Spring 2011

Evaluation of curing criteria for cold in-place recycling of asphalt

Adam Michael Woods
University of Iowa

EVALUATION OF CURING CRITERIA FOR COLD IN-PLACE RECYCLING OF ASPHALT

by

Adam Michael Woods

A thesis submitted in partial fulfillment
of the requirements for the Master of
Science degree in Civil and Environmental Engineering
in the Graduate College of
The University of Iowa

May 2012

Thesis Supervisor: Professor Hosin Lee

Graduate College
The University of Iowa
Iowa City, Iowa

CERTIFICATE OF APPROVAL

_____

MASTER'S THESIS

_____

This is to certify that the Master's thesis of

Adam Michael Woods

has been approved by the Examining Committee
for the thesis requirement for the Master of Science
degree in Civil and Environmental Engineering at the May 2012 graduation.

Thesis Committee: _____
Hosin Lee, Thesis Supervisor

_____
Wilfred Nixon

_____
Paul Hanley

TABLE OF CONTENTS

LIST OF TABLES v

LIST OF FIGURES vi

CHAPTER 1: INTRODUCTION 1

1.1 Objective 1
1.2 Benefits of the Study 2

CHAPTER 2: SUMMARY FROM PREVIOUS STUDY 3

CHAPTER 3: MOISTURE LOSS INDEX DEVELOPED BY PREVIOUS STUDY 5

3.1 Moisture Content and Temperature of CIR-CSS-1-emulsion Layer 5
3.2 Moisture Content and Temperature of CIR-foam Layer 6
3.3 Moisture Loss Index for CIR Layer 7
3.3.1 Moisture Loss Index for CIR-CSS-1-emulsion Layer 8
3.3.2 Moisture Loss Index for CIR-foam Layer 9

CHAPTER 4: LABORATORY EVALUATION OF CAPACITANCE MOISTURE SENSOR 18

CHAPTER 5: MEASUREMENT OF MOISTURE CONTENT FROM CIR-EMULSION PROJECT IN CLINTON COUNTY 23

5.1 Measurement of Field Moisture Content and Temperature 23
5.2 Measurement of Density and Stiffness 25
5.2.1 Density Measurements using Nuclear Gauge 25
5.2.2 Stiffness Measurements using Geo-Gauge 25

CHAPTER 6: MEASUREMENT OF MOISTURE CONTENT FROM CIR-FOAM PROJECT IN IOWA COUNTY 39

6.1 Measurement of Field Moisture Content and Temperature 39
6.2 Stiffness Measurements using Geo-Gauge 40

CHAPTER 7: MEASUREMENT OF MOISTURE CONTENT FROM CIR-FOAM PROJECT IN BENTON COUNTY 50

7.1 Measurement of Field Moisture Content and Temperature 50
7.2 Stiffness Measurements using Geo-Gauge 51

CHAPTER 8: MEASUREMENT OF MOISTURE CONTENT FROM CIR-FOAM PROJECT IN MARSHALL COUNTY 61

8.1 Measurement of Field Moisture Content and Temperature 61
8.2 Measurement of Density and Stiffness 63
8.2.1 Density Measurements using Nuclear Gauge 63
8.2.2 Stiffness Measurements using Geo-Gauge 63

CHAPTER 9: MEASUREMENT OF MOISTURE CONTENT FROM CIR-FOAM PROJECT IN DELAWARE COUNTY 77

9.1 Measurement of Field Moisture Content and Temperature 77
9.2 Stiffness Measurements using Geo-Gauge 78

CHAPTER 10: MEASUREMENT OF MOISTURE CONTENT FROM CIR-FOAM PROJECT IN DELAWARE COUNTY 86

10.1 Measurement of Field Moisture Content and Temperature 86
10.2 Measurement of Density and Stiffness 87
10.2.1 Density Measurements using Nuclear Gauge 88
10.2.2 Stiffness Measurements using Geo-Gauge 88

CHAPTER 11: MEASUREMENT OF MOISTURE CONTENT FROM CIR-FOAM PROJECT IN BLACK HAWK COUNTY 100

11.1 Measurement of Field Moisture Content and Temperature 100
11.2 Measurement of Density and Stiffness 101
11.2.1 Density Measurements using Nuclear Gauge 101
11.2.2 Stiffness Measurements using Geo-Gauge 102

CHAPTER 12: DEVELOPMENT OF MOISTURE LOSS INDEX FOR CIR LAYER 114

12.1 CIR-HFMS-2S-emulsion Project Site in Clinton County 114
12.2 CIR-foam Project Site in Iowa County 116
12.3 CIR-foam Project Site in Benton County 117
12.4 CIR-foam Project Site in Marshall County 118
12.5 CIR-foam Project Site in Delaware County 2010 119
12.6 CIR-foam Project Site in Delaware County 2011 120
12.7 CIR-foam Project Site in Black Hawk County 121
12.8 Compilation of Moisture Data from all CIR-foam Sites 122

CHAPTER 13: DEVELOPMENT OF STIFFNESS CRITERIA 144

13.1 Background and Other Studies 144
13.2 Examination of Stiffness from Project Sites 145

CHAPTER 14: SUMMARY AND CONCLUSIONS 151

14.1 Conclusions 151
14.2 Recommendations/Future Studies 152

REFERENCES 154

LIST OF TABLES

Table 4-1. Comparisons between moisture content from six sensors and moisture content from real weight 20

Table 12-1. Comparisons between moisture loss indices for each project site 143

Table 13-1. Stiffness Results for 12 Portland Concrete Cement Projects in White et. al Study 2003 147

Table 13-2. Stiffness Results for 3 Test Sections in Mohammad et. al 2003 Study.....148

Table 13-3. Base Rankings in regards to Stiffness from Chen et. al Study 148

LIST OF FIGURES

Figure 3-1. Locations of CIR-foam and CIR-emulsion project sites in Iowa 10

Figure 3-2. Plots of moisture contents against the curing time from three moisture sensors embedded in the CIR-CSS-1-emulsion layer 11

Figure 3-3. Plots of temperature from two sensors embedded in the CIR-CSS-1-emulsion layer against air temperature from weather station 12

Figure 3-4. Plots of moisture contents against the curing time from three sensors embedded in the CIR-foam layer 13

Figure 3-5. Plots of temperature from two sensors embedded in the CIR-foam layer against air temperature from weather station 14

Figure 3-6. Plots of moisture change per hour against each of three independent variables at 3.5 inches of surface from for CIR-CSS-1-emulsion layer 15

Figure 3-7. Plots of moisture change per hour against each of three independent variables at 2.0 inches of surface from CIR-foam layer 16

Figure 3-8. Plots of moisture change per hour against each of three independent variables at 3.5 inches of surface from CIR-foam layer 17

Figure 4-1. Verification of capacitance moisture sensors in the laboratory 19

Figure 4-2. Plots of moisture content changes from six sensors buried at 2.0 inches from the surface 21

Figure 4-3. Plots of moisture content from six sensors buried at 2.0 inches from the surface against moisture content from real weight 22

Figure 5-1. Locations of CIR-HFMS-2S-emulsion project sites in Clinton County 26

Figure 5-2. Embedded moisture and temperature sensors installed 2.0 inches from the surface of the CIR- HFMS-2S layer 27

Figure 5-3. Plots of moisture contents against the curing period from three sensors embedded in the CIR-HMFS-2S layer 28

Figure 5-4. Plots of rainfalls against the curing period from weather station device 28

Figure 5-5. Plots of temperature against the curing period from three sensors embedded in the CIR-HFMS-2S-emulsion layer and air temperature from weather station device 29

Figure 5-6. Plots of humidity against the curing period from weather station device 30

Figure 5-7. Plots of temperature from three sensors embedded in the CIR-HFMS-2S-emulsion layer against air temperature from weather station device 30

Figure 5-8. Moisture measurements for each of three locations using a portable TDR and nuclear gauge in CIR-HFMS-2S-emulsion project site 31

Figure 5-9. Plots of field moisture contents measured by a portable TDR in CIR-HFMS-2S-emulsion project site 31

Figure 5-10. Plots of field moisture contents measured by nuclear gauge in CIR-HFMS-2S-emulsion project site 32

Figure 5-11. Plots of field moisture content measured by a potable TDR (or moisture sensors) against field moisture content measured by a nuclear gauge 33

Figure 5-12. Plots of field moisture content measured by a potable TDR against field moisture content measured by moisture sensors 34

Figure 5-13. Location of three spots for measuring density and stiffness 35

Figure 5-14. Plots of density against curing period from three locations in the CIR-HFMS-2S-emulsion layer 35

Figure 5-15. Plots of stiffness against the curing period from three locations in the CIR-HFMS-2S-emulsion layer 36

Figure 5-16. Plots of density measured by a nuclear gauge against stiffness measured by geo-gauge at three different locations 37

Figure 5-17. Plots of stiffness measured by a geo-gauge against moisture content measured by embedded sensors at three different locations 38

Figure 6-1. Locations of CIR-foam project sites in Iowa County 41

Figure 6-2. Embedded moisture and temperature sensors installed 2.0 inches from the surface of the CIR- foam layer 42

Figure 6-3. Plots of moisture contents against the curing period from three sensors embedded in the CIR-foam layer 43

Figure 6-4. Plots of rainfalls against the curing period from weather station device 43

Figure 6-5. Plots of temperature against the curing period from three sensors embedded in the CIR-foam layer and air temperature from weather station device 44

Figure 6-6. Plots of humidity against the curing period from weather station device 44

Figure 6-7. Plots of temperature from three sensors embedded in the CIR-foam layer against air temperature from weather station device 45

Figure 6-8. Plots of field moisture contents measured by a portable TDR in CIR-foam project site 46

Figure 6-9. Plots of field moisture content measured by a potable TDR against field moisture content measured by moisture sensors 47

Figure 6-10. Plots of stiffness against the curing period from three locations in the CIR-foam layer 48

Figure 6-11. Plots of stiffness measured by a geo-gauge against moisture content measured by embedded sensors at three different locations 49

Figure 7-1. Locations of CIR-foam project site in Benton County 52

Figure 7-2. Embedded moisture and temperature sensors installed 2.0 inches from the surface of the CIR- foam layer....53

Figure 7-3. Plots of moisture contents against the curing period from three sensors embedded in the CIR-foam layer....54

Figure 7-4. Plots of rainfalls against the curing period from weather station device 54

Figure 7-5. Plots of temperature against the curing period from three sensors embedded in the CIR-foam layer and air temperature from weather station device 55

Figure 7-6. Plots of humidity against the curing period from weather station device 55

Figure 7-7. Plots of temperature from three sensors embedded in the CIR-foam layer against air temperature from weather station device 56

Figure 7-8. Plots of field moisture contents measured by a portable TDR in CIR-foam project site....57

Figure 7-9. Plots of field moisture content measured by a potable TDR against field moisture content measured by moisture sensors....58

Figure 7-10. Plots of stiffness against the curing period from three locations in the CIR-foam layer 59

Figure 7-11. Plots of stiffness measured by a geo-gauge against moisture content measured by embedded sensors at three different locations 60

Figure 8-1. Location of CIR-foam project site in Marshall County 64

Figure 8-2. Embedded moisture and temperature sensors installed 2.0 inches from the surface of the CIR- foam layer....65

Figure 8-3. Plots of moisture contents against the curing period from three sensors embedded in the CIR-foam layer....66

Figure 8-4. Plots of rainfalls against the curing period from weather station device 66

Figure 8-5. Plots of temperature against the curing period from two sensors embedded in the CIR-foam layer and air temperature from weather station device 67

Figure 8-6. Plots of humidity against the curing period from weather station device 67

Figure 8-7. Plots of temperature from three sensors embedded in the CIR-foam layer against air temperature from weather station device 68

Figure 8-8. Plots of field moisture contents measured by a portable TDR in CIR-foam project site.....69

Figure 8-9. Plots of field moisture contents measured by nuclear gauge in CIR-foam project site.....70

Figure 8-10. Plots of field moisture content measured by a potable TDR (or moisture sensors) against field moisture content measured by a nuclear gauge.....71

Figure 8-11. Plots of field moisture content measured by a potable TDR against field moisture content measured by moisture sensors 72

Figure 8-12. Plots of density against curing period from three locations in the CIR-foam layer 73

Figure 8-13. Plots of stiffness against the curing period from three locations in the CIR-foam layer 74

Figure 8-14. Plot of density measured by a nuclear gauge against stiffness measured by geo-gauge.....75

Figure 8-15. Plots of stiffness measured by a geo-gauge against moisture content measured by embedded sensors at three different locations 76

Figure 9-1. Locations of CIR-foam project site in Delaware County.....79

Figure 9-2. Embedded moisture and temperature sensors installed 2.0 inches from the surface of the CIR- foam layer.....80

Figure 9-3. Plots of moisture contents against the curing period from three sensors embedded in the CIR-foam layer.....81

Figure 9-4. Plots of rainfalls against the curing period from weather station device 81

Figure 9-5. Plots of temperature against the curing period from three sensors embedded in the CIR-foam layer and air temperature from weather station device 82

Figure 9-6. Plots of humidity against the curing period from weather station device 82

Figure 9-7. Plots of temperature from three sensors embedded in the CIR-foam layer against air temperature from weather station device 83

Figure 9-8. Plots of stiffness against the curing period from three locations in the CIR-foam layer 84

Figure 9-9. Plots of stiffness measured by a geo-gauge against moisture content measured by embedded sensors at three different locations 85

Figure 10-1. Location of CIR-foam project site in Delaware County 89

Figure 10-2. Embedded moisture and temperature sensors installed 2.0 inches from the surface of the CIR- foam layer 90

Figure 10-3. Plots of moisture contents against the curing period from three sensors embedded in the CIR-foam layer 91

Figure 10-4. Plots of rainfalls against the curing period from weather station device 91

Figure 10-5. Plots of temperature against the curing period from three sensors embedded in the CIR-foam layer and air temperature from weather station device 92

Figure 10-6. Plots of humidity against the curing period from weather station device 92

Figure 10-7. Plots of temperature from three sensors embedded in the CIR-foam layer against air temperature from weather station device 93

Figure 10-8. Plots of field moisture contents measured by nuclear gauge in CIR-foam project site 94

Figure 10-9. Plots of field moisture content measured by a nuclear gauge against field moisture content measured by the embedded moisture sensors 95

Figure 10-10. Plots of density against curing period from three locations in the CIR-foam layer 96

Figure 10-11. Plots of stiffness against the curing period from three locations in the CIR-foam layer 97

Figure 10-12. Plot of density measured by a nuclear gauge against stiffness measured by geo-gauge 98

Figure 10-13. Plots of stiffness measured by a geo-gauge against moisture content measured by embedded sensors at three different locations 99

Figure 11-1. Location of CIR-foam project site in Black Hawk County 103

Figure 11-2. Embedded moisture and temperature sensors installed 2.0 inches from the surface of the CIR- foam layer 104

Figure 11-3. Plots of moisture contents against the curing period from three sensors embedded in the CIR-foam layer 105

Figure 11-4. Plots of rainfalls against the curing period from weather station device 105

Figure 11-5. Plots of temperature against the curing period from three sensors embedded in the CIR-foam layer and air temperature from weather station device 106

Figure 11-6. Plots of humidity against the curing period from weather station device 106

Figure 11-7. Plots of temperature from three sensors embedded in the CIR-foam layer against air temperature from weather station device 107

Figure 11-8. Plots of field moisture contents measured by nuclear gauge in CIR-foam project site.....108

Figure 11-9. Plots of field moisture content measured by a nuclear gauge against field moisture content measured by the embedded moisture sensors 109

Figure 11-10. Plots of density against curing period from three locations in the CIR-foam layer 110

Figure 11-11. Plots of stiffness against the curing period from three locations in the CIR-foam layer 111

Figure 11-12. Plot of density measured by a nuclear gauge against stiffness measured by geo-gauge.....112

Figure 11-13. Plots of stiffness measured by a geo-gauge against moisture content measured by embedded sensors at three different locations 113

Figure 12-1. Plots of moisture change per hour against each of three independent variables at sensor A 123

Figure 12-3. Plots of moisture change per hour against each of three independent variables at sensor C 125

Figure 12-4. Plots of moisture change per hour against each of three independent variables at sensor A 126

Figure 12-5. Plots of moisture change per hour against each of three independent variables at sensor B 127

Figure 12-6. Plots of moisture change per hour against each of three independent variables at sensor C 128

Figure 12-7. Plots of moisture change per hour against each of three independent variables at sensor A 129

Figure 12-8. Plots of moisture change per hour against each of three independent variables at sensor B 130

Figure 12-9. Plots of moisture change per hour against each of three independent variables at sensor C 131

Figure 12-10. Plots of moisture change per hour against each of three independent variables at sensor A 132

Figure 12-11. Plots of moisture change per hour against each of three independent variables at sensor C 133

Figure 12-12. Plots of moisture change per hour against each of three independent variables at sensor A 134

Figure 12-13. Plots of moisture change per hour against each of three independent variables at sensor B 135

Figure 12-14. Plots of moisture change per hour against each of three independent variables at sensor C 136

Figure 12-15. Plots of moisture change per hour against each of three independent variables at sensor A 137

Figure 12-16. Plots of moisture change per hour against each of three independent variables at sensor B 138

Figure 12-17. Plots of moisture change per hour against each of three independent variables at sensor C 139

Figure 12-18. Plots of moisture change per hour against each of three independent variables at sensor A 140

Figure 12-19. Plots of moisture change per hour against each of three independent variables at sensor B 141

Figure 12-20. Plots of moisture change per hour against each of three independent variables at sensor C 142

Figure 13-1. Plots of Stiffness Against the Curing Period for 2009 and 2010 Project Sites 149

Figure 13-2. Plots of Stiffness Against the Curing Period for 2011 Project Sites 150

CHAPTER 1: INTRODUCTION

The current practice in Iowa simply controls the maximum moisture content in the cold in-place recycling (CIR) of 1.5 percent, whereas many CIR projects, struggling with unfavorable climate, have been overlaid successfully with higher amounts of moisture. The prior research was conducted to explore technically sound and more effective ways to identify minimum in-place CIR properties necessary to permit placement of the HMA overlay.

Moisture loss indices were developed based on the field measurements from one CIR-foam and one CIR-emulsion construction sites. To calibrate the moisture loss indices, six CIR construction sites that include two CIR-foam sites, two CIR-emulsion (CSS-1) sites and two CIR-emulsion (HFMS-2s) sites, were proposed to be monitored using embedded moisture and temperature sensors. However, due to the lack of available CIR-emulsion sites nearby, one CIR-HFMS-2S emulsion site and four CIR-foam sites were monitored.

The potential of using the stiffness measured by geo-gauge to supplement (or possibly replace) the moisture measurement by a nuclear gauge was explored in this study. A correlation between stiffness and moisture content was developed.

1.1 Objective

The main objectives of the study are to: 1) measure the moisture contents and temperature throughout a CIR layer from six CIR project sites, 2) calibrate the developed moisture loss indies using the field measurement from six CIR project sites, and 3) develop stiffness/density gain model to supplement (or possibly replace) the moisture criteria.

1.2 Benefits of the Study

During the previous study, both moisture and temperature conditions were measured in the field by embedding the sensors in the CIR layer. Based upon the field measurements, moisture loss indices were developed as a function of initial moisture condition and cumulative pavement temperature per hour. However, it is necessary to calibrate the moisture loss indices so that they can be applied to various CIR construction projects in Iowa. The results of the research are presented as more accurate and rational moisture loss indices for various types of CIR construction. The moisture loss index will be a truly useful tool for all pavement engineers, which can help them accurately determine an optimum timing of an overlay without continually measuring moisture conditions in the field using a nuclear gauge. The moisture loss indices will rationalize the way the quality of CIR layer is inspected for the optimum timing of an HMA overlay and significantly enhance the long-term performance of CIR pavements. In addition, the stiffness of CIR layer measured by the Geo-gage can be used to supplement (or possibly replace) the moisture measurement during a curing period.

CHAPTER 2: SUMMARY FROM PREVIOUS STUDY

During phase 1 study, to represent the curing process of CIR layer in the field construction, three different laboratory curing procedures were examined: 1) uncovered, 2) semi-covered and 3) covered specimens. Indirect tensile strengths and moisture contents of the CIR specimens cured for various curing periods were measured. To predict the field performance of CIR pavements during the curing process, dynamic modulus and dynamic creep tests were conducted using Simple Performance Testing (SPT) equipment.

Upon completion of phase 1 study, the following conclusions were derived:

- The indirect tensile strength of CIR specimens in all three curing conditions did not increase during the early stage of curing but increased during a later stage of curing, usually when the moisture content fell below 1.5%.
- Dynamic modulus and flow number increased as a curing time increased and a moisture content decreased.
- Given the same curing time, CIR-foam specimens exhibited the higher tensile strength, dynamic modulus and flow number than CIR-emulsion. This might have been caused by the higher moisture content in the CIR-emulsion specimens than the CIR-foam for the equivalent curing time.
- The curing method, temperature and duration had a significant impact on indirect tensile strength, dynamic modulus, and flow number of the CIR mixtures.

During phase 2 study, to develop a set of moisture loss indices, the moisture contents and temperatures of one CIR-foam and one CIR-emulsion layers were monitored for five

months. The moisture contents were measured by embedded capacitance moisture sensors at a midpoint and a bottom of the CIR layer and they were compared against the moisture content measured by a nuclear gauge. The modulus and stiffness were measured using a falling weight deflectometer (FWD) and a geo-gauge during the curing time. Moisture loss indices were developed based on the initial moisture content and temperature of CIR-foam and CIR-emulsion layers.

Upon completion of phase 2 study, the following conclusions were derived:

- The moisture condition of a CIR layer can be monitored accurately using a capacitance moisture sensor.
- The moisture loss index for a CIR layer is a viable tool in determining the optimum timing for an overlay.
- The modulus of a CIR layer back-calculated from deflection measured by FWD seemed to be in a good agreement with the stiffness measured by geo-gauge.
- The stiffness of a CIR layer increased as curing time increased. The layer stiffness seemed to be affected by the pavement temperature.
- The geo-gauge should be considered for measuring the stiffness of a CIR layer that can be used to determine the optimum timing of an overlay.

CHAPTER 3: MOISTURE LOSS INDEX DEVELOPED BY PREVIOUS STUDY

To develop moisture loss index for CIR layer, as shown in Figure 3-1, the field moisture contents and temperature were measured from CIR-emulsion and CIR-foam layers in 2008.

3.1 Moisture Content and Temperature of CIR-CSS-1-emulsion Layer

To measure the field moisture contents and temperature of CIR-emulsion layer, CIR with CSS-1 emulsified asphalt (CIR-CSS-1-emulsion) project site in Scott County was selected. The 2.5-mile section of County Road Y-40 was rehabilitated from Iowa Highway 22 in the town of Buffalo to Mayne Street in the town of Blue Grass, Iowa between June 5th and June 6th, 2008. The existing 10-cm thick Type B HMA layer on top of the concrete pavement was milled and mixed with CSS-1 emulsified asphalt to produce 4-inch thick CIR-CSS-1-emulsion layer. The 2-inch thick HMA intermediate course was overlaid on June 26th, 2008 followed by the 1.5-inch thick HMA wearing course overlaid on July 3rd, 2008.

To monitor actual moisture contents and temperatures of the CIR-CSS-1-emulsion layer in the field, three ECH2O moisture sensors and two temperature sensors were installed at 3.5 inches from surface. A weather station was also installed to collect air temperature, humidity, and rainfall.

Figure 3-2 shows plots of moisture contents measured by three sensors along with dates and amounts of the fourteen rainfalls (with a total of 6.38 inches) measured during

the curing period of 19 days. The moisture contents at the bottom of CIR-CSS-1-emulsion layer before the intermediate HMA overlay were measured as 9.4% from sensor A, 11.1% from sensor B, and 9.4% from sensor C. Despite the actual moisture content of CIR-CSS-1-emulsion layer being above 1.5%, the intermediate HMA overlay was constructed after 19 days of curing.

Figure 3-3 shows plots of temperatures measured by two sensors embedded in the CIR-CSS-1-emulsion layer against air temperatures from the weather station. This air-to-pavement temperature relationship was used to estimate the temperature of CIR-emulsion layer based on the air temperature.

3.2 Moisture Content and Temperature of CIR-foam Layer

To measure the field moisture contents and temperature of CIR-foam layer, CIR with foamed asphalt (CIR-foam) project site in Grundy County was selected. The 6.5-mile section of County Road T 55 was rehabilitated from I-175 north to County Road D 25 starting on July 31, 2008. The top 3.5-inch of the existing 9-inch thick Type B HMA layer was milled and mixed with foamed asphalt to produce 3.5-inch thick CIR-foam layer. Upon completion of tack coating process on top of CIR-foam layer, the 1.5-inch thick HMA intermediate course was overlaid on August 22nd, 2008 followed by the 1.5-inch thick HMA wearing course overlaid on September 1st, 2008.

To monitor actual moisture contents and temperatures of the CIR-foam layer in the field, two ECH2O moisture sensors and one temperature sensor were installed at 3.5 inches from surface and one ECH2O moisture sensor and one temperature sensor were installed at 2 inches from surface. A weather station was also installed to collect air temperature, humidity, and rainfall.

Figure 3-4 shows plots of moisture contents measured by three sensors along with dates and amounts of the eleven rainfalls (with a total of 1.54 inches) measured during the curing period of 22 days. The moisture contents in the middle of the CIR-foam layer before the intermediate HMA overlay were measured as 12.1% from sensor A', 7.2% from sensor A at the bottom, and 14.5% from sensor B at the bottom. Despite the actual moisture contents of CIR-foam layer remaining above 1.5%, the intermediate HMA overlay was constructed after 22 days of curing.

Figure 3-5 shows plots of temperatures from two sensors embedded in the CIR-foam layer against air temperature from the weather station. This air-to-pavement temperature relationship was used to estimate the temperature of CIR-foam layer based on the air temperature.

3.3 Moisture Loss Index for CIR Layer

In order to develop a better analysis tool to monitor the CIR layer in preparation for a timely placement of the wearing surface, a moisture loss index concept was introduced. The main objective of the moisture loss index is to determine an optimal timing of an overlay based on the initial moisture and climate conditions without continually measuring moisture contents using a nuclear gauge. To develop moisture loss indices for CIR layer, the actual moisture content of CIR layer was measured by ECH_2O moisture sensors and climate data were collected from the weather stations installed at CIR project sites.

To predict the moisture change in the CIR layer over time, using a multiple linear regression technique, the following moisture loss index formula was developed as a

function of initial moisture condition, average CIR layer temperature, and average humidity.

$$\Delta MC/hr = a_1 + a_2\ IMC + a_3\ Temp + a_4\ Hum$$

Where, $\Delta MC/hr$ = Moisture change per hour during curing time

IMC = Initial moisture content of CIR layer right after construction

Temp = Average CIR layer temperature (°C) during curing time

Hum = Average humidity (%) during curing time

a_1, a_2, a_3, a_4 = multiple linear regression coefficients

3.3.1 Moisture Loss Index for CIR-CSS-1-emulsion Layer

Moisture contents and climatic data were collected from the CIR-CSS-1-emulsion layer in Scott County. A new set of moisture content data was created when the rainfall had occurred. After discarding the initial moisture contents above 12% (unusually high due to 200-year flood), three moisture content data sets from sensor A, six sets from sensor B, and fourteen sets from sensor C were obtained.

Figure 3-6 shows plots of moisture content change per hour against three independent variables. As can be seen from Figure 3-6, a positive correlation of moisture content change per hour against initial moisture content and CIR-CSS-1-emulsion layer temperature indicates that the rate of moisture change in CIR layer increases as the initial moisture content and average CIR layer temperature increase. A negative correlation of moisture content change per hour against the average humidity indicates that the rate of moisture change in CIR layer decreases as the average humidity increases.

As shown in the regression equation below, Δmoisture content per hour in CIR-CSS-1-emulsion layer can be predicted as a function of the initial moisture content and the average CIR pavement temperature and the average humidity.

$$\Delta MC/hr = 0.123 + 0.015\ IMC + 0.005\ Temp - 0.002\ Hum \quad (R\text{-square} = 71.6\%)$$

3.3.2 Moisture Loss Index for CIR-foam Layer

Moisture contents and climatic data were collected from the CIR-foam layer in Grundy County. After discarding the initial moisture contents above 12% (unusually high due to 200-year flood), thirty moisture content data sets from sensor A', twenty-three sets from sensor A, and sixteen sets from sensor B were obtained.

Figure 3-7 and Figure 3-8 show plots of moisture content change per hour against three independent variables for sensor A' at 2.0 inches from surface of CIR-foam layer and for sensor A and B at 3.5 inches from surface of CIR-foam layer, respectively. As can be seen from Figure 3-7 and Figure 3-8, a positive correlation of moisture content change per hour against initial moisture content and CIR-foam layer temperature indicates that the rate of moisture change in CIR layer increases as the initial moisture content and average CIR layer temperature increase. A negative correlation of moisture content change per hour against the average humidity indicates that the rate of moisture change in CIR layer decreases as the average humidity increases.

As shown in the regression equation below, Δmoisture content per hour in CIR-foam layer can be predicted as a function of the initial moisture content and the average CIR pavement temperature and the average humidity.

A' (2.0 inches): $\Delta MC/hr = -0.005 + 0.033\ IMC + 0.003\ Temp - 0.001\ Hum$

$(R\text{-square} = 82.8\%)$

A&B (3.5 inches): ΔMC/hr = -0.012 + 0.042 IMC - 0.003 Temp - 0.002 Hum

(R-square = 62.7%)

Figure 3-1. Locations of CIR-foam and CIR-emulsion project sites in Iowa

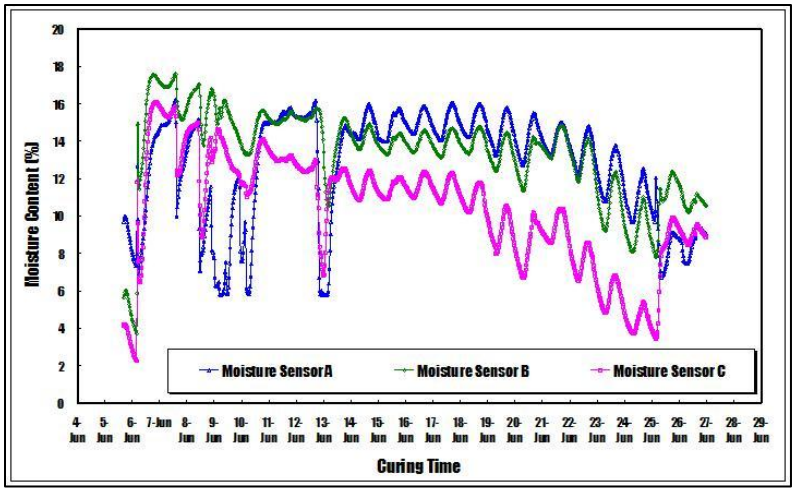

Figure 3-2. Plots of moisture contents against the curing time from three moisture sensors embedded in the CIR-CSS-1-emulsion layer

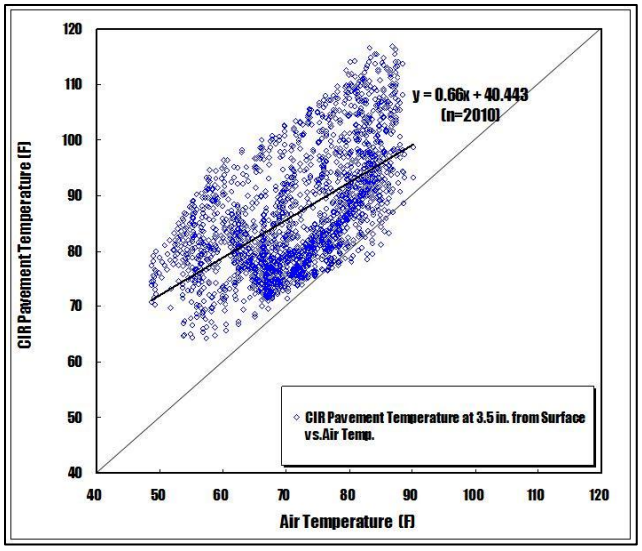

Figure 3-3. Plots of temperature from two sensors embedded in the CIR-CSS-1-emulsion layer against air temperature from weather station

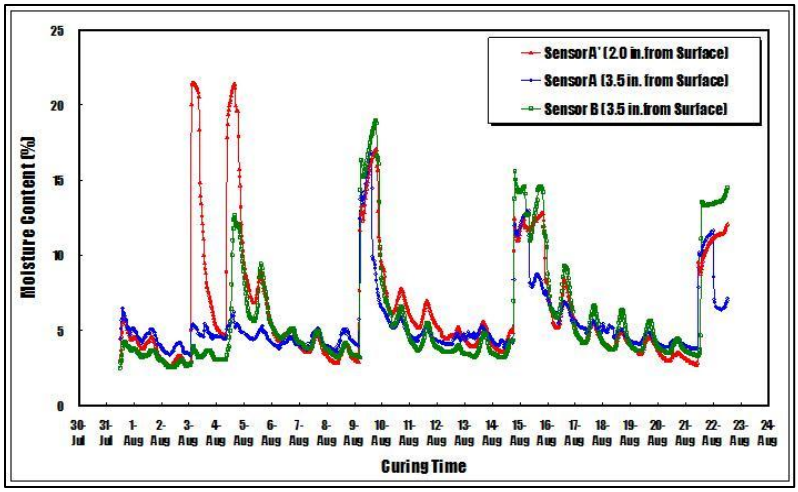

Figure 3-4. Plots of moisture contents against the curing time from three sensors embedded in the CIR-foam layer

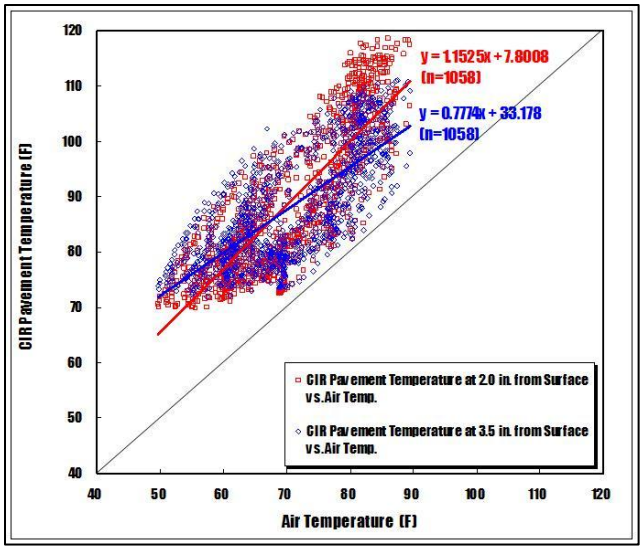

Figure 3-5. Plots of temperature from two sensors embedded in the CIR-foam layer against air temperature from weather station

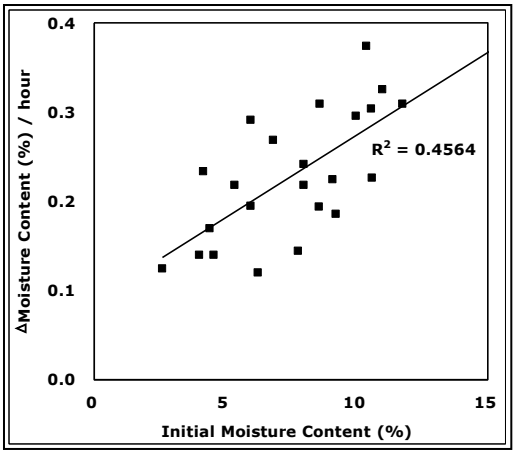

(a) ΔMC/h vs. IMC

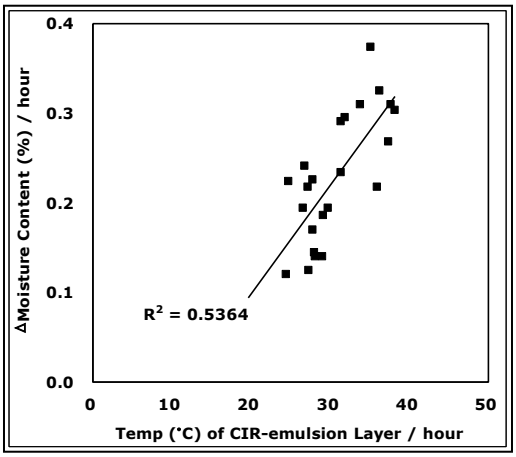

(b) ΔMC/hour vs. Temperature

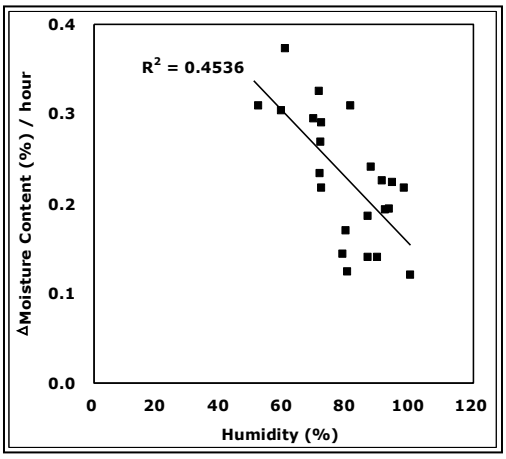

(c) ΔMC/h vs. Humidity

Figure 3-6. Plots of moisture change per hour against each of three independent variables at 3.5 inches of surface from for CIR-CSS-1-emulsion layer

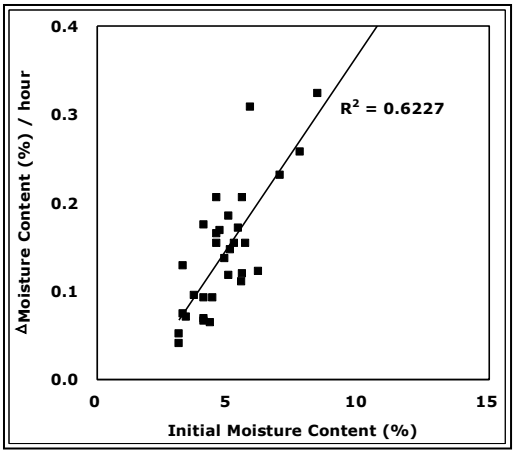

(a) ΔMC/h vs. IMC

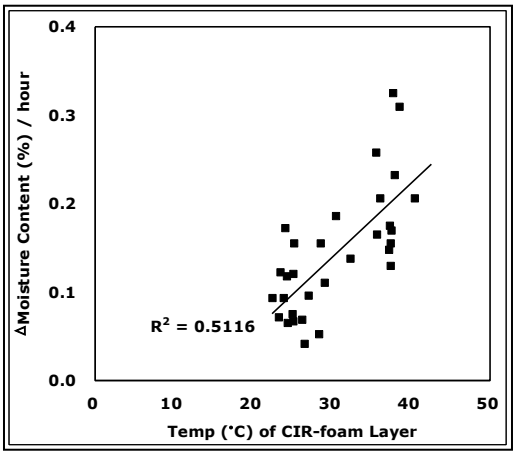

(b) ΔMC/h vs. Temperature

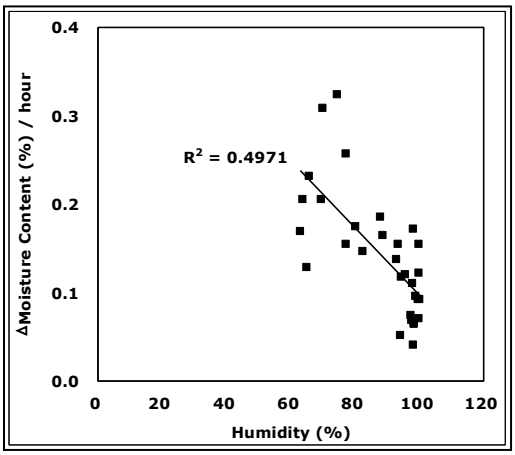

(c) ΔMC/h vs. Humidity

Figure 3-7. Plots of moisture change per hour against each of three independent variables at 2.0 inches of surface from CIR-foam layer

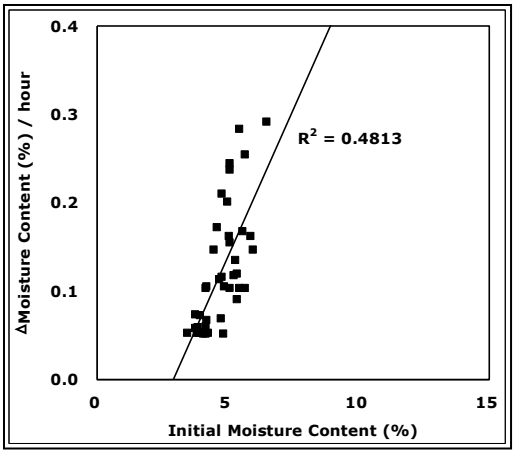

(a) ΔMC/h vs. IMC

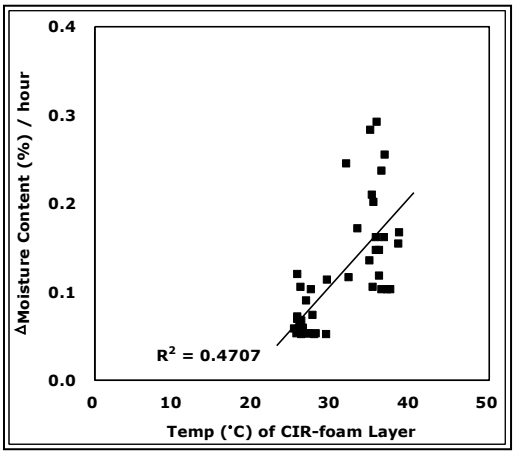

(b) ΔMC/h vs. Temperature

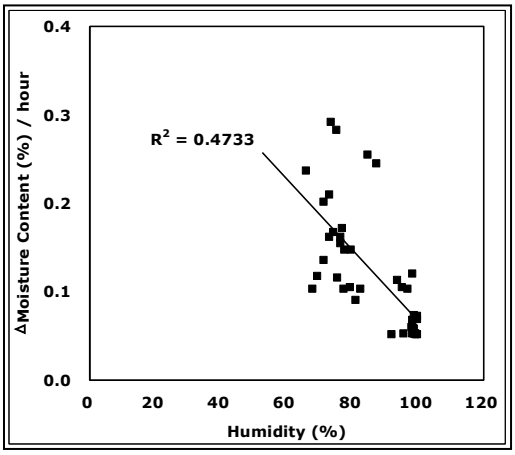

(c) ΔMC/h vs. Humidity

Figure 3-8. Plots of moisture change per hour against each of three independent variables at 3.5 inches of surface from CIR-foam layer

CHAPTER 4: LABORATORY EVALUATION OF CAPACITANCE MOISTURE SENSOR

To verify the capacitance moisture sensor against the actual moisture content, three RAP specimens were prepared in the rectangular container. The RAP materials were mixed with water at 2.0%, 4.0%, and 6.0% of RAP weight of 2700g. As shown in Figure 4-1 (a), for each RAP specimens, two capacitance moisture sensors were buried at 2.0 inches from the surface (2.0% MC for sensor A and B, 4.0% MC for sensor C and D, and 6.0% MC for sensor E and F) and RAP specimens were then compacted using a manual Marshall hammer. As shown in Figure 4-1 (b), the RAP specimens were cured at 40°C for 50 days to achieve at 0% of the moisture content. As summarized shown in Figure 4-2, changes of moisture content from six sensors were monitored for 50 days and the actual moisture contents from real weight were computed.

Table 4-1 summarizes the moisture contents measured from six sensors buried at 2.0 inches from the surface at three different moisture levels and the moisture contents measured from by measuring the weight loss of three RAP specimens during the curing period. Figure 4-2 shows plots of the moisture contents from six sensors buried at 2.0 inches from the surface against the actual moisture content.

(a) Moisture sensors buried at 2.0 inches

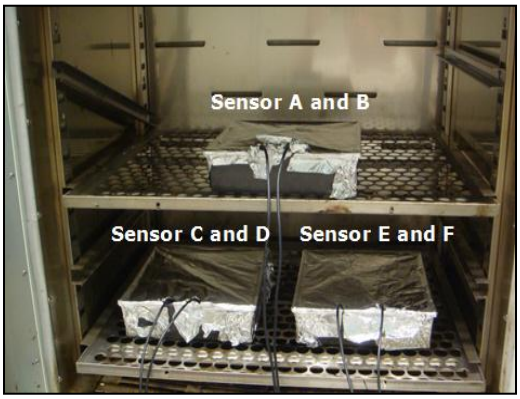

(b) Curing process at 40°C

Figure 4-1. Verification of capacitance moisture sensors in the laboratory

Table 4-1. Comparisons between moisture content from six sensors and moisture content from real weight

Curing day	Measured moisture content (%) from sensor						Measured moisture (%) content from actual weight		
							A, B	C, D	E, F
1 day	.8	.7	.4	.7	.7	.4	1.3	2.5	3.4
3 days	.6	.5	.1	.3	.3	.1	0.9	2.1	2.7
4 days	.3	.3	.1	.2	.1	.0	0.7	1.7	2.4
5 days	.9	.9	.9	.9	.8	.7	0.5	1.3	1.9
9 days	.4	.4	.6	.4	.7	.3	0.0	0.6	0.6
10 days	.4	.4	.1	.3	.1	.7	0.0	0.3	0.4
11 days	.4	.3	.1	.3	.7	.6	0.0	0.2	0.2
12 days	.3	.2	.1	.3	.4	.5	0.0	0.1	0.1
13 days	.3	.2	.1	.2	.4	.4	0.0	0.0	0.0
19 days	.2	.1	.0	.0	.1	.1	0.0	0.0	0.0
20 days	.2	.1	.0	.0	.1	.1	0.0	0.0	0.0
21 days	.2	.1	.0	.0	.1	.1	0.0	0.0	0.0
50 days	.0	.0	.0	.0	.0	.0	0.0	0.0	0.0

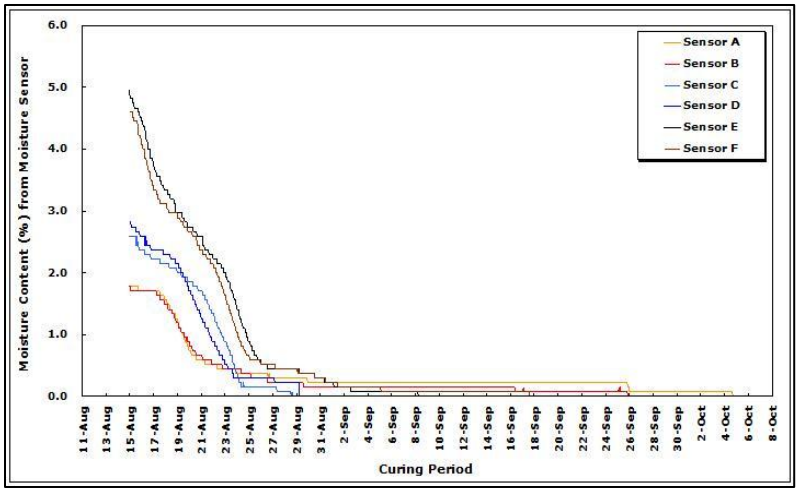

Figure 4-2. Plots of moisture content changes from six sensors buried at 2.0 inches from the surface

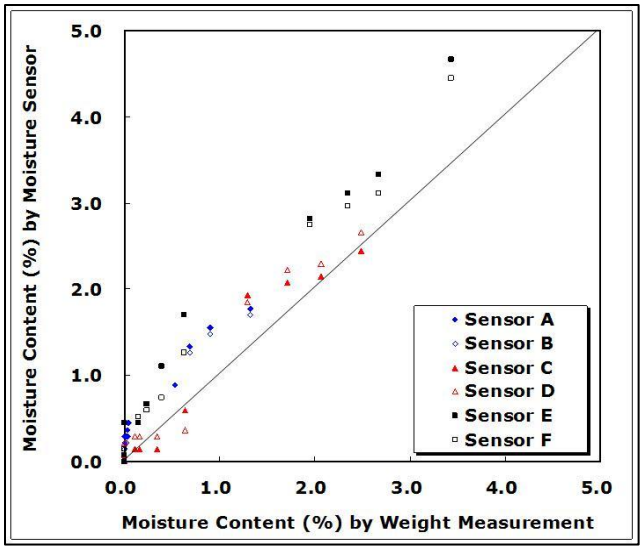

Figure 4-3. Plots of moisture content from six sensors buried at 2.0 inches from the surface against moisture content from real weight

CHAPTER 5: MEASUREMENT OF MOISTURE CONTENT FROM CIR-EMULSION PROJECT IN CLINTON COUNTY

To measure the field moisture contents and temperature of CIR-emulsion layer, as shown in Figure 5-1, cold in-place recycling with high float medium setting-high viscosity with solvent emulsified asphalt (HFMS-2S-emulsion) project site in Clinton County was selected. HFMS-2S-emulsion project site is located from 11th street north in city of Dewitt to Iowa Highway 136, Iowa. The 11.2-mile section of County Road Y-70 and Z2E was rehabilitated from 11th street north in city of Dewitt to Iowa Highway 136, Iowa from August 18th to September 24th, 2009.

5.1 Measurement of Field Moisture Content and Temperature

To monitor actual moisture contents of the CIR-HFMS-2S-emulsion layer in the field, as shown in Figure 5-2, three ECH2O moisture sensors and three temperature sensors were embedded at 2.0 inches from the surface of the CIR-HFMS-2S layer. A weather station was also installed to collect air temperature, humidity, rainfall and wind speed.

Figure 5-3, Figure 5-4, Figure 5-5, and Figure 5-6 show plots of moisture content, rainfall, temperature, and humidity, respectively, measured during the curing duration of 36 days when ten rainfalls with a total amount of 6.18 inches have occurred. The moisture contents measured by three sensors are consistent with the time and amount of rainfall. The moisture contents at 2.0 inches from the surface of the CIR- HFMS-2S layer were measured as 3.6% from sensor A, 3.35% from sensor B, and 3.30% from

sensor C. Despite the actual moisture content of CIR-HFMS-2S-emulsion layer being above 1.5%, the base HMA overlay was constructed after 37 days of curing. Figure 5-7 shows plots of temperature from three sensors embedded in the CIR-HFMS-2S-emulsion layer against air temperature from the weather station. As shown in Figure 5-7, as expected, temperature of CIR-HFMS-2S-emulsion layer was significantly higher than air temperature.

As shown in Figure 5-8 (a), using a portable TDR device, field moisture contents were measured from three different locations between 9:30 a.m. to 3:30 p.m. for 37 days between August 18th and September 24th, 2009. Three measurements by a portable TDR device were made from each of three locations and the average value was recorded for each day. Figure 5-9 shows plots of moisture contents measured between August 18th and September 24th, 2009.

As shown in Figure 5-8 (b), using nuclear gauge, field moisture contents were measured from three different locations between 9:00 a.m. to 9:30 a.m. for 6 days between August 19th and August 24th, 2009. A single measurement was made by nuclear gauge from each of three locations. Figure 5-10 shows plots of moisture contents measured between August 19th and August 24th, 2009.

Figure 5-11 shows plots of field moisture content measured by a potable TDR device (or by moisture sensors) against field moisture content measured by a nuclear gauge. It should be noted that the moisture contents measured using a portable TDR, a nuclear gauge, and moisture sensors represent the moisture contents between the surface and 1.5 inches to 2.0 inches from the surface and they were above the minimum moisture content of 1.5% required before an HMA overlay. As shown in Figure 5-11, overall, the

moisture content measured by a portable TDR device is higher than those measured by a nuclear gauge but the moisture content measured by moisture sensors is lower than those measured by a nuclear gauge.

Figure 5-12 shows plots of field moisture content measured by a potable TDR against field moisture content measured by moisture sensors. As shown in Figure 5-12, the moisture content measured by a portable TDR device is higher than ones measured by moisture sensors.

5.2 Measurement of Density and Stiffness

The density and stiffness of the CIR-HFMS-2S-emulsion layer was measured using a nuclear gauge and geo-gauge, respectively, throughout the duration of curing. As shown in Figure 5-13, the density and stiffness were measured at three different locations: 1) A (Sensor A), 2) B (Sensor B) and 3) C (Sensor C).

5.2.1 Density Measurements using Nuclear Gauge

A nuclear gauge was used to measure densities of CIR-HFMS-2S-emulsion layer. As shown in Figure 5-14, density values were measured four times between August 19th and August 24th, 2009 from three locations between 9:00 a.m. to 9:30 a.m. The density value of CIR-HFMS-2S layer slightly increased as the curing time increased at the early stage of curing and remained constant in the remaining curing period.

5.2.2 Stiffness Measurements using Geo-Gauge

The geo-gauge was used to measure the stiffness of CIR-HFMS-2S-emulsion layer. The geo-gauge is a portable device capable of measuring the in-situ stiffness of soil. As shown in Figure 5-15, stiffness was measured thirteen times between August

18th and September 24th, 2009 from three locations (all stiffness measurements were made between 9:30 a.m. to 3:30 p.m.). Right after the construction, the stiffness of CIR-HFMS-2S-emulsion layer increased in three days. However, after reaching the stiffness of approximately 30 MN/m, the stiffness remained constant for one month. Figure 5-16 shows plots of density measured by a nuclear gauge against stiffness measured by geo-gauge at three different locations between August 19th and August 21st, 2009. Figure 5-17 shows there too be little correlation between stiffness and moisture content measured by the embedded sensors. Moisture contents above 7% were considered outliers for Figure 5-17.

Figure 5-1. Locations of CIR-HFMS-2S-emulsion project sites in Clinton County

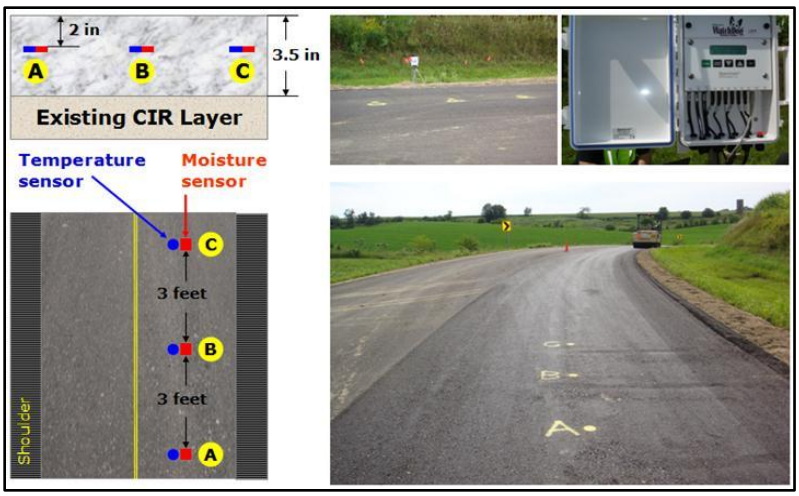

Figure 5-2. Embedded moisture and temperature sensors installed 2.0 inches from the surface of the CIR- HFMS-2S layer

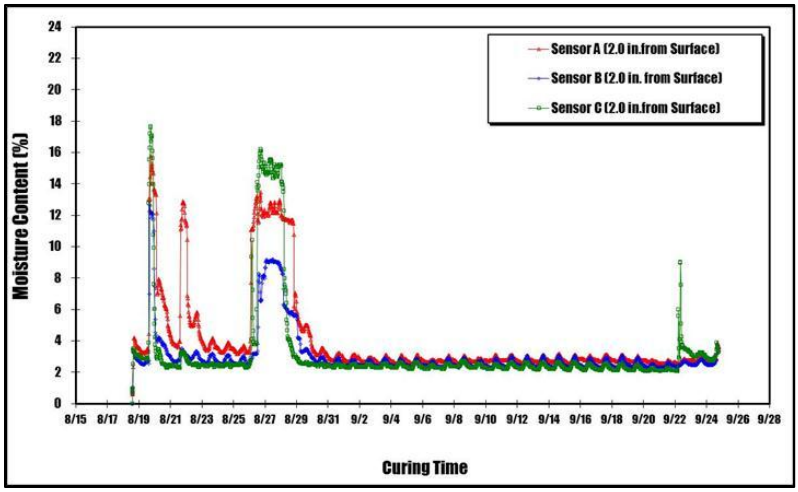

Figure 5-3. Plots of moisture contents against the curing period from three sensors embedded in the CIR-HMFS-2S layer

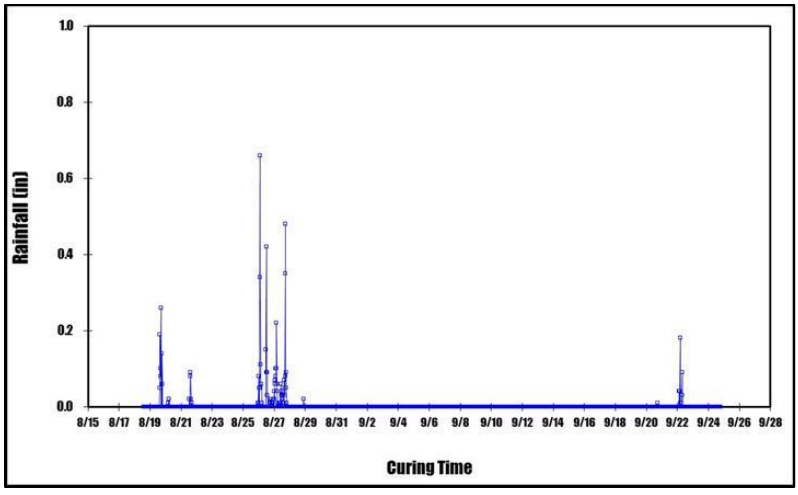

Figure 5-4. Plots of rainfalls against the curing period from weather station device

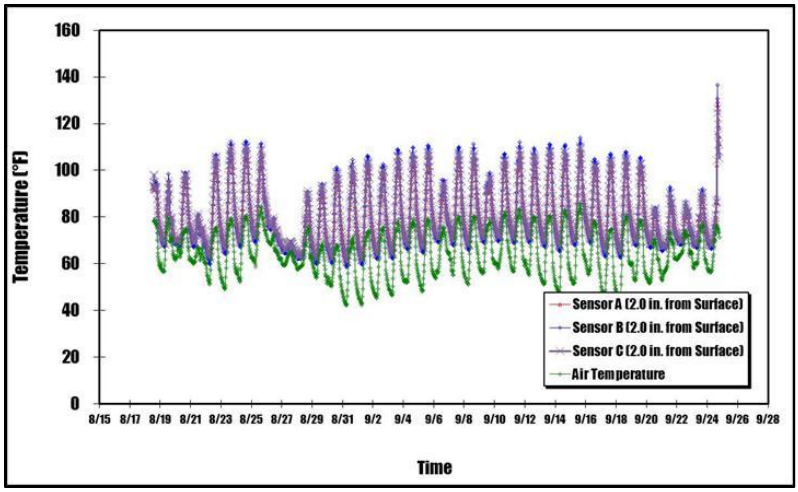

Figure 5-5. Plots of temperature against the curing period from three sensors embedded in the CIR-HFMS-2S-emulsion layer and air temperature from weather station device

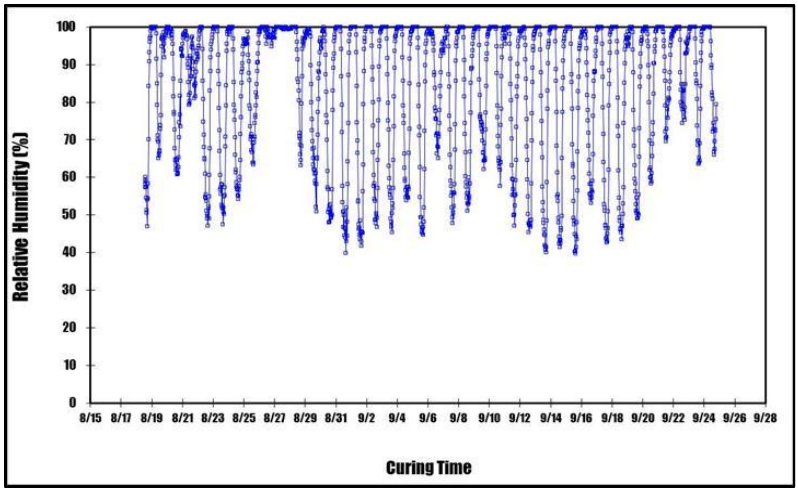

Figure 5-6. Plots of humidity against the curing period from weather station device

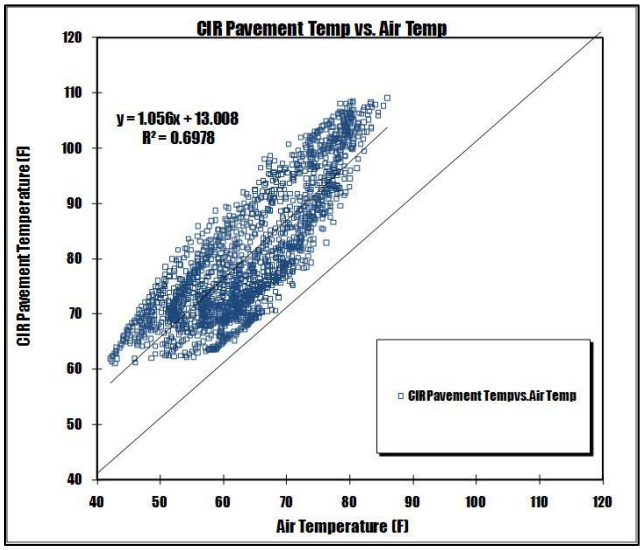

Figure 5-7. Plots of temperature from three sensors embedded in the CIR-HFMS-2S-emulsion layer against air temperature from weather station device

(a) Portable TDR device (b) Nuclear gauge

Figure 5-8. Moisture measurements for each of three locations using a portable TDR and nuclear gauge in CIR-HFMS-2S-emulsion project site

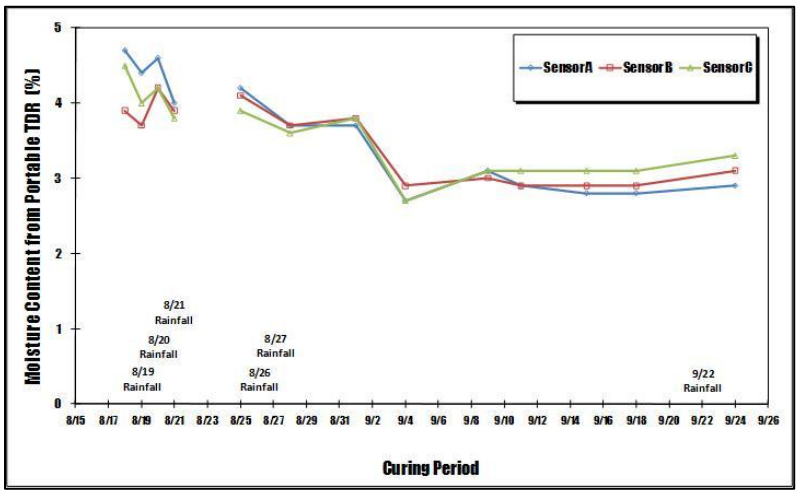

Figure 5-9. Plots of field moisture contents measured by a portable TDR in CIR-HFMS-2S-emulsion project site

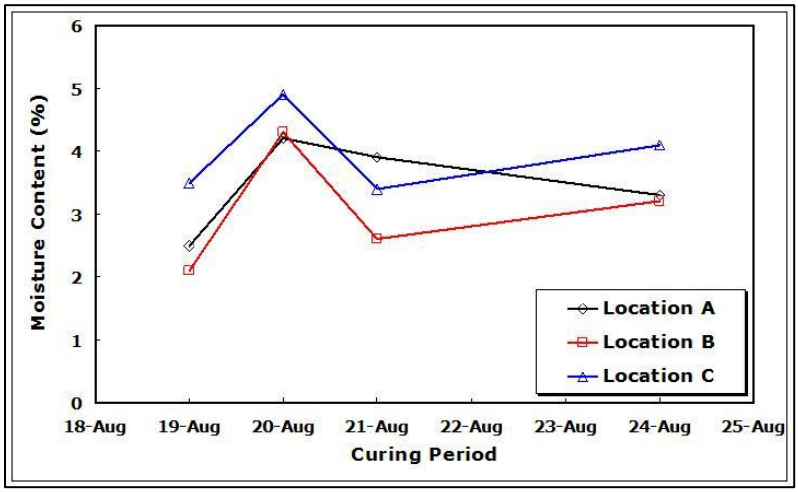

Figure 5-10. Plots of field moisture contents measured by nuclear gauge in CIR-HFMS-2S-emulsion project site

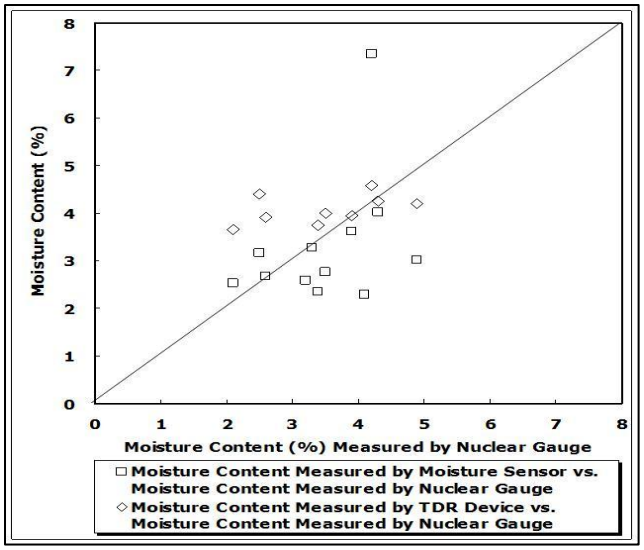

Figure 5-11. Plots of field moisture content measured by a potable TDR (or moisture sensors) against field moisture content measured by a nuclear gauge

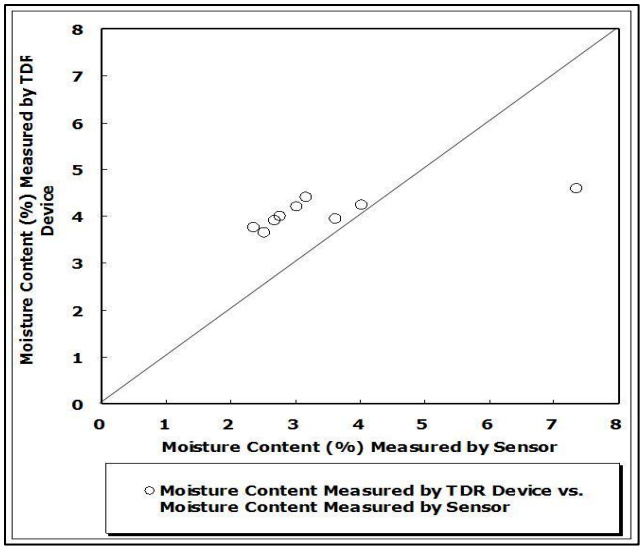

Figure 5-12. Plots of field moisture content measured by a potable TDR against field moisture content measured by moisture sensors

Figure 5-13. Location of three spots for measuring density and stiffness

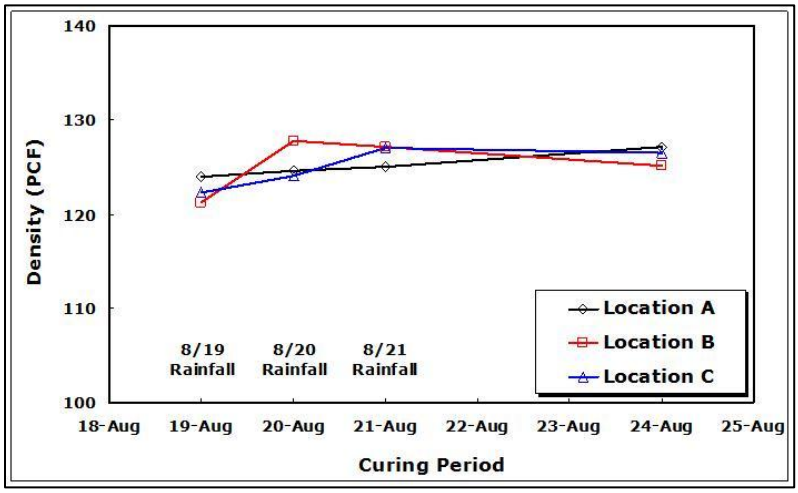

Figure 5-14. Plots of density against curing period from three locations in the CIR-HFMS-2S-emulsion layer

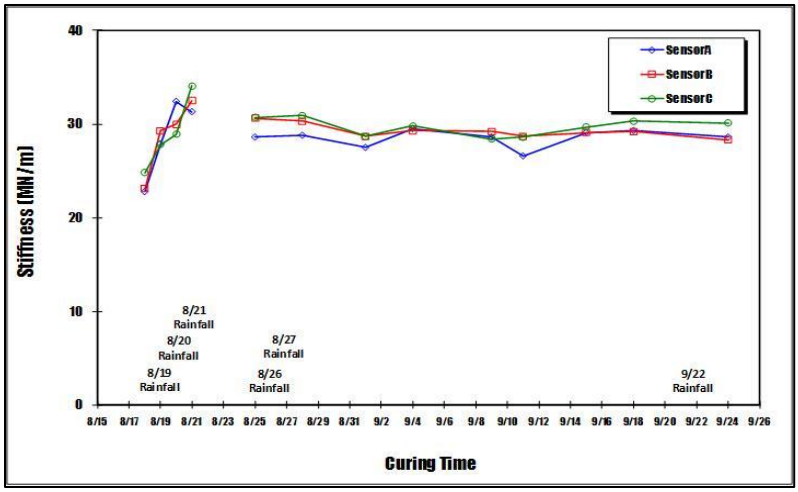

Figure 5-15. Plots of stiffness against the curing period from three locations in the CIR-HFMS-2S-emulsion layer

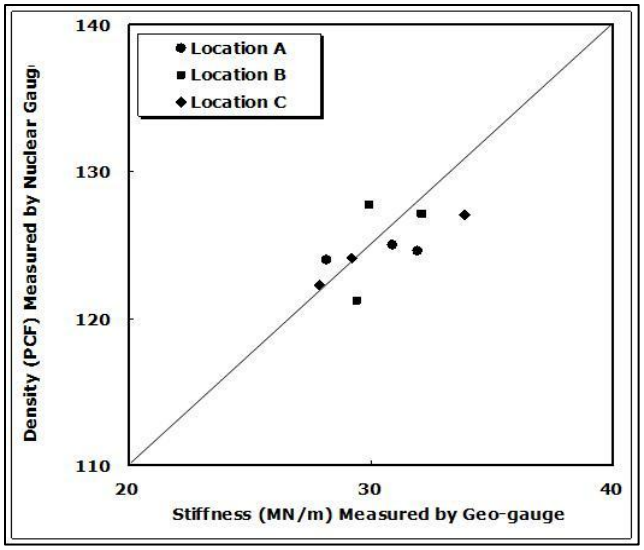

Figure 5-16. Plots of density measured by a nuclear gauge against stiffness measured by geo-gauge at three different locations

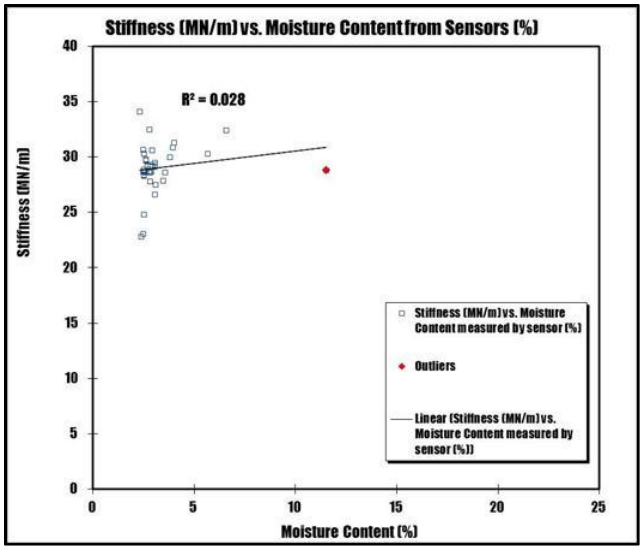

Figure 5-17. Plots of stiffness measured by a geo-gauge against moisture content measured by embedded sensors at three different locations

CHAPTER 6: MEASUREMENT OF MOISTURE CONTENT FROM CIR-FOAM PROJECT IN IOWA COUNTY

To measure the field moisture contents and temperature of CIR-foam layer, as shown in Figure 6-1, cold in-place recycling with foamed asphalt (CIR-foam) project site in Iowa County was selected. The CIR-foam project site is located from West of North English on County Road F 67 to Keswick on County G 13, Iowa. 5.0-mile section of Country road F 67 and G 13 was rehabilitated from West of North English on County Road F 67 to Keswick on County G 13, Iowa between August 20th and September 16th, 2009.

6.1 Measurement of Field Moisture Content and Temperature

To monitor actual moisture contents of the CIR-foam-emulsion layer in the field, as shown in Figure 6-2, three ECH2O moisture sensors and three temperature sensors were embedded at 2.0 inches from the surface of the CIR-foam layer. A weather station was also installed to collect air temperature, humidity, rainfall and wind speed.

Figure 6-3, Figure 6-4, Figure 6-5, and Figure 6-6 show plots of moisture content, rainfall, temperature, and humidity, respectively, measured during the curing time of 27 days when four rainfalls with a total amount of 4.65 inches have occurred. The moisture contents measured by three sensors peaked when there was a heavy rainfall on August 27. This supports that the moisture sensors are accurate. The moisture contents at 2.0 inches from the surface of the CIR-foam layer were measured as 2.74% from sensor A, 3.22% from sensor B, and 2.85% from sensor C. Despite the actual moisture content of

CIR-foam layer being above 1.5%, the base HMA overlay was constructed after 36 days of curing. Figure 6-7 shows plots of temperature from three sensors embedded in the CIR-foam layer against air temperature from weather station device. As shown in Figure 6-7, as expected, temperature of CIR-foam layer is higher than air temperature.

Using a portable TDR device, field moisture contents were measured from three different locations between 9:30 a.m. to 3:30 p.m. for 36 days between August 20th and September 14th, 2009. Two measurements by a potable TDR device were made from each of three locations and the average value was recorded. Figure 6-8 shows plots of moisture contents measured between August 20th and September 16th, 2009. As can be seen from Figure 6-8, the moisture content as measured by the TDR device continuously decreased despite the heavy rainfall on August 26 and 27. It indicates that the TDR device may not be accurate in measuring the moisture content of the CIR-foam layer.

Figure 6-9 shows plots of field moisture content measured by a potable TDR against field moisture content measured by moisture sensors. It should be noted that the moisture contents measured using a portable TDR and moisture sensors represent the moisture contents between the surface and 1.5 inches to 2.0 inches from the surface and they were above the minimum moisture content of 1.5% required before an HMA overlay. As shown in Figure 6-9, the moisture content measured by a portable TDR device is higher than ones measured by moisture sensors.

6.2 Stiffness Measurements using Geo-Gauge

The stiffness of the CIR-foam layer was measured using a geo-gauge throughout the duration of curing. The stiffness was measured at three different locations that were spaced at approximately 3 feet: 1) A (Sensor A), 2) B (Sensor B) and 3) C (Sensor C).

As shown in Figure 6-10, stiffness was measured thirteen times between August 20th and September 16th, 2009 from three locations (all stiffness measurements were made between 9:30 a.m. to 3:30 p.m.). Despite a heavy rainfall on August 27, the stiffness of CIR-foam layer steadily increased and stabilizing at between 25 and 30 MN/m as curing time increased. Figure 6-11 shows that stiffness and moisture content had little correlation.

Figure 6-1. Locations of CIR-foam project sites in Iowa County

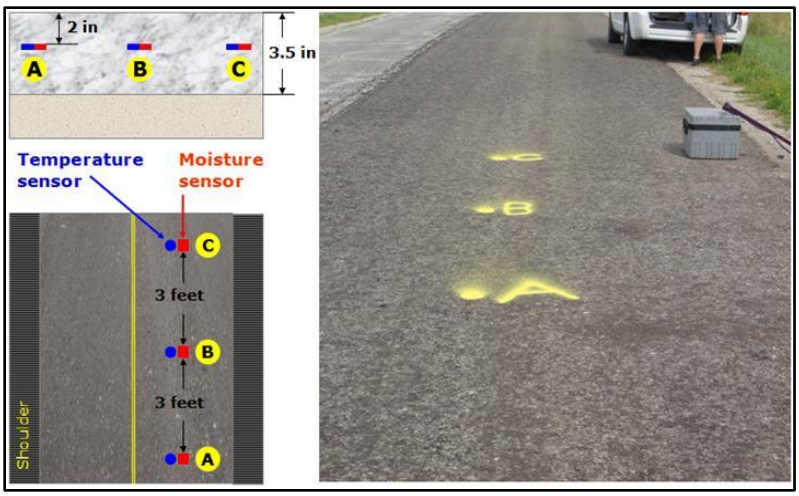

Figure 6-2. Embedded moisture and temperature sensors installed 2.0 inches from the surface of the CIR- foam layer

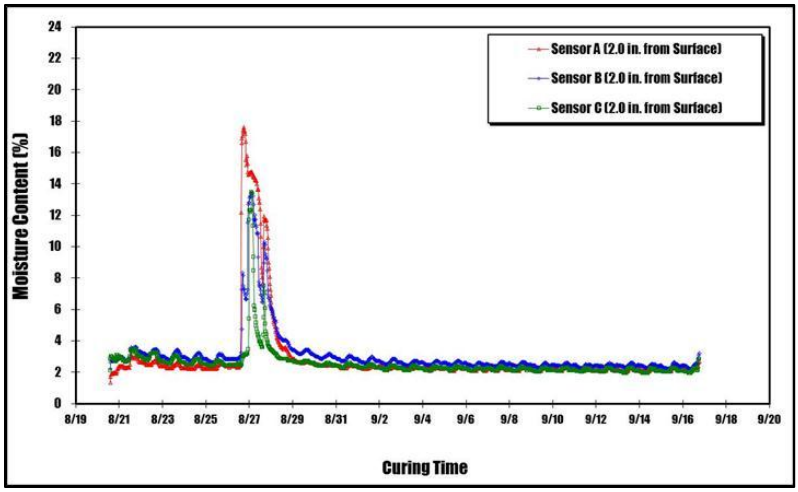

Figure 6-3. Plots of moisture contents against the curing period from three sensors embedded in the CIR-foam layer

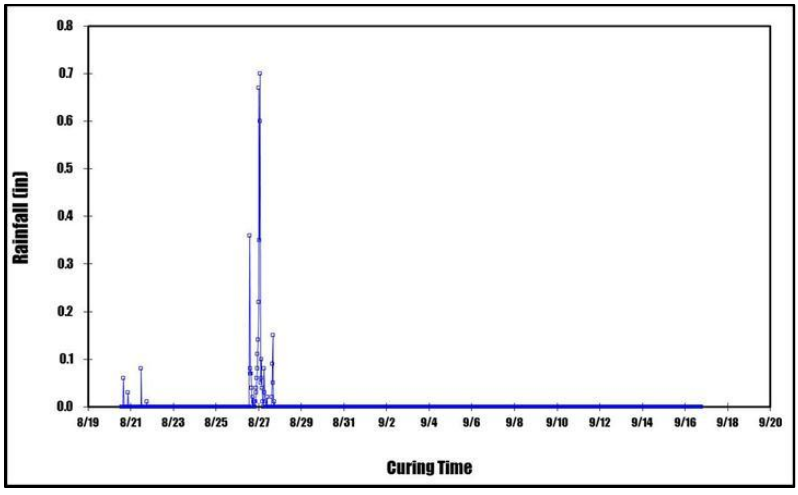

Figure 6-4. Plots of rainfalls against the curing period from weather station device

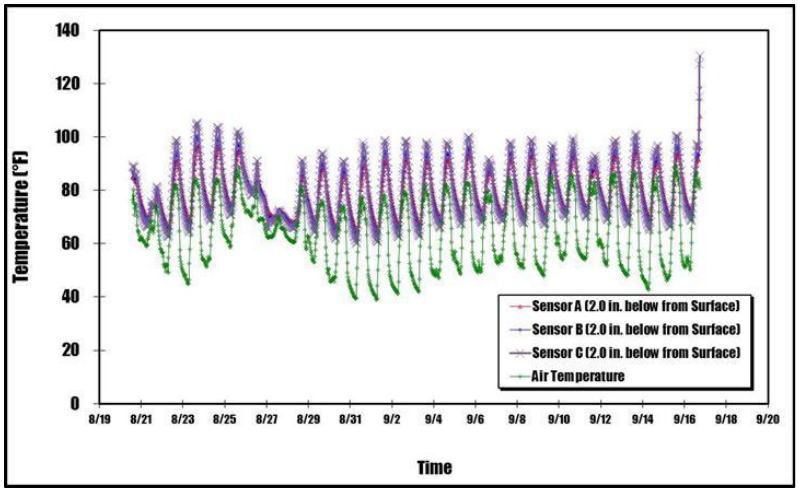

Figure 6-5. Plots of temperature against the curing period from three sensors embedded in the CIR-foam layer and air temperature from weather station device

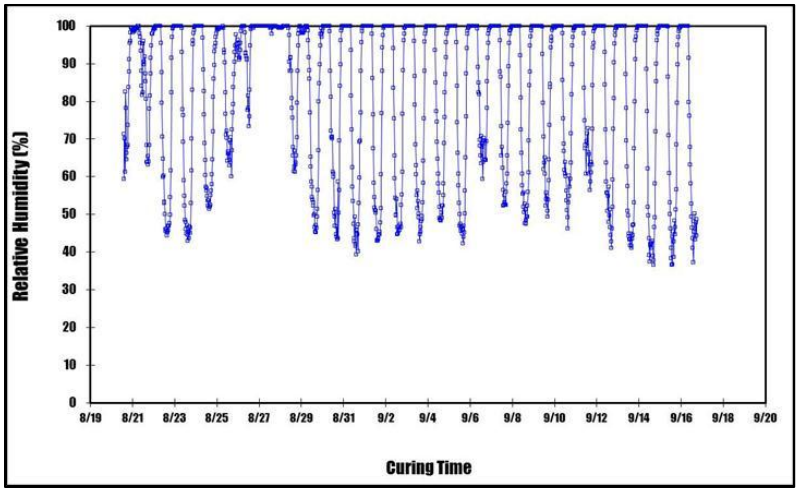

Figure 6-6. Plots of humidity against the curing period from weather station device

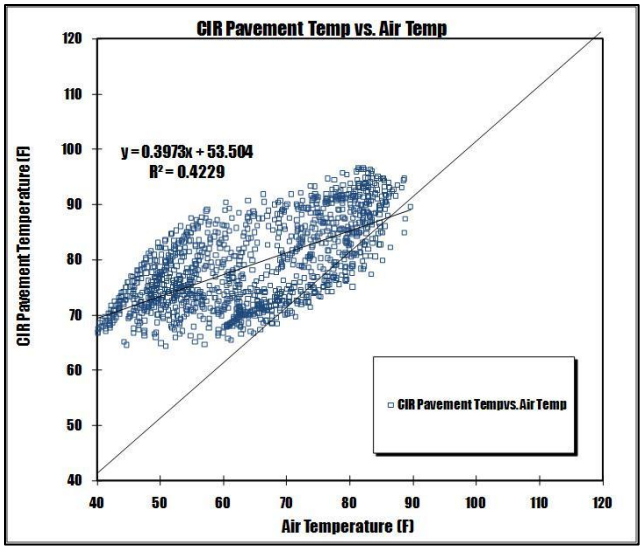

Figure 6-7. Plots of temperature from three sensors embedded in the CIR-foam layer against air temperature from weather station device

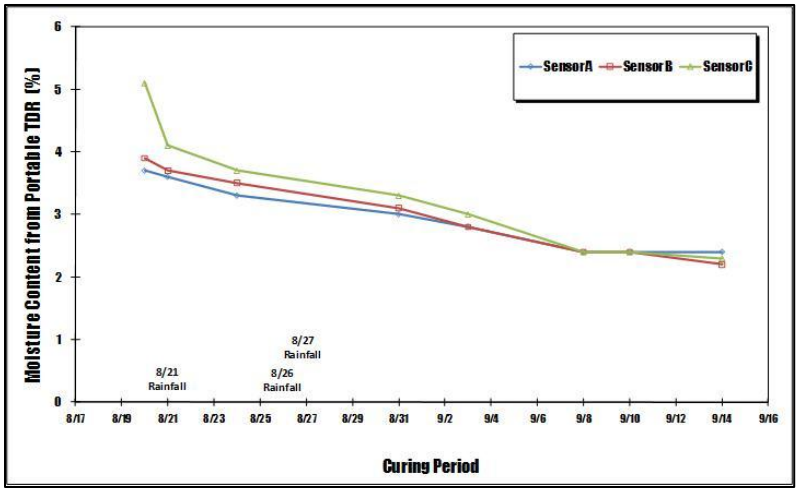

Figure 6-8. Plots of field moisture contents measured by a portable TDR in CIR-foam project site

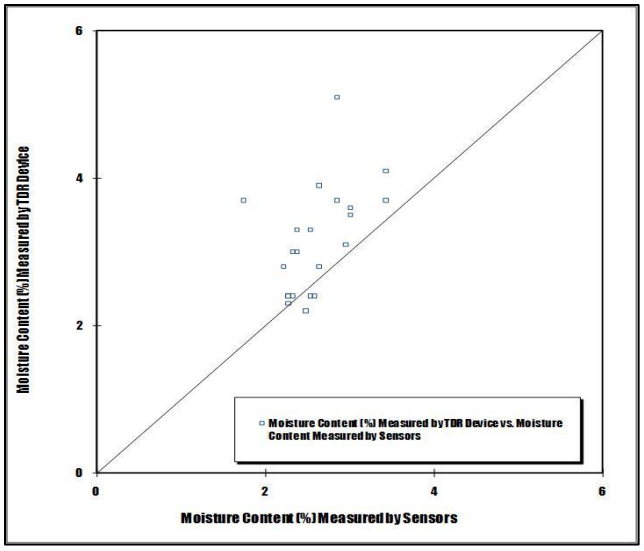

Figure 6-9. Plots of field moisture content measured by a potable TDR against field moisture content measured by moisture sensors

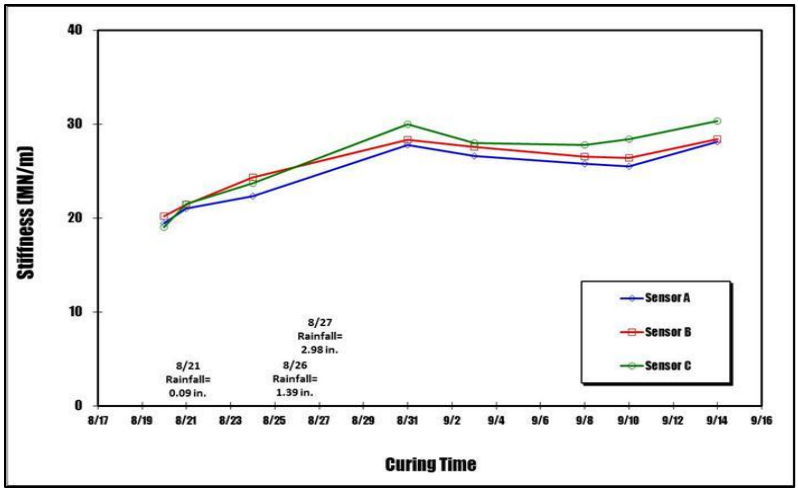

Figure 6-10. Plots of stiffness against the curing period from three locations in the CIR-foam layer

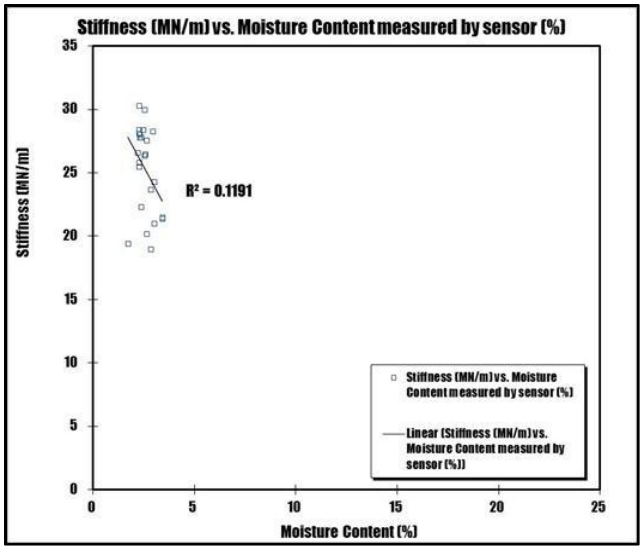

Figure 6-11. Plots of stiffness measured by a geo-gauge against moisture content measured by embedded sensors at three different locations

CHAPTER 7: MEASUREMENT OF MOISTURE CONTENT FROM CIR- FOAM PROJECT IN BENTON COUNTY

To measure the field moisture contents and temperature of CIR-foam layer, as shown in Figure 7-1, CIR-foam project site in Benton County was selected. The CIR-foam project site is located on highway 30 and was rehabilitated between June 3rd and June 30th 2010.

7.1 Measurement of Field Moisture Content and Temperature

To monitor actual moisture contents of the CIR-foam layer in the field, as shown in Figure 7-2, three ECH2O moisture sensors and three temperature sensors were embedded at 2.0 inches from the surface of the CIR-foam layer. A weather station was also installed to collect air temperature, humidity, rainfall and wind speed.

Figure 7-3, Figure 7-4, Figure 7-5, and Figure 7-6 show plots of moisture content, rainfall, temperature, and humidity, respectively, measured during the curing duration of 28 days when eighteen rainfalls with a total amount of 7.81 inches have occurred. Due to the heavy rainfall throughout the curing period, the moisture contents remained high from 4% to 24%. The moisture contents before the intermediate HMA overlay were measured at 8.9% from sensor A, 3.6% from sensor B, and 4.45% from sensor C. Despite the actual moisture contents of CIR-foam layer remaining above 1.5%, the intermediate HMA overlay was constructed after 28 days of curing. Figure 7-7 shows plots of temperature from three sensors embedded in the CIR-foam layer against air temperature

from the weather station. As shown in Figure 7-7, as expected, temperature of CIR-foam layer was significantly higher than air temperature.

Using a portable TDR device, field moisture contents were measured from three different locations between 9:30 a.m. to 3:30 p.m. for 18 days between June 3rd and June 21st, 2010. Three measurements by a portable TDR device were made from each of three locations and the average value was recorded. Figure 7-8 shows plots of moisture contents measured between June 3rd and June 21st, 2010. As can be seen from Figure 7-8, the moisture content remained high between 14 to 28% and it stabilized at around 14% as the curing time increased.

Figure 7-9 shows plots of field moisture content measured by a potable TDR against field moisture content measured by moisture sensors. As shown in Figure 7-9, the moisture content measured by a portable TDR device were significantly higher than ones measured by moisture sensors. It should be noted that the moisture contents measured were above the minimum moisture content of 1.5% required before an HMA overlay.

7.2 Stiffness Measurements using Geo-Gauge

The stiffness of the CIR-foam layer was measured using a geo-gauge throughout the duration of curing. The stiffness was measured at three different locations: 1) A (Sensor A), 2) B (Sensor B) and 3) C (Sensor C).

The geo-gauge was used to measure the stiffness of the CIR-foam layer. As shown in Figure 7-10, stiffness was measured six times between June 3rd and June 21st, 2010 from three locations (all stiffness measurements were made between 9:30 a.m. to 3:30 p.m.). Right after the construction, the stiffness of the CIR-foam layer increased up to 20 MN/m in three days. When there was continuous rainfall between June 8th and

15th, however, the stiffness decreased. Despite continuous rainfall, however, the stiffness remained above the initial stiffness right after the construction. Figure 7-11 shows there was little correlation between stiffness and moisture content. Moisture contents above 7% were considered high and outliers for Figure 7-11.

Figure 7-1. Locations of CIR-foam project site in Benton County

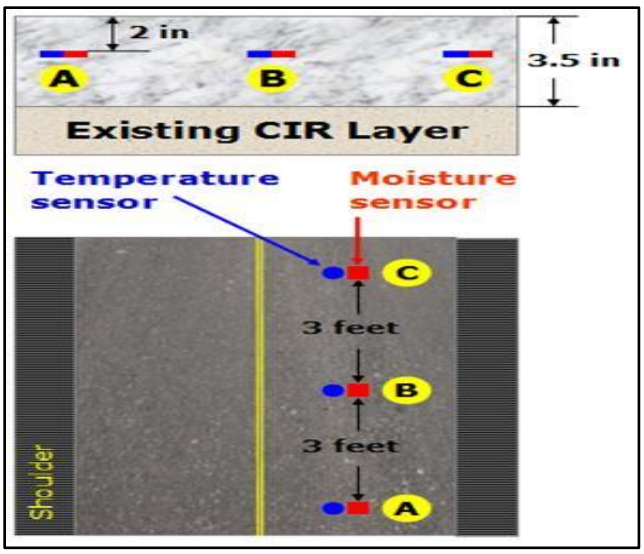

Figure 7-2. Embedded moisture and temperature sensors installed 2.0 inches from the surface of the CIR- foam layer

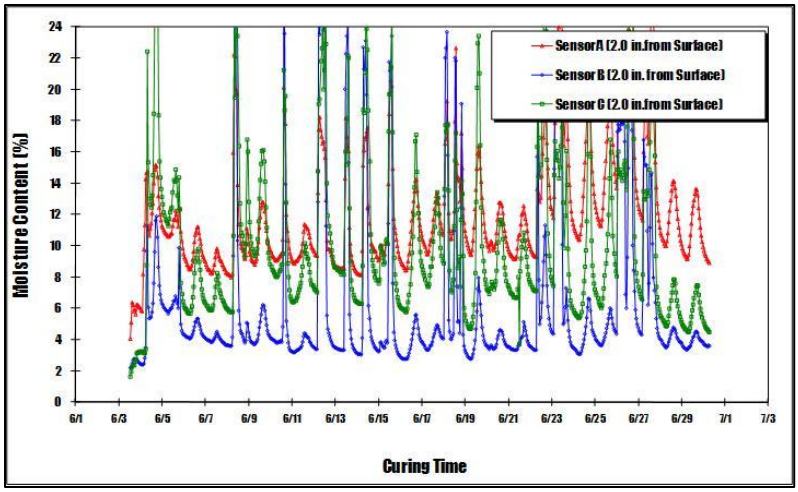

Figure 7-3. Plots of moisture contents against the curing period from three sensors embedded in the CIR-foam layer

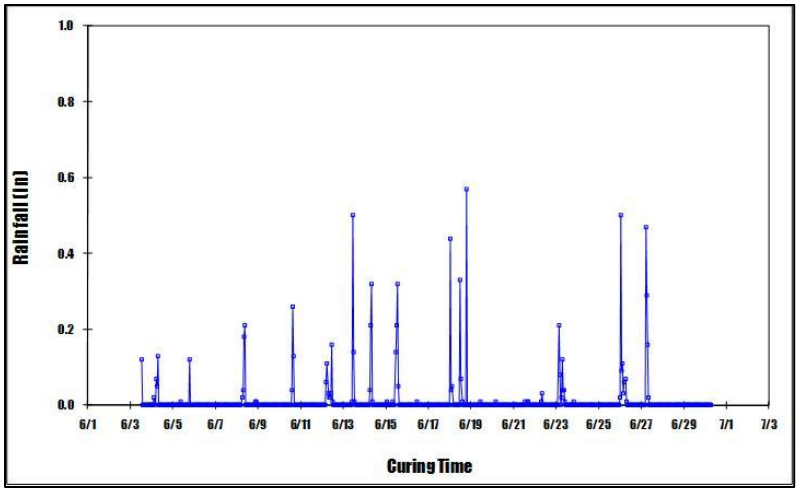

Figure 7-4. Plots of rainfalls against the curing period from weather station device

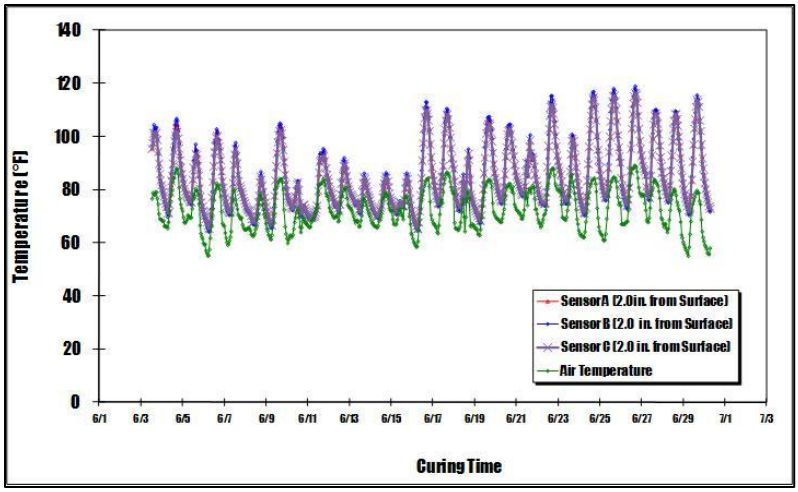

Figure 7-5. Plots of temperature against the curing period from three sensors embedded in the CIR-foam layer and air temperature from weather station device

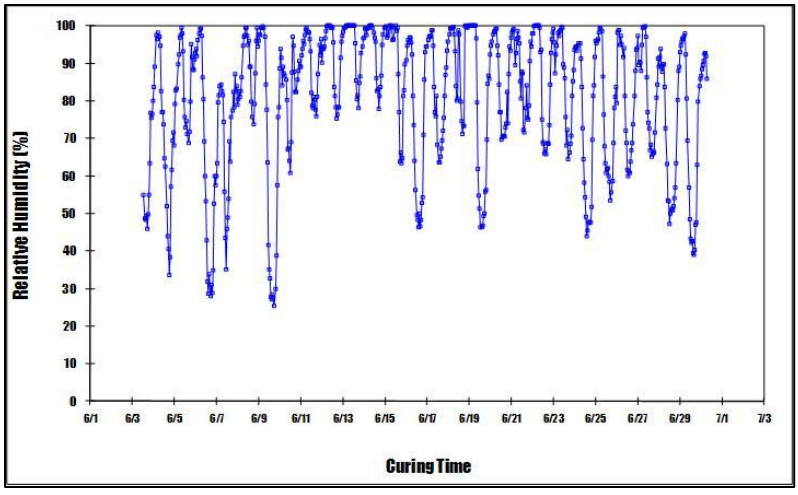

Figure 7-6. Plots of humidity against the curing period from weather station device

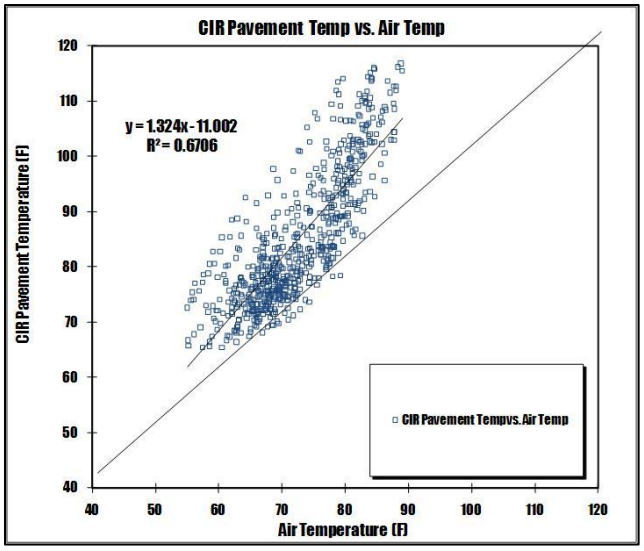

Figure 7-7. Plots of temperature from three sensors embedded in the CIR-foam layer against air temperature from weather station device

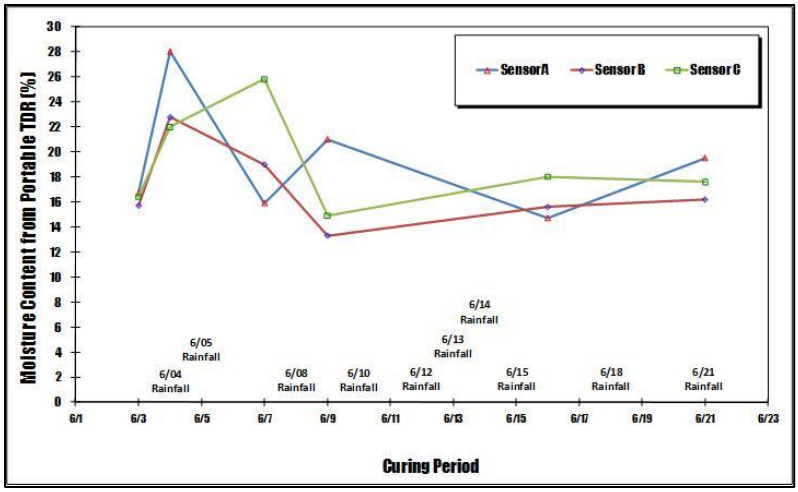

Figure 7-8. Plots of field moisture contents measured by a portable TDR in CIR-foam project site

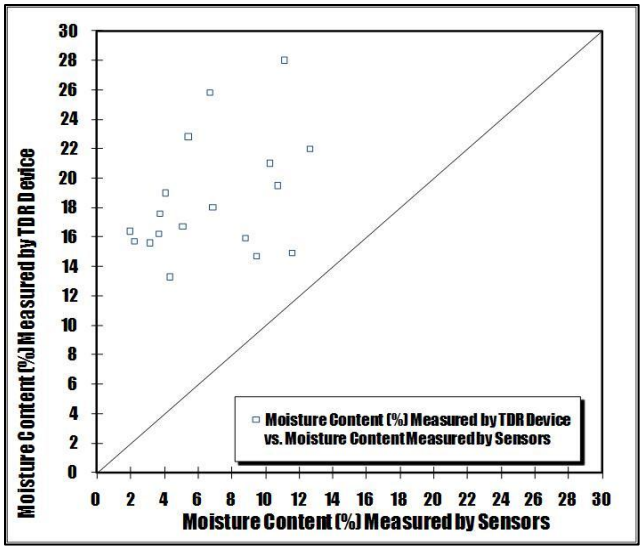

Figure 7-9. Plots of field moisture content measured by a potable TDR against field moisture content measured by moisture sensors

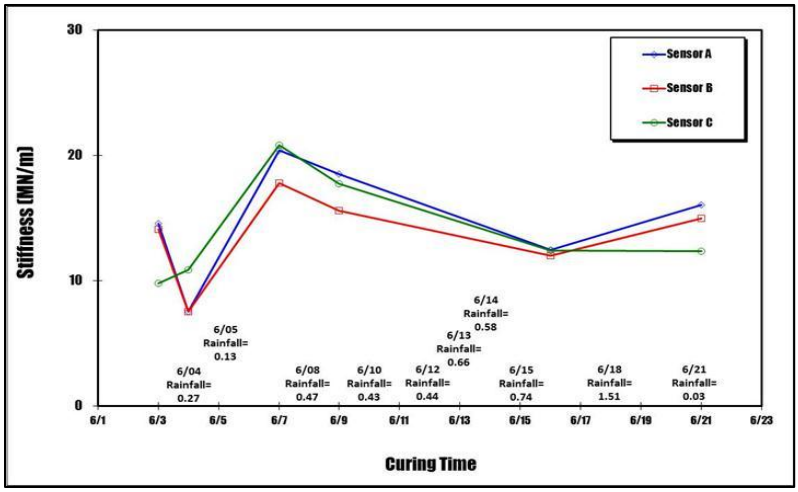

Figure 7-10. Plots of stiffness against the curing period from three locations in the CIR-foam layer

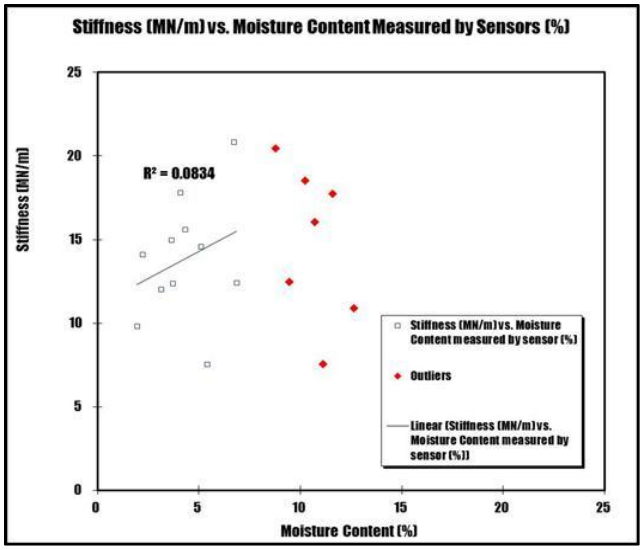

Figure 7-11. Plots of stiffness measured by a geo-gauge against moisture content measured by embedded sensors at three different locations

CHAPTER 8: MEASUREMENT OF MOISTURE CONTENT FROM CIR-FOAM PROJECT IN MARSHALL COUNTY

To measure the field moisture contents and temperature of CIR-foam layer, as shown in Figure 8-1, CIR-foam project site in Marshall County was selected. The CIR-foam project site is located on 330th Street west of Highway 14. The road was rehabilitated between August 23rd and September 20th, 2010.

8.1 Measurement of Field Moisture Content and Temperature

To monitor actual moisture contents of the CIR-foam layer in the field, as shown in Figure 8-2, three ECH2O moisture sensors and three temperature sensors were embedded at 2.0 inches from the surface of the CIR-foam layer. The temperature sensor at location B was damaged during the installation process. A weather station was also installed to collect air temperature, humidity, rainfall and wind speed.

Figure 8-3, Figure 8-4, Figure 8-5, and Figure 8-6 show plots of moisture content, rainfall, temperature, and humidity, respectively, measured during the curing duration of 28 days when four rainfalls with a total amount of 4.22 inches have occurred. Throughout the curing period, the moisture contents measured by three sensors were consistent with rainfalls. The moisture contents before the intermediate HMA overlay were measured at 2.68% from sensor A, 4.07% from sensor B, and 4.51% from sensor C. Despite the actual moisture contents of CIR-foam layer remaining above 1.5%, the intermediate HMA overlay was constructed after 28 days of curing. Figure 8-7 shows plots of temperature from two sensors embedded in the CIR-foam layer against air temperature

from the weather station. As shown in Figure 8-7, as expected, temperature of the CIR-foam layer was significantly higher than air temperature.

As shown in Figure 8-8, using a portable TDR device, field moisture contents were measured from three different locations between 9:30 a.m. to 3:30 p.m. for 14 days between August 25th and September 8th, 2010. Three measurements by a portable TDR device were made from each of three locations and the average value was recorded. Figure 8-8 shows plots of moisture contents measured between August 25th and September 8th, 2010. Although there was no major rainfall until September 1, the moisture content measured by TDR device peaked at 28% on August 27 and decreased to 4% on September 2 right after the heavy rainfall. It support that the TDR device is not consistent with rainfalls.

As shown in Figure 8-9, using nuclear gauge, field moisture contents were measured from one location between 9:00 a.m. to 9:30 a.m. for 5 days between August 23rd and August 28th, 2010. As can be seen from Figure 8-9, the moisture content remained relatively constant between 2.5% and 4.0%. It is interesting to note that the moisture content increased on August 27 although there was no rainfall since construction

Figure 8-10 shows plots of field moisture content measured by a potable TDR device or moisture sensors against field moisture content measured by a nuclear gauge. It should be noted that the moisture contents measured using a portable TDR, a nuclear gauge, and moisture sensors represent the moisture contents between the surface and 1.5 inches to 2.0 inches from the surface and they were above the minimum moisture content of 1.5% required before an HMA overlay. As shown in Figure 8-10, overall, the moisture

contents measured by a portable TDR device or the moisture sensors were higher than those measured by a nuclear gauge.

Figure 8-11 shows plots of field moisture content measured by a potable TDR against field moisture content measured by moisture sensors. As shown in Figure 8-11, the moisture content measured by a portable TDR device is significantly higher than ones measured by moisture sensors.

8.2 Measurement of Density and Stiffness

The density and stiffness of the CIR-foam layer were measured using a nuclear gauge and geo-gauge, respectively, throughout the duration of curing. The stiffness was measured at three locations, while the density was measured at only one location.

8.2.1 Density Measurements using Nuclear Gauge

A nuclear gauge was used to measure densities of the CIR-foam layer. As shown in Figure 8-12, density values were measured six times between August 23rd and August 28th, 2010. The density value of CIR-foam layer slightly decreased as the curing time increased but increased at the last day of measurement.

8.2.2 Stiffness Measurements using Geo-Gauge

The geo-gauge was used to measure the stiffness of the CIR-foam layer. As shown in Figure 8-13, stiffness was measured six times between August 25th and September 13th, 2010 from three locations (all stiffness measurements were made between 9:30 a.m. to 3:30 p.m.). The stiffness of the CIR-foam layer remained constant during the early stage of curing from August 25 to September 9 but increased significantly above 20 MN/m when the stiffness was measured on September 13. Figure

8-14 shows plots of density measured by a nuclear gauge against stiffness measured by geo-gauge for August 25th, 2010 but there was no correlation between them likely due to a lack of data points. Figure 8-15 showed little correlation between stiffness and moisture content.

Figure 8-1. Location of CIR-foam project site in Marshall County

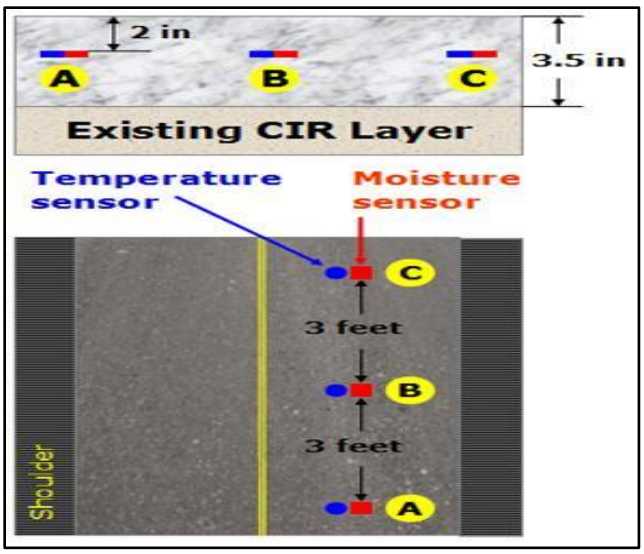

Figure 8-2. Embedded moisture and temperature sensors installed 2.0 inches from the surface of the CIR- foam layer

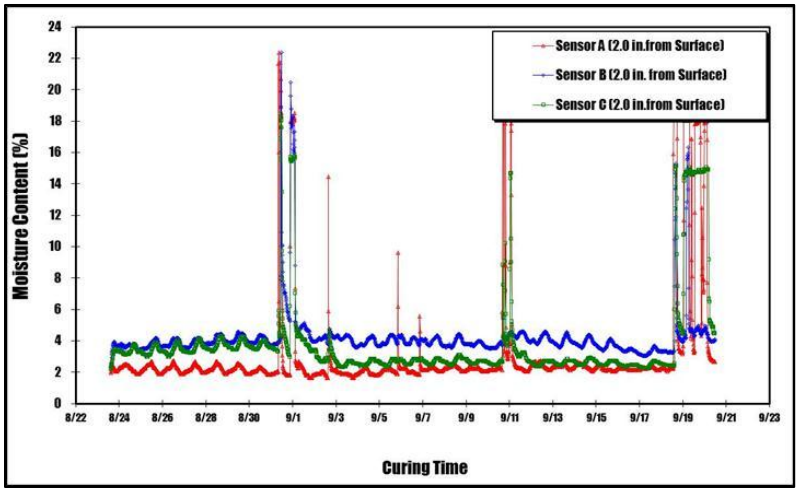

Figure 8-3. Plots of moisture contents against the curing period from three sensors embedded in the CIR-foam layer

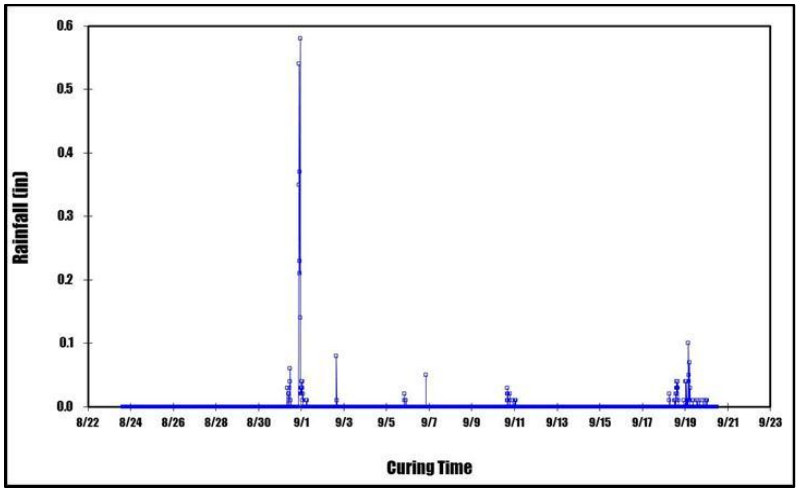

Figure 8-4. Plots of rainfalls against the curing period from weather station device

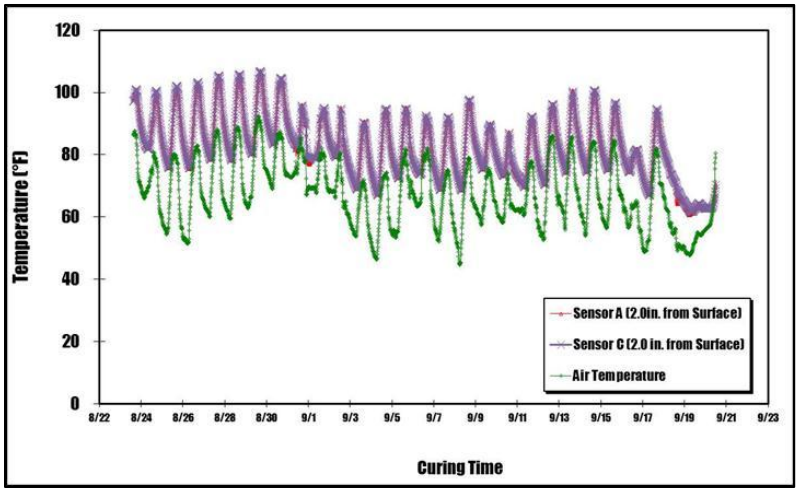

Figure 8-5. Plots of temperature against the curing period from two sensors embedded in the CIR-foam layer and air temperature from weather station device

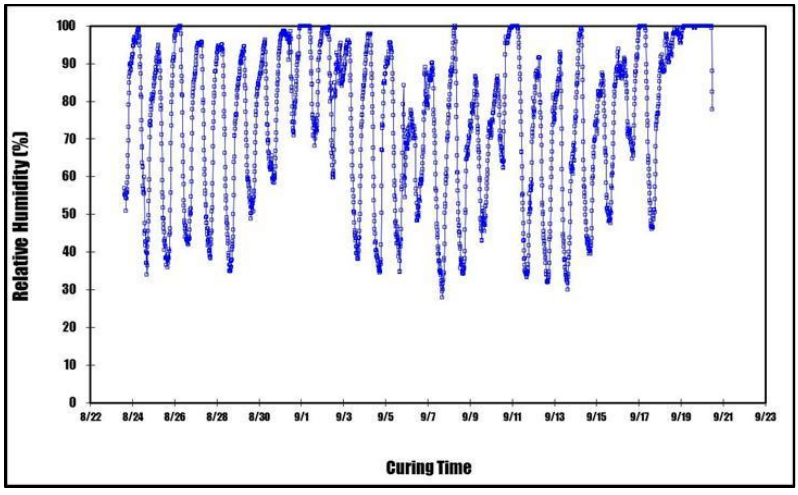

Figure 8-6. Plots of humidity against the curing period from weather station device

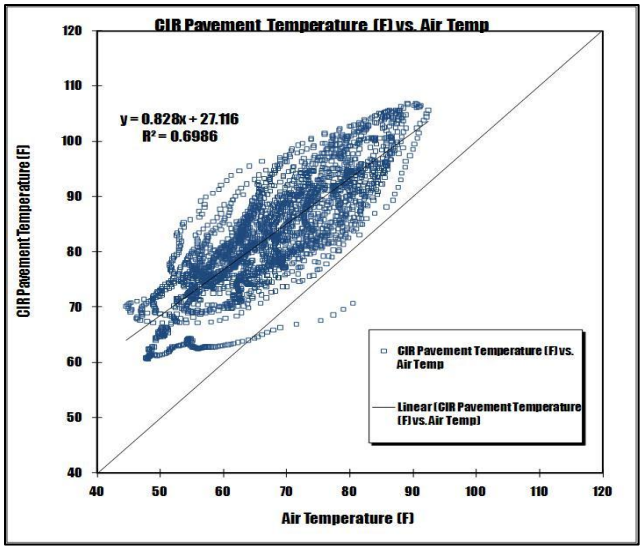

Figure 8-7. Plots of temperature from three sensors embedded in the CIR-foam layer against air temperature from weather station device

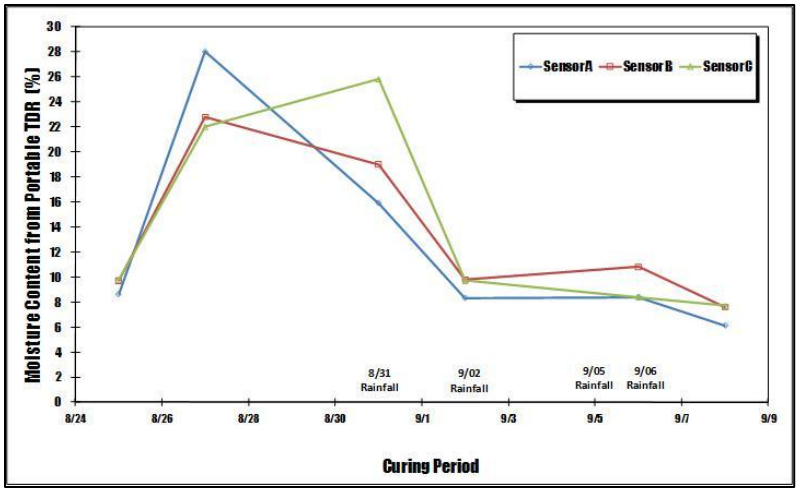

Figure 8-8. Plots of field moisture contents measured by a portable TDR in CIR-foam project site

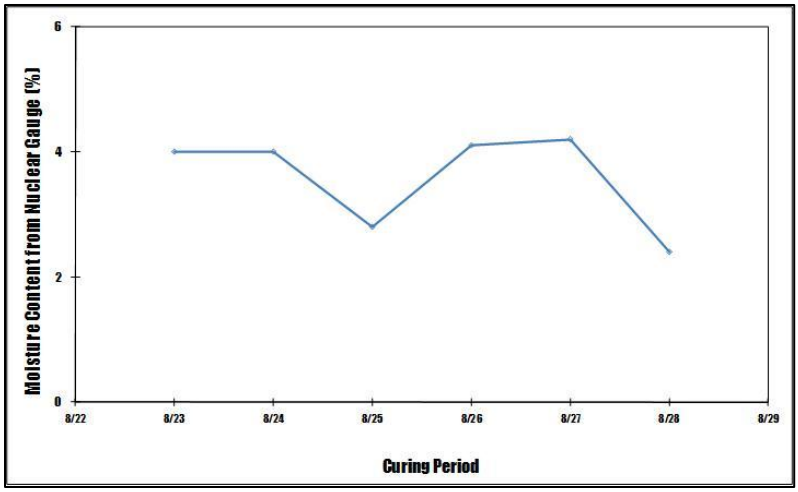

Figure 8-9. Plots of field moisture contents measured by nuclear gauge in CIR-foam project site

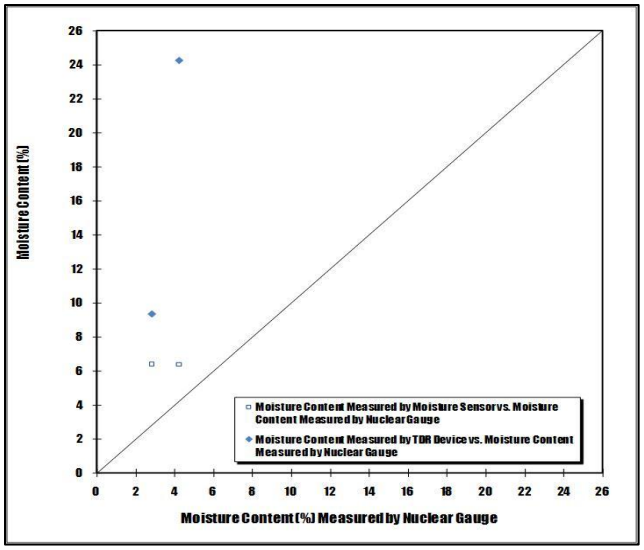

Figure 8-10. Plots of field moisture content measured by a potable TDR (or moisture sensors) against field moisture content measured by a nuclear gauge

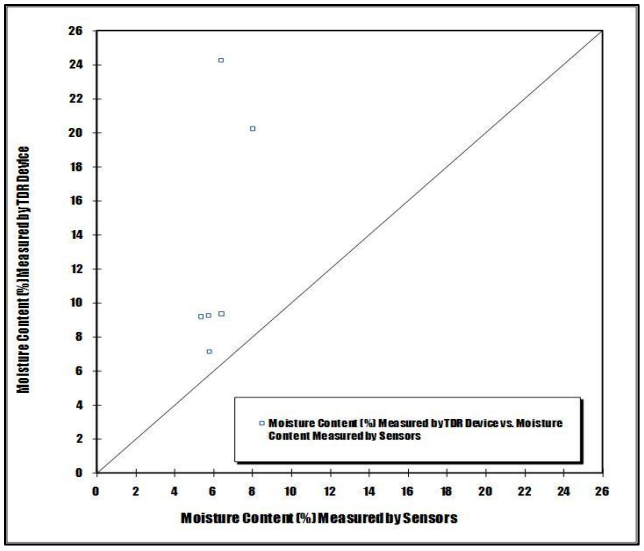

Figure 8-11. Plots of field moisture content measured by a potable TDR against field moisture content measured by moisture sensors

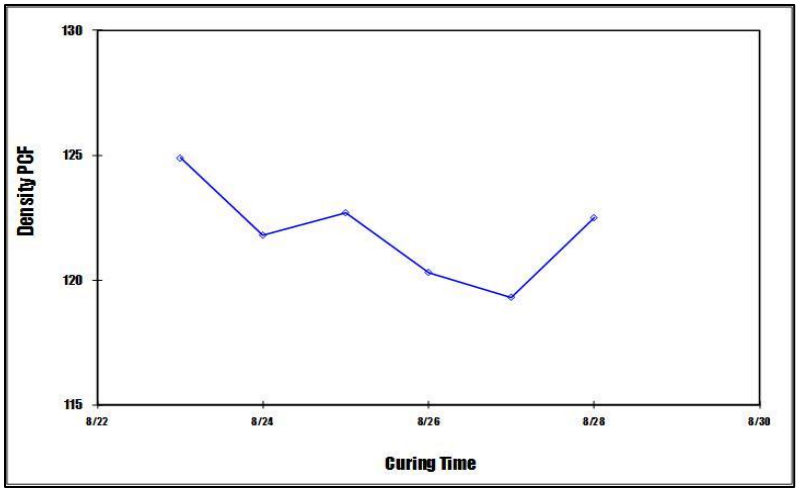

Figure 8-12. Plots of density against curing period from three locations in the CIR-foam layer

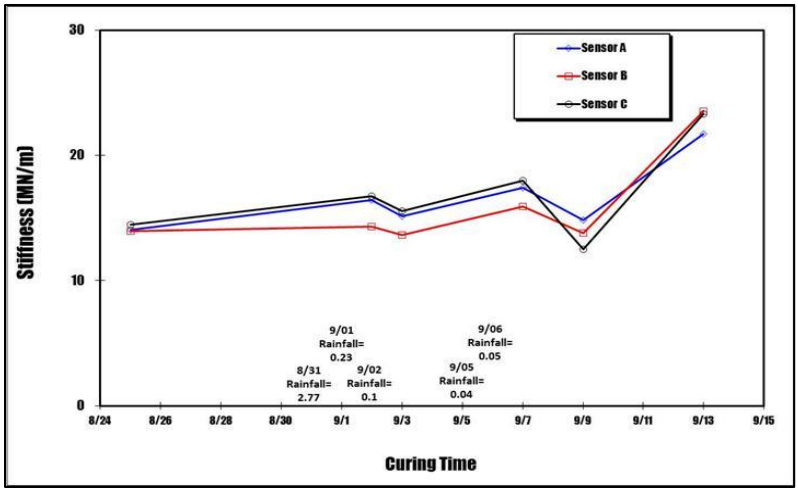

Figure 8-13. Plots of stiffness against the curing period from three locations in the CIR-foam layer

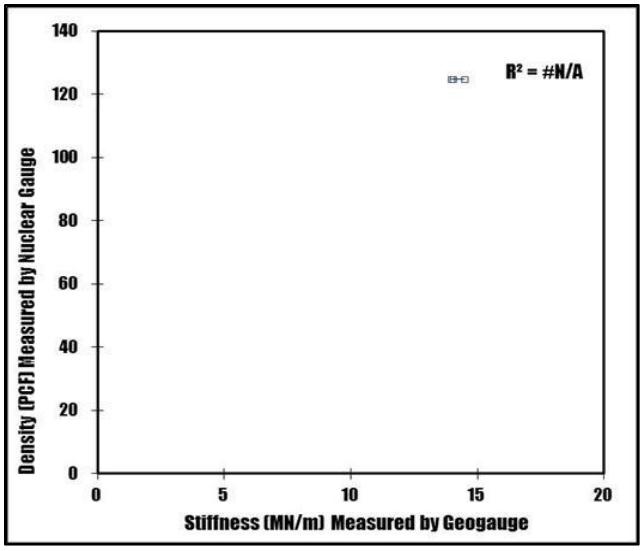

Figure 8-14. Plot of density measured by a nuclear gauge against stiffness measured by geo-gauge

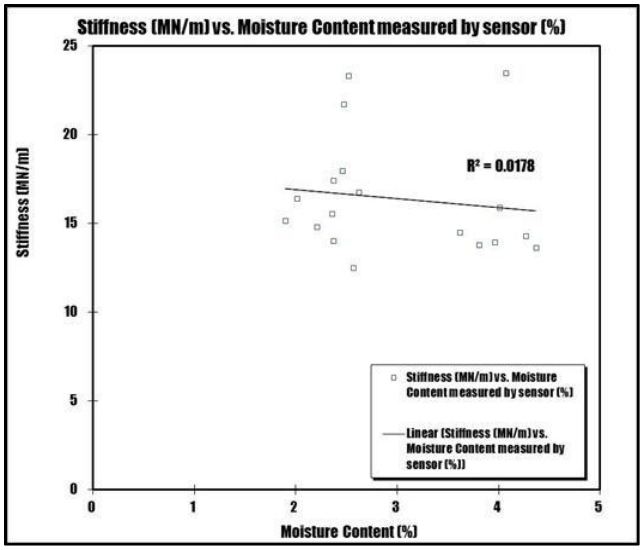

Figure 8-15. Plots of stiffness measured by a geo-gauge against moisture content measured by embedded sensors at three different locations

CHAPTER 9: MEASUREMENT OF MOISTURE CONTENT FROM CIR-FOAM PROJECT IN DELAWARE COUNTY

To measure the field moisture contents and temperature of CIR-foam layer, as shown in Figure 9-1, CIR-foam project site in Delaware County was selected. The CIR-foam project site is located on Floyd Rd. north of Highway 136 and was rehabilitated between September 14th and October 25th, 2010.

9.1 Measurement of Field Moisture Content and Temperature

To monitor actual moisture contents of the CIR-HFMS-2S-emulsion layer in the field, as shown in Figure 9-2, three ECH2O moisture sensors and three temperature sensors were embedded at 2.0 inches from the surface of the CIR-foam layer. A weather station was also installed to collect air temperature, humidity, rainfall and wind speed.

Figure 9-3, Figure 9-4, Figure 9-5, and Figure 9-6 show plots of moisture content, rainfall, temperature, and humidity, respectively, measured during the curing duration of 41 days when nine rainfalls with a total amount of 2.00 inches occurred. Due to a relatively small amount of rainfall, the moisture content measured by the moisture sensors A and C remained slightly above 2.0%. The moisture content measured by sensor B was consistently significantly higher and its values should be considered inaccurate. The moisture contents before the intermediate HMA overlay were measured at 2.5% from sensor A, 7.7% from sensor B, and 2.0% from sensor C. Despite the actual moisture contents of CIR-foam layer remaining above 1.5%, the intermediate HMA overlay was constructed after 35 days of curing. Figure 9-7 shows plots of temperature

from three sensors embedded in the CIR-foam layer against air temperature from the weather station. As shown in Figure 9-7, temperature of CIR-foam layer was slightly higher than air temperature because the weather was cooler in September. The TDR device was damaged and not used at this project site. Due to its inconsistencies in measurement the TDR device was not used for any project sites after this.

9.2 Stiffness Measurements using Geo-Gauge

The stiffness of the CIR-foam layer was measured using a geo-gauge throughout the curing period. The stiffness was measured at three different locations: 1) A (Sensor A), 2) B (Sensor B) and 3) C (Sensor C).

The geo-gauge was used to measure the stiffness of the CIR-foam layer. As shown in Figure 9-8, stiffness was measured six times between September 15th and September 27th, 2010 from three locations (all stiffness measurements were made between 9:30 a.m. to 3:30 p.m.). The stiffness right after the construction was relatively high at around 25 MN/m and the CIR layer did not gain stiffness throughout the curing period. It should be noted that there was no rain and the project was constructed in a late season when the pavement temperature was relatively low. Figure 9-9 shows that there was little correlation between stiffness and moisture content. Moisture contents above 7% were considered outliers for Figure 9-9.

Figure 9-1. Locations of CIR-foam project site in Delaware County

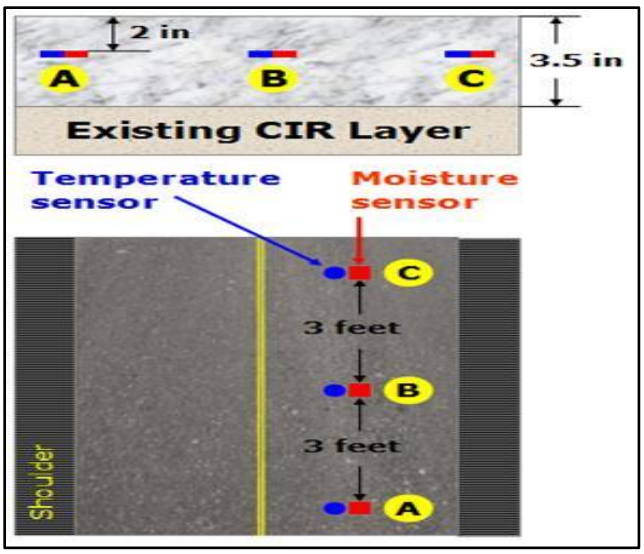

Figure 9-2. Embedded moisture and temperature sensors installed 2.0 inches from the surface of the CIR- foam layer

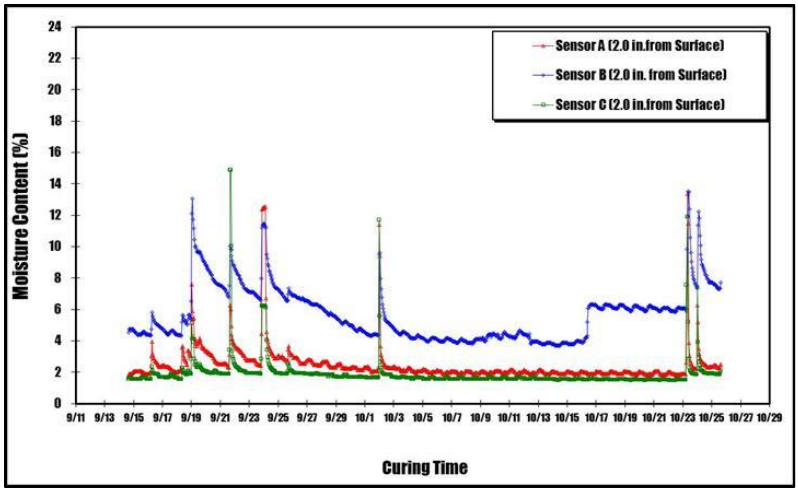

Figure 9-3. Plots of moisture contents against the curing period from three sensors embedded in the CIR-foam layer

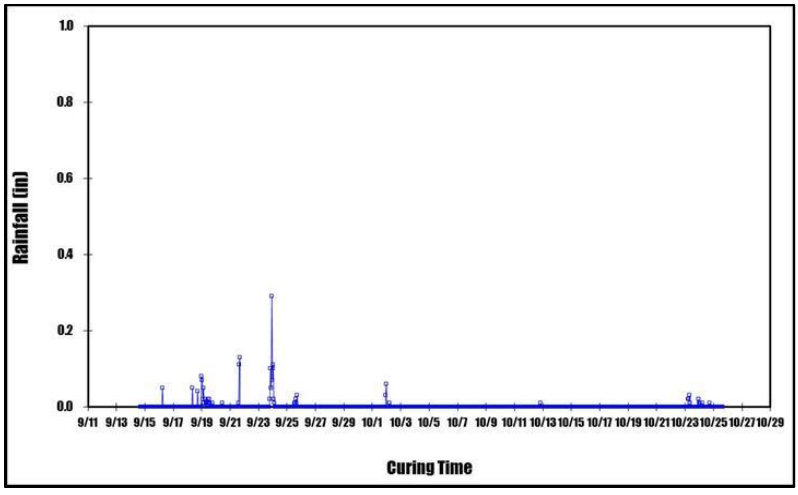

Figure 9-4. Plots of rainfalls against the curing period from weather station device

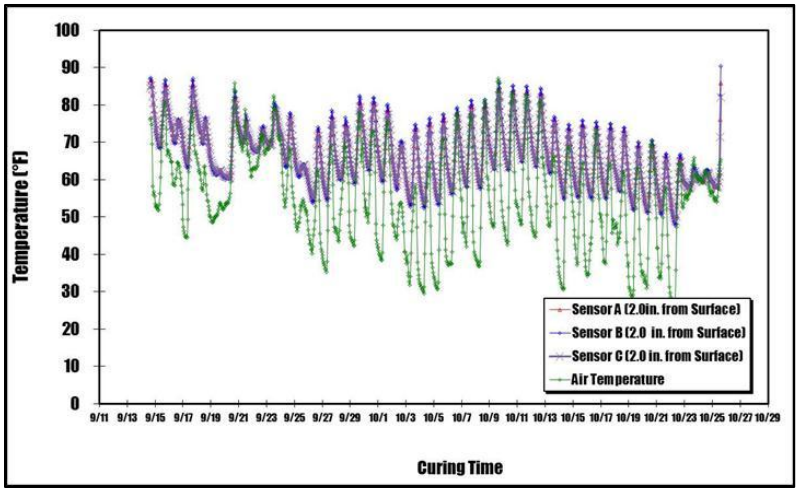

Figure 9-5. Plots of temperature against the curing period from three sensors embedded in the CIR-foam layer and air temperature from weather station device

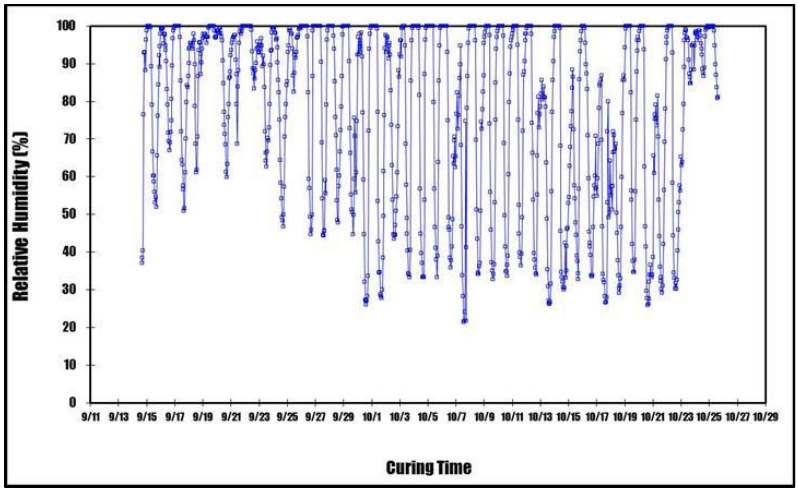

Figure 9-6. Plots of humidity against the curing period from weather station device

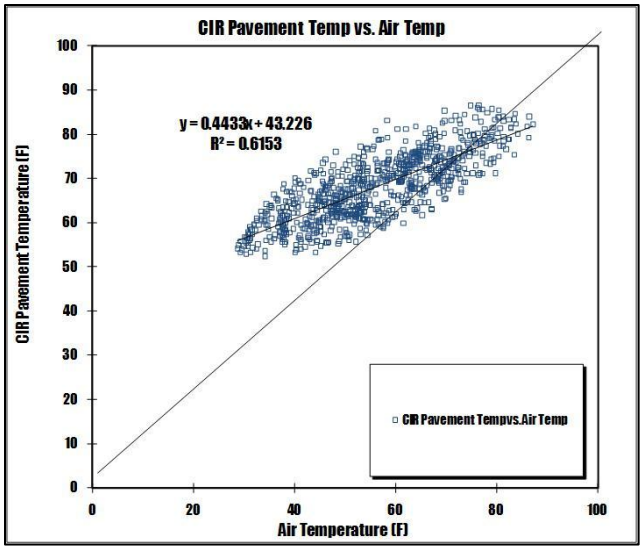

Figure 9-7. Plots of temperature from three sensors embedded in the CIR-foam layer against air temperature from weather station device

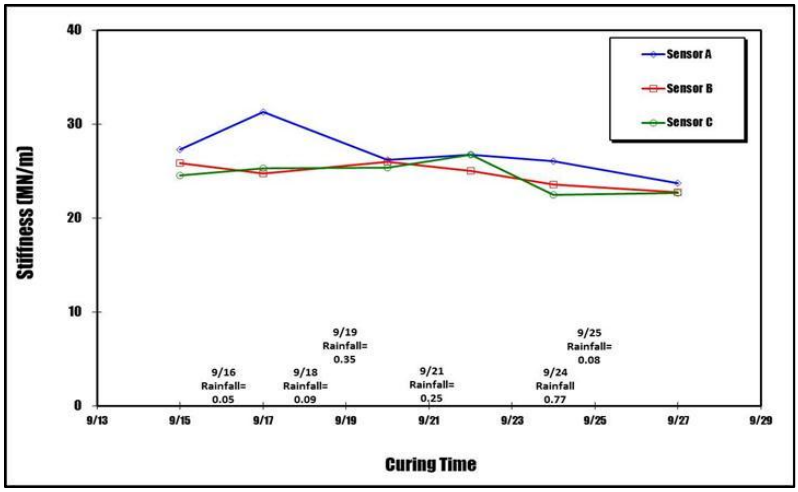

Figure 9-8. Plots of stiffness against the curing period from three locations in the CIR-foam layer

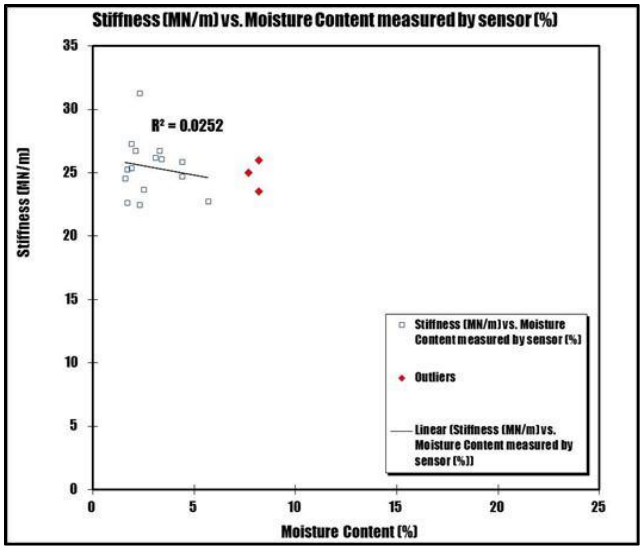

Figure 9-9. Plots of stiffness measured by a geo-gauge against moisture content measured by embedded sensors at three different locations

CHAPTER 10: MEASUREMENT OF MOISTURE CONTENT FROM CIR-FOAM PROJECT IN DELAWARE COUNTY

To measure the field moisture contents and temperature of CIR-foam layer, as shown in Figure 10-1, CIR-foam project site in Delaware County was selected. The CIR-foam project site is located on the corner of Canfield and Wellman Rd. The road was rehabilitated between July 11th and August 3rd, 2011.

10.1 Measurement of Field Moisture Content and Temperature

To monitor actual moisture contents of the CIR-foam layer in the field, as shown in Figure 10-2, three ECH2O moisture sensors and three temperature sensors were embedded at 2.0 inches from the surface of the CIR-foam layer. The moisture sensor at location A became disconnected after 4 days of curing. A weather station was also installed to collect air temperature, humidity, rainfall and wind speed.

Figure 10-3, Figure 10-4, Figure 10-5, and Figure 10-6 show plots of moisture content, rainfall, temperature, and humidity, respectively, measured during the curing duration of 24 days when seven rainfalls with a total amount of 8.05 inches have occurred. Throughout the curing period, the moisture contents measured by three sensors were consistent with rainfalls. The moisture contents before the intermediate HMA overlay were measured at 9.26% from sensor B and 9.42% from sensor C. Despite the actual moisture contents of CIR-foam layer remaining above 1.5%, the intermediate HMA overlay was constructed after 24 days of curing. Figure 10-7 shows plots of temperature from the three sensors embedded in the CIR-foam layer against air

temperature from the weather station. As shown in Figure 10-7, as expected, temperature of CIR-foam layer was significantly higher than air temperature.

Based off of portable TDR moisture data from the previous sites it was decided that the portable TDR device was unreliable for measuring moisture content of asphalt pavement. Furthermore, the TDR device was not used to measure moisture content on the 2 projects monitored in the summer of 2011.

As shown in Figure 10-8, using a nuclear gauge, field moisture contents were measured from one location between 9:00 a.m. to 9:30 a.m. for 5 days between July 11th and July 15th, 2011. As can be seen from Figure 10-8, the moisture content decreased slightly from 10.8% to 9.8%. It should be noted that these moisture contents are fairly high.

Figure 10-9 shows plots of field moisture content measured by the nuclear gauge against moisture contents measured by the embedded moisture sensors. It should be noted that the moisture contents measured using a nuclear gauge and moisture sensors represent the moisture contents between the surface and 1.5 inches to 2.0 inches from the surface and they were above the minimum moisture content of 1.5% required before an HMA overlay. As shown in Figure 10-9, overall, the moisture contents measured by the embedded sensors were higher than those measured by the nuclear gauge.

10.2 Measurement of Density and Stiffness

The density and stiffness of the CIR-foam layer were measured using a nuclear gauge and geo-gauge, respectively, throughout the duration of curing. The stiffness was measured at three locations, while the density was measured at only one location.

10.2.1 Density Measurements using Nuclear Gauge

A nuclear gauge was used to measure densities of the CIR-foam layer. As shown in Figure 10-10, density values were measured five times between July 11th and July 15th, 2011. The density value of CIR-foam layer increased at first then had a decrease on 7/13. The density then increased during the rest of the measurement period.

10.2.2 Stiffness Measurements using Geo-Gauge

The geo-gauge was used to measure the stiffness of the CIR-foam layer. In previous projects the stiffness was measured every 2-3 days during the curing period. For all projects during the summer of 2011 it was decided to measure stiffness every day in order to see a more detailed trend. As shown in Figure 10-11, stiffness was measured between July 11th and August 1st, 2011 from three locations (all stiffness measurements were made between 9:30 a.m. to 12:00 p.m.). The stiffness of the CIR-foam layer began by increasing after construction. There were some noticeable decreases in stiffness after rainfalls throughout the curing period with the most notable occurring a little after 7/14, in which a rainfall of 0.07 in. occurred. There was another dip beginning on 7/22 after an extremely large rainfall of 4.85 in. and again on 7/28 after a rainfall of 1.6 in. The stiffness tended to decrease after significant rain and then began to start increasing again each time. Overall, the stiffness fluctuated but was overlay occurred at roughly the same stiffness that the project bean at. Figure 10-12 shows plots of density measured by a nuclear gauge against stiffness measured by geo-gauge for July 11th, July 13th, July 14th and July 15th but there was little correlation between them. Figure 10-13 shows that there is little correlation between stiffness and moisture content. Moisture contents above

7.0% were considered outliers for the correlation and as seen every data point was an outlier.

Figure 10-1. Location of CIR-foam project site in Delaware County

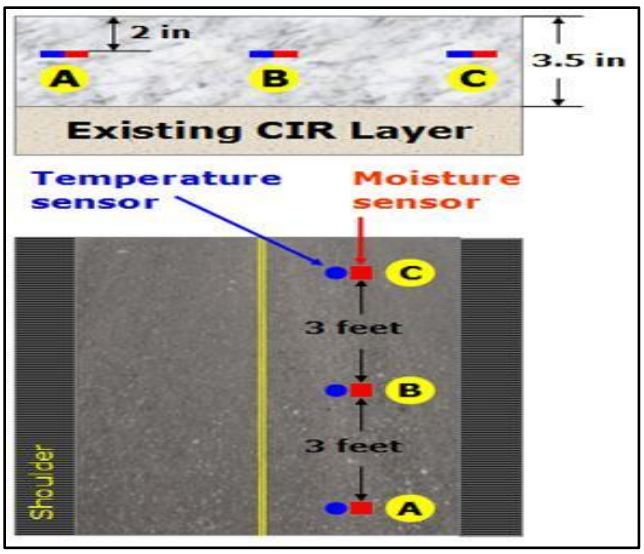

Figure 10-2. Embedded moisture and temperature sensors installed 2.0 inches from the surface of the CIR- foam layer

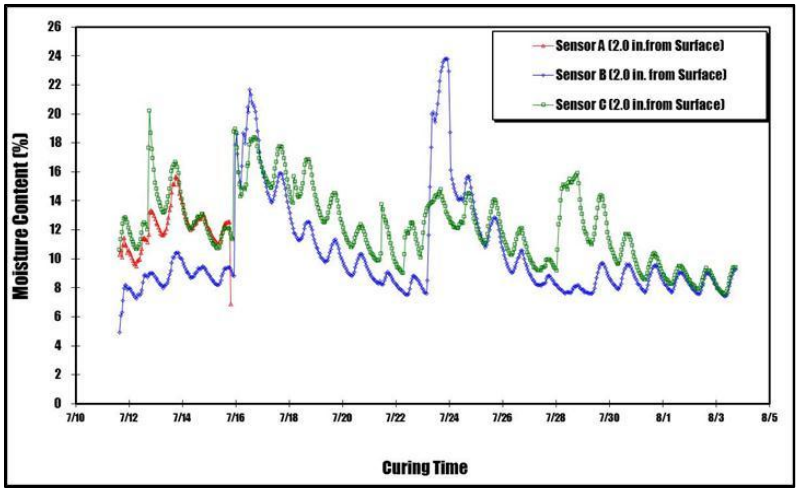

Figure 10-3. Plots of moisture contents against the curing period from three sensors embedded in the CIR-foam layer

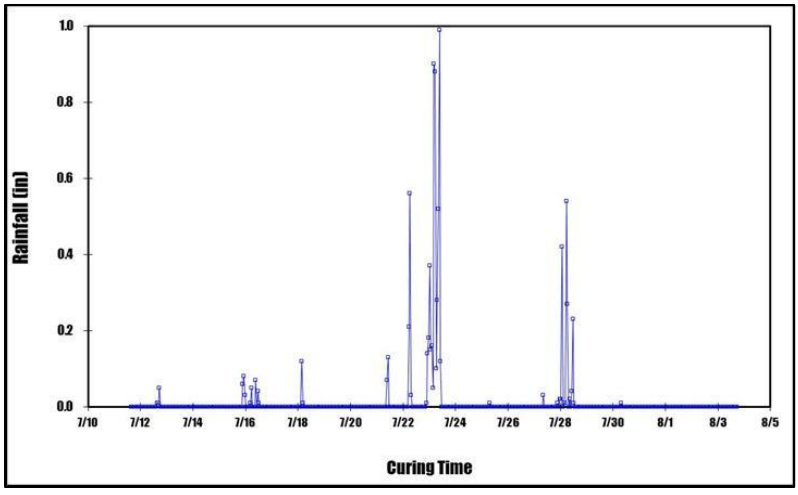

Figure 10-4. Plots of rainfalls against the curing period from weather station device

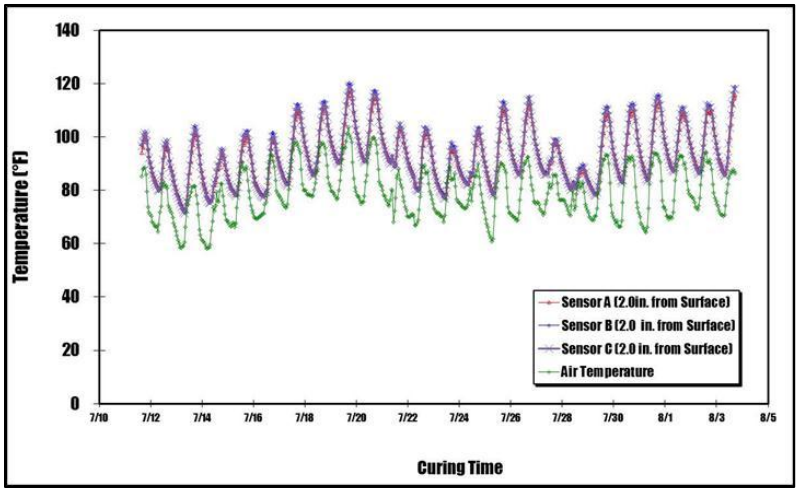

Figure 10-5. Plots of temperature against the curing period from three sensors embedded in the CIR-foam layer and air temperature from weather station device

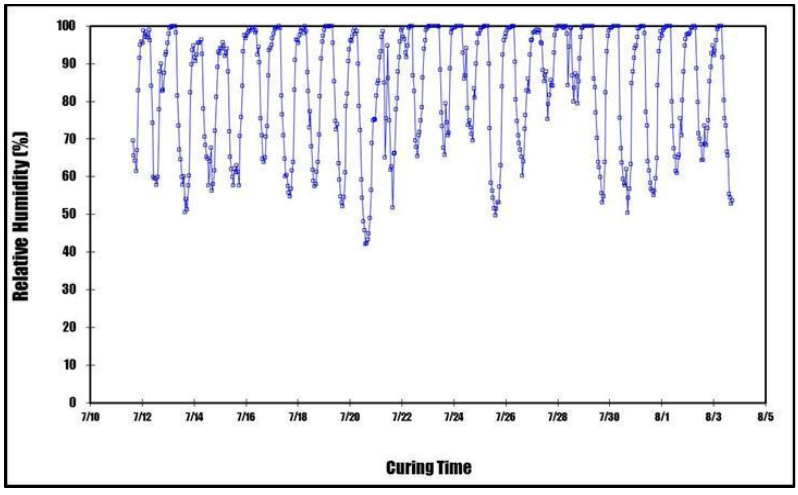

Figure 10-6. Plots of humidity against the curing period from weather station device

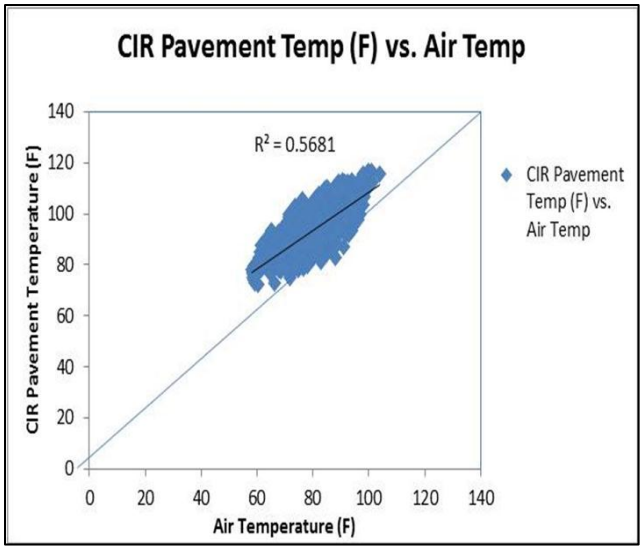

Figure 10-7. Plots of temperature from three sensors embedded in the CIR-foam layer against air temperature from weather station device

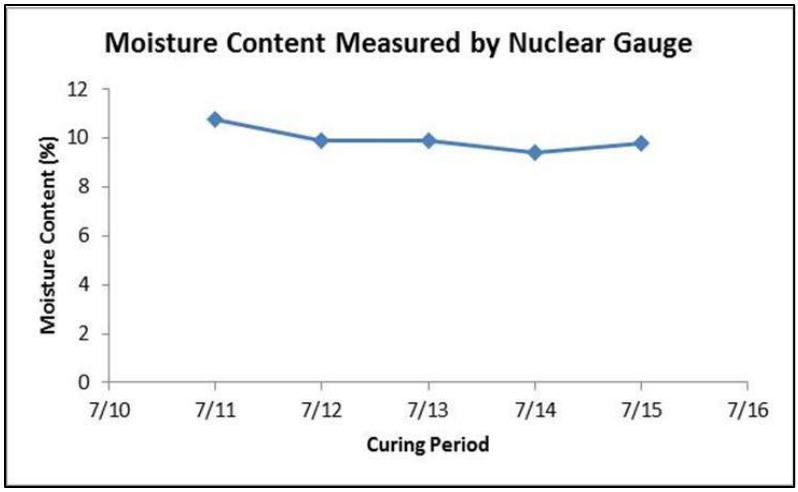

Figure 10-8. Plots of field moisture contents measured by nuclear gauge in CIR-foam project site

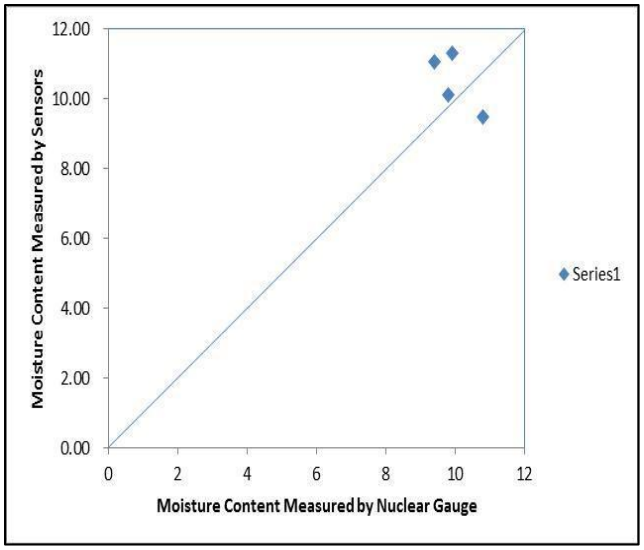

Figure 10-9. Plots of field moisture content measured by a nuclear gauge against field moisture content measured by the embedded moisture sensors

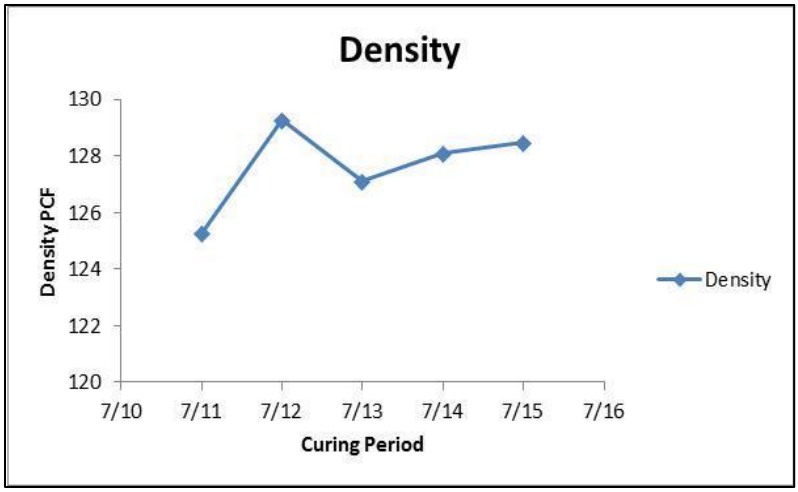

Figure 10-10. Plots of density against curing period from three locations in the CIR-foam layer

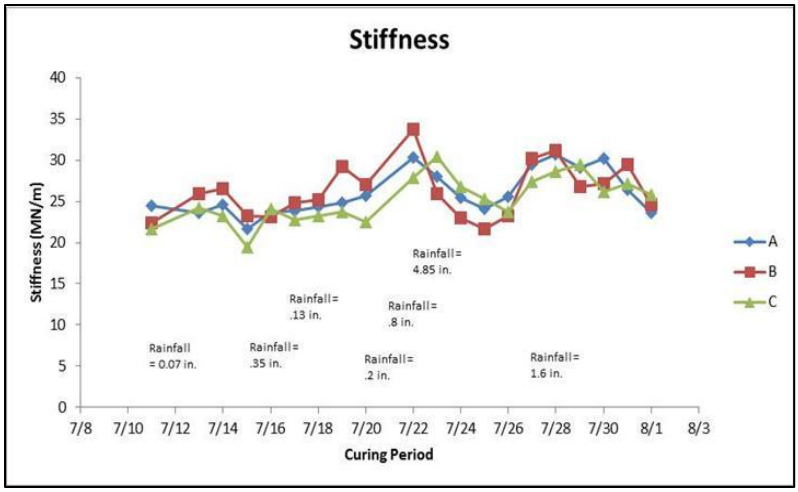

Figure 10-11. Plots of stiffness against the curing period from three locations in the CIR-foam layer

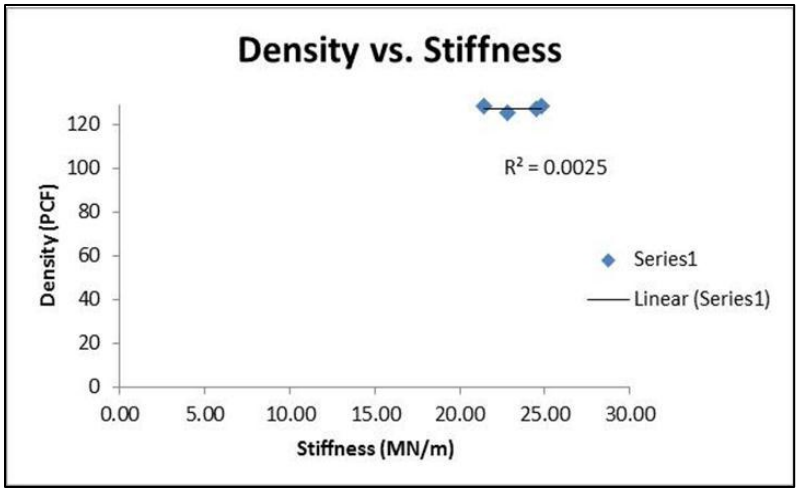

Figure 10-12. Plot of density measured by a nuclear gauge against stiffness measured by geo-gauge

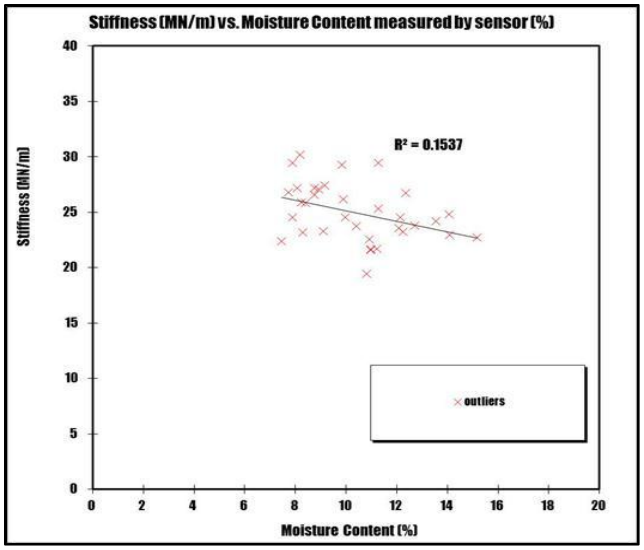

Figure 10-13. Plots of stiffness measured by a geo-gauge against moisture content measured by embedded sensors at three different locations

CHAPTER 11: MEASUREMENT OF MOISTURE CONTENT FROM CIR-FOAM PROJECT IN BLACK HAWK COUNTY

To measure the field moisture contents and temperature of CIR-foam layer, as shown in Figure 11-1, CIR-foam project site in Black Hawk County was selected. The CIR-foam project site is located on County Highway D13 in Manchester, Iowa. The road was rehabilitated between July 21st and August 11th, 2011.

11.1 Measurement of Field Moisture Content and Temperature

To monitor actual moisture contents of the CIR-foam layer in the field, as shown in Figure 11-2, three ECH2O moisture sensors and three temperature sensors were embedded at 2.0 inches from the surface of the CIR-foam layer. A weather station was also installed to collect air temperature, humidity, rainfall and wind speed.

Figure 11-3, Figure 11-4, Figure 11-5, and Figure 11-6 show plots of moisture content, rainfall, temperature, and humidity, respectively, measured during the curing duration of 21 days when four rainfalls with a total amount of 3.91 inches have occurred. Throughout the curing period, the moisture contents measured by three sensors were consistent with rainfalls. The moisture contents before the intermediate HMA overlay were measured at 6.48% from sensor A, 6.90% from sensor B and 4.63% from sensor C. Despite the actual moisture contents of CIR-foam layer remaining above 1.5%, the intermediate HMA overlay was constructed after 21 days of curing. Figure 11-7 shows plots of temperature from the three sensors embedded in the CIR-foam layer against air

temperature from the weather station. As shown in Figure 11-7, as expected, temperature of CIR-foam layer was significantly higher than air temperature.

As stated earlier, the TDR device was not used to measure moisture content on the 2 projects monitored in the summer of 2011.

As shown in Figure 11-8, using a nuclear gauge, field moisture contents were measured from one location between 9:00 a.m. to 9:30 a.m. on 3 days between July 22nd and July 26th, 2011. As can be seen from Figure 11-8, the moisture content decreased slightly from 12.0% to 11.0%.

Figure 11-9 shows plots of field moisture content measured by the nuclear gauge against moisture contents measured by the embedded moisture sensors. It should be noted that the moisture contents measured using a nuclear gauge and moisture sensors represent the moisture contents between the surface and 1.5 inches to 2.0 inches from the surface and they were above the minimum moisture content of 1.5% required before an HMA overlay. As shown in Figure 11-9, overall, the moisture contents measured by the embedded sensors were higher than those measured by the nuclear gauge.

11.2 Measurement of Density and Stiffness

The density and stiffness of the CIR-foam layer were measured using a nuclear gauge and geo-gauge, respectively, throughout the duration of curing. The stiffness was measured at three locations, while the density was measured at only one location.

11.2.1 Density Measurements using Nuclear Gauge

A nuclear gauge was used to measure densities of the CIR-foam layer. As shown in Figure 11-10, density values were measured three times between July 22nd and July

26th, 2011. The density value of CIR-foam layer increased in a liner fashion during the measurement period.

11.2.2 Stiffness Measurements using Geo-Gauge

The geo-gauge was used to measure the stiffness of the CIR-foam layer. In previous projects the stiffness was measured every 2-3 days during the curing period. For all projects during the summer of 2011 it was decided to measure stiffness every day in order to see a more detailed trend. As shown in Figure 11-11, stiffness was measured between July 22nd and August 10th, 2011 from three locations (all stiffness measurements were made between 9:30 a.m. to 12:00 p.m.). The stiffness of the CIR-foam layer began by increasing after construction. There were some noticeable decreases in stiffness after rainfalls throughout the curing period with the most notable occurring a little after 7/23, in which an extremely large rainfall of 2.19 in. occurred. There was another dip beginning on 7/29 after a 0.65 in. rainfall and 8/8 after a 0.50 in. rainfall. The stiffness tended to decrease after significant rain and then began to start increasing again each time. Overall, the stiffness increased from around the 25 MN/m range to the low 30 MN/m range. Figure 11-12 shows plots of density measured by a nuclear gauge against stiffness measured by geo-gauge for July 22nd, July 25th, and July 26th but there was little correlation between them. Figure 11-13 shows little correlation between stiffness and moisture content. Moisture contents above 7% were considered outliers for Figure 11-13.

Figure 11-1. Location of CIR-foam project site in Black Hawk County

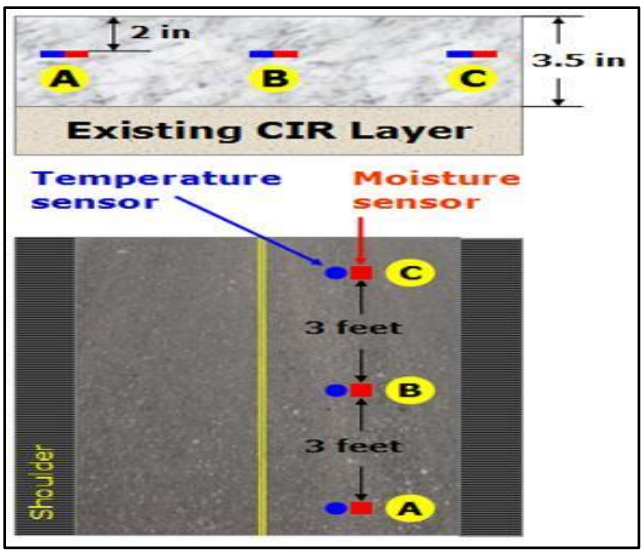

Figure 11-2. Embedded moisture and temperature sensors installed 2.0 inches from the surface of the CIR- foam layer

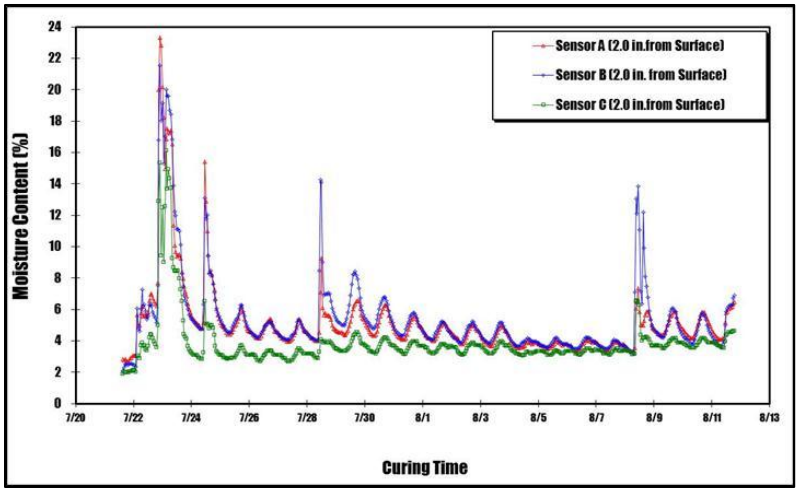

Figure 11-3. Plots of moisture contents against the curing period from three sensors embedded in the CIR-foam layer

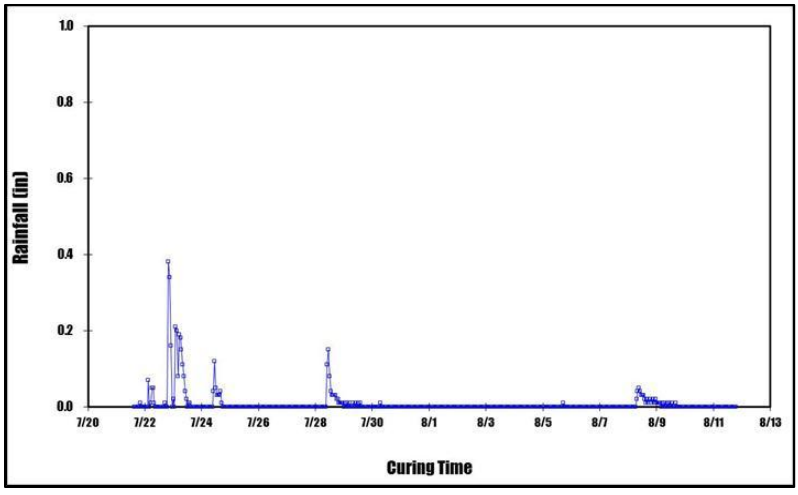

Figure 11-4. Plots of rainfalls against the curing period from weather station device

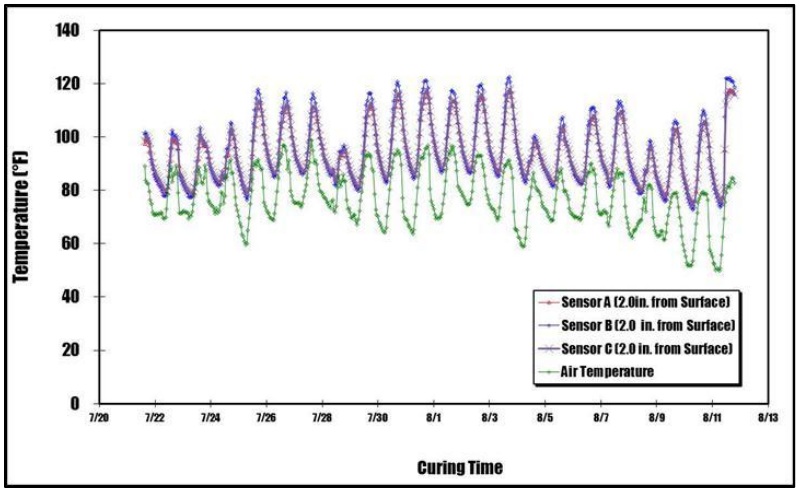

Figure 11-5. Plots of temperature against the curing period from three sensors embedded in the CIR-foam layer and air temperature from weather station device

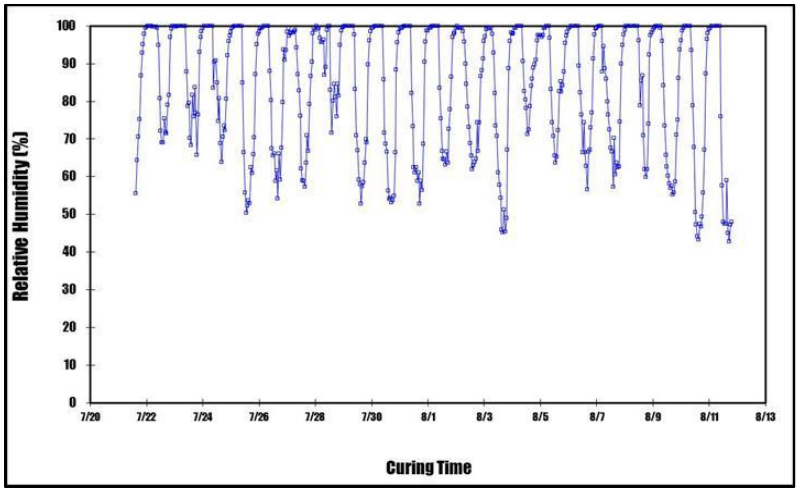

Figure 11-6. Plots of humidity against the curing period from weather station device

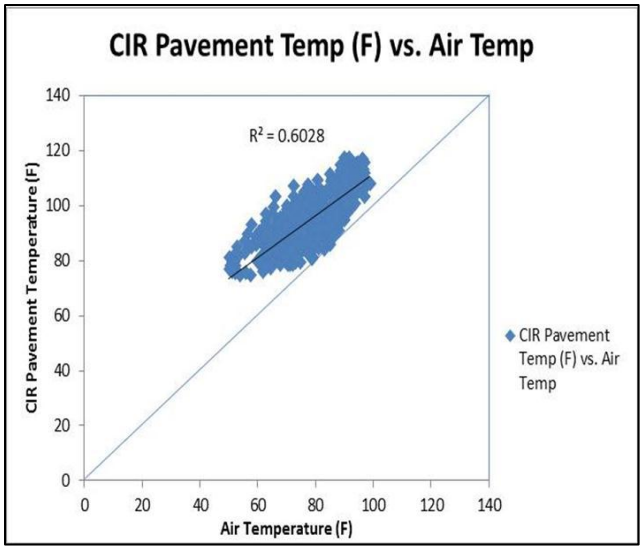

Figure 11-7. Plots of temperature from three sensors embedded in the CIR-foam layer against air temperature from weather station device

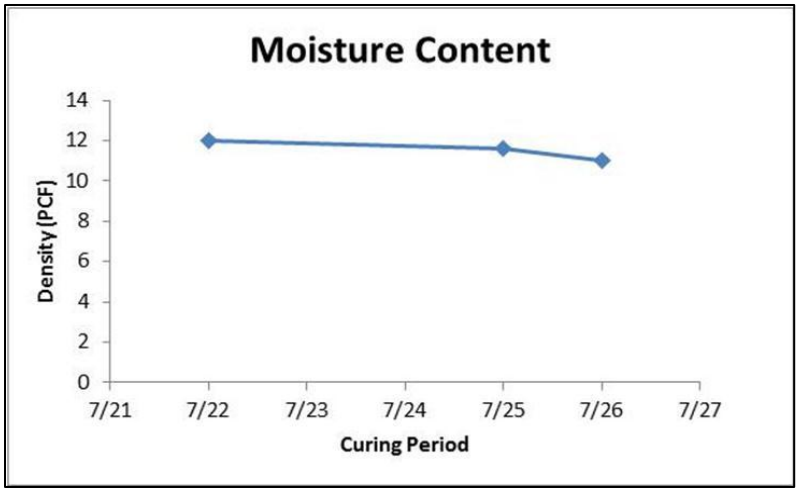

Figure 11-8. Plots of field moisture contents measured by nuclear gauge in CIR-foam project site

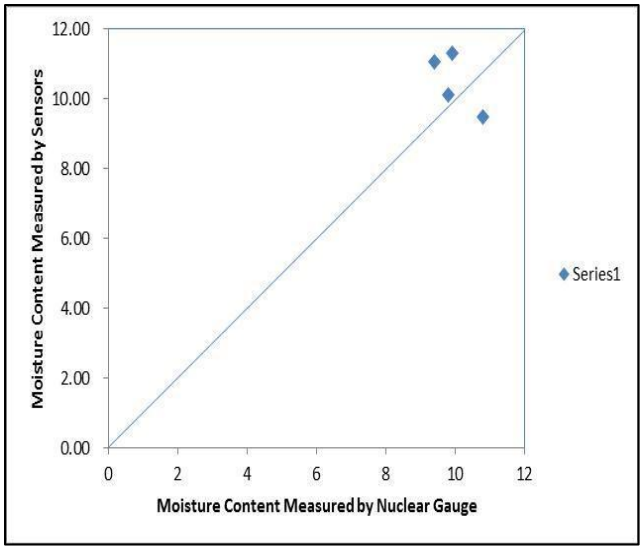

Figure 11-9. Plots of field moisture content measured by a nuclear gauge against field moisture content measured by the embedded moisture sensors

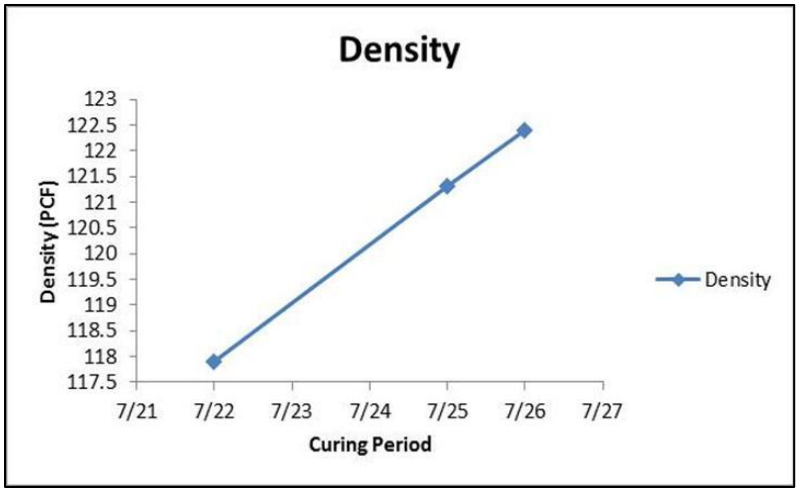

Figure 11-10. Plots of density against curing period from three locations in the CIR-foam layer

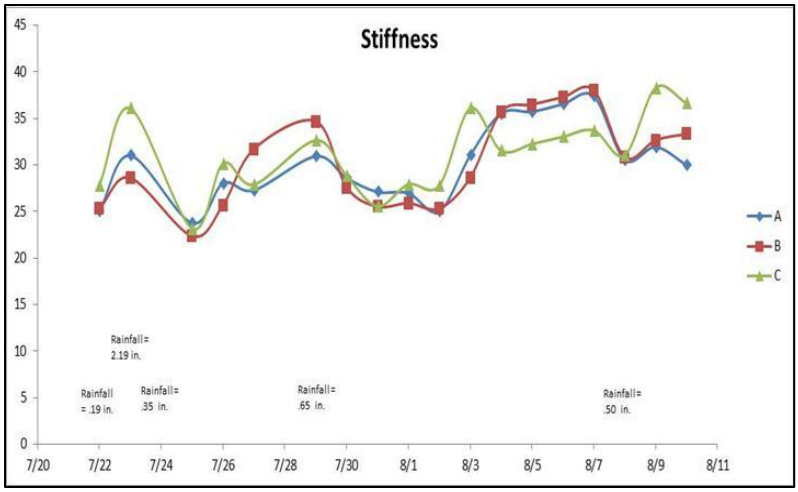

Figure 11-11. Plots of stiffness against the curing period from three locations in the CIR-foam layer

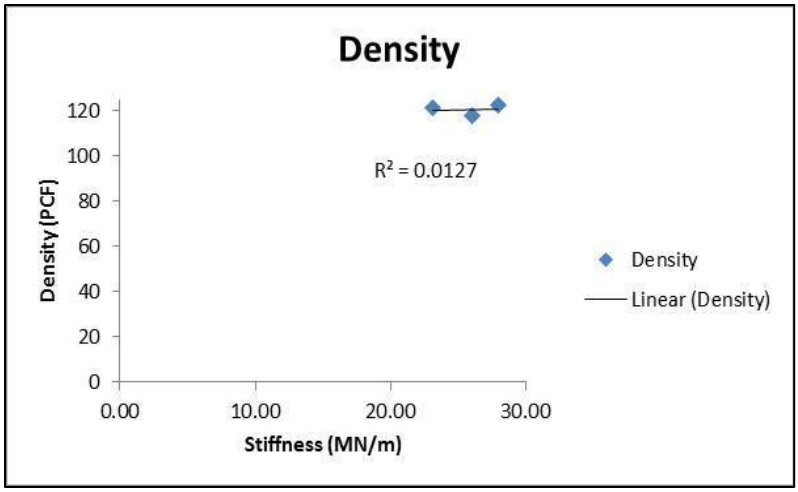

Figure 11-12. Plot of density measured by a nuclear gauge against stiffness measured by geo-gauge

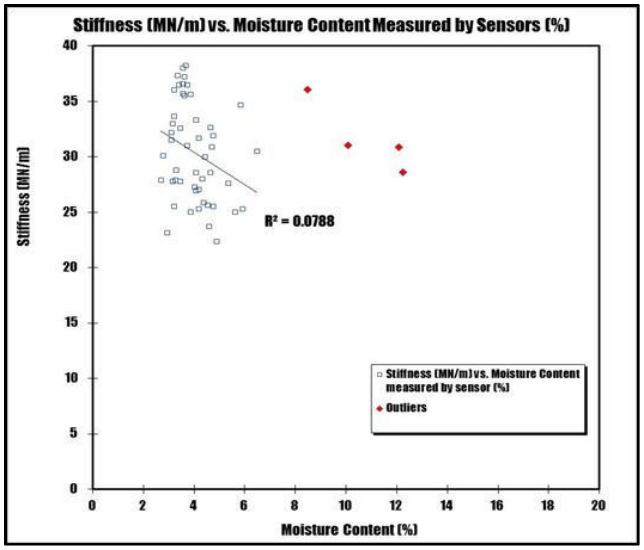

Figure 11-13. Plots of stiffness measured by a geo-gauge against moisture content measured by embedded sensors at three different locations

CHAPTER 12: DEVELOPMENT OF MOISTURE LOSS INDEX FOR CIR LAYER

To develop moisture loss indices for CIR layer, the actual moisture content of CIR layer was measured by ECH2O moisture sensors and climate data were collected from the weather stations installed at CIR project sites.

To predict the moisture change in the CIR layer over time, using a multiple linear regression technique, the following moisture loss index formula was developed as a function of initial moisture condition, average CIR layer temperature, and average humidity and average wind speed.

$$\Delta MC/hr = a1 + a2\ IMC + a3\ Temp + a4\ Hum + a5\ Wind$$

where, $\Delta MC/hr$ = Moisture change per hour during curing time

IMC = Initial moisture content of CIR layer right after construction

Temp = Average CIR layer temperature (°F) during curing time

Hum = Average humidity (%) during curing time

Wind= Average wind speed (mph) during curing time

a1, a2, a3, a4, a5 = multiple linear regression coefficients

12.1 CIR-HFMS-2S-emulsion Project Site in Clinton County

Moisture contents and climatic data were collected from the CIR-HFMS-2S-emulsion layer in Clinton County. A new set of moisture content data was created when the rainfall had occurred. After discarding the initial moisture contents above 12%

(unusually high), thirty-two moisture content data sets from sensor A, thirty-four sets from sensor B, and thirty nine sets from sensor C were obtained.

Figure 12-1, Figure 12-2 and Figure 12-3 show plots of moisture content change per hour against three independent variables for sensor A, B and C. As can be seen from Figures 12-1, 12-2, 12-3 initial moisture content had the largest R-square value.

As shown in the regression equations below, Δmoisture content per hour in CIR-HFMS-2S-emulsion layer can be predicted as a function of the initial moisture content, the average CIR pavement temperature, the average humidity and the average wind speed.

A: $\Delta MC/hr = 0.03092 + 0.045002\ IMC + 0.00024\ Temp + 0.00135\ Hum + 0.02339\ Wind$ (R-square = 94.0%)

B: $\Delta MC/hr = 0.112077 + 0.022621\ IMC + 0.00062\ Temp + 0.00212\ Hum + 0.02106\ Wind$ (R-square = 88.4%)

C: $\Delta MC/hr = -0.57029 + 0.067176\ IMC + 0.002025\ Temp + 0.002852\ Hum + 0.010132\ Wind$ (R-square = 64.8%)

A, B and C: $\Delta MC/hr = -0.3094 + 0.38766\ IMC + 0.000954\ Temp + 0.001692\ Hum + 0.002683\ Wind$ (R-square = 51.8%)

Overall, the R-square value for this project was reasonable, which suggests this equation can be used for predicting moisture level in a typical CIR-HFMS-2S emulsion project. The individual sensors offered higher R-square values than the overall equation because of a significant variation among moisture contents measured by three different sensors.

12.2 CIR-foam Project Site in Iowa County

Moisture contents and climatic data were collected from the CIR-foam layer in Iowa County. After discarding the initial moisture contents above 12% (unusually high), twenty-three moisture content data sets from sensor A, twenty-three sets from sensor B, and twenty-four sets from sensor C were obtained.

Figure 12-4, Figure 12-5 and Figure 12-6 show plots of moisture content change per hour against three independent variables for sensor A, B and C. As can be seen from Figures 12-4, 12-5, 12-6 initial moisture content had the largest R-square value.

As shown in the regression equations below, Δmoisture content per hour in CIR-foam layer can be predicted as a function of the initial moisture content, the average CIR pavement temperature, the average humidity and the average wind speed.

A: $\Delta MC/hr = -0.04831 + 0.02247\ IMC + 0.00056\ Temp + 0.00038\ Hum + 0.00358\ Wind$ (R-square = 88.1%)

B: $\Delta MC/hr = -0.06945 + 0.02523\ IMC + 0.0002\ Temp + 0.00006\ Hum - 0.03893\ Wind$ (R-square = 89.8%)

C: $\Delta MC/hr = -0.0747 + 0.02262\ IMC + 0.00018\ Temp + 0.00029\ Hum - 0.01302\ Wind$ (R-square = 86.7%)

A, B and C: $\Delta MC/hr = -0.01005 + 0.02104\ IMC + 0.00014\ Temp - 0.00037\ Hum - 0.00586\ Wind$ (R-square = 85.5%)

Overall, the R-square value for this project was relatively high, which suggests this equation is more reliable for predicting moisture level in a typical CIR-foam project than the one developed for CIR-HFMS-2S-emulsion. Overall R-square value was close to ones developed for individual sensors, which indicates that the data from three sensors are consistent among them.

12.3 CIR-foam Project Site in Benton County

Moisture contents and climatic data were collected from the CIR-foam layer in Benton County. After discarding the initial moisture contents above 12% (unusually high), eleven moisture content data sets from sensor A, thirty sets from sensor B, and twenty-five sets from sensor C were obtained.

Figure 12-7, Figure 12-8 and Figure 12-9 show plots of moisture content change per hour against three independent variables for sensor A, B and C. As can be seen from Figures 12-7, 12-8, 12-9 initial moisture content had the largest R-square value.

As shown in the regression equations below, Δmoisture content per hour in CIR-foam layer can be predicted as a function of the initial moisture content, the average CIR pavement temperature, the average humidity and the average wind speed.

A: ΔMC/hr = 0.11712 + 0.034418 IMC - 0.0006 Temp - 0.00281 Hum - 0.01432 Wind (R-square = 50.9%)

B: ΔMC/hr = -0.31646 + 0.052826 IMC – 0.000014 Temp + 0.00205 Hum + 0.007106 Wind (R-square = 77.4%)

C: ΔMC/hr = -0.4607 + 0.041376 IMC + 0.002876 Temp + 0.000893 Hum - 0.01359 Wind (R-square = 59.1%)

A, B and C: ΔMC/hr = -0.4363 + 0.029607 IMC + 0.003342 Temp + 0.001343 Hum + 0.012037 Wind (R-square = 53.3%)

Overall, the R-square value for this project was reasonable, which suggests this equation can be used for predicting moisture level in a typical CIR-foam project. Overall R-square value was close to ones developed for individual sensors, which indicates that the data from three sensors are consistent among them.

12.4 CIR-foam Project Site in Marshall County

Moisture contents and climatic data were collected from the CIR-foam layer in Marshall County. After discarding the initial moisture contents above 12% (unusually high), twenty-six moisture content data sets from sensor A, and twenty-nine sets from sensor C were obtained.

Figure 12-10 and Figure 12-11 show plots of moisture content change per hour against three independent variables for sensor A and C. As can be seen from Figures 12-10 and 12-11 initial moisture content had the largest R-square value.

As shown in the regression equations below, Δmoisture content per hour in CIR-foam layer can be predicted as a function of the initial moisture content, the average CIR pavement temperature, the average humidity and the average wind speed.

A: ΔMC/hr = -0.28486 + 0.081042 IMC + 0.001235 Temp + 0.000497 Hum - 0.00161 Wind (R-square = 80.5%)

C: ΔMC/hr = 0.092117 + 0.071668 IMC - 0.00231 Temp - 0.00126 Hum + 0.009859 Wind (R-square = 86.6%)

A and C: ΔMC/hr = -0.0076 + 0.064511 IMC - 0.00058 Temp - 0.00114 Hum + 0.003648 Wind (R-square = 64.7%)

Overall, the R-square value for this project was relatively high, which suggests this equation is reliable for predicting moisture level in a typical CIR-foam project. Overall R-square value was lower than the ones developed for individual sensors, which indicates that the data from three sensors are variable.

12.5 CIR-foam Project Site in Delaware County 2010

Moisture contents and climatic data were collected from the CIR-foam layer in Iowa County. After discarding the initial moisture contents above 12% (unusually high), twenty-four moisture content data sets from sensor A, twenty-one sets from sensor B, and twenty-two sets from sensor C were obtained.

Figure 12-12, Figure 12-13 and Figure 12-14 show plots of moisture content change per hour against three independent variables for sensor A, B and C. As can be seen from Figures 12-12, 12-13, 12-14 initial moisture content had the largest R-square value.

As shown in the regression equations below, Δmoisture content per hour in CIR-foam layer can be predicted as a function of the initial moisture content, the average CIR pavement temperature, the average humidity and the average wind speed.

A: ΔMC/hr = -0.0329 + 0.042869 IMC - 0.00065 Temp - 0.00022 Hum + 0.00242 Wind (R-square = 57.8%)

B: ΔMC/hr = -0.07285 + 0.00689 IMC + 0.000065 Temp + 0.00066 Hum – 0.00763 Wind (R-square = 63.7%)

C: ΔMC/hr = 0.009026 + 0.069285 IMC - 0.00143 Temp - 0.00036 Hum - 0.01874 Wind (R-square = 72.7%)

A, B and C: ΔMC/hr = -0.13562 + 0.005781 IMC - 0.000081 Temp + 0.001739 Hum + 0.017054 Wind (R-square = 29.5%)

Overall, the R-square value for this project was low, which suggests this equation would not be reliable for predicting moisture level in a typical CIR-foam project. Overall R-square value was significantly lower than ones developed for individual sensors, which indicates that the data from three sensors are not consistent among them. It can be

postulated that the low R-squared value was obtained because there was little moisture loss over the curing period.

12.6 CIR-foam Project Site in Delaware County 2011

Moisture contents and climatic data were collected from the CIR-foam layer in Delaware County. A new set of moisture content data was created when the rainfall had occurred. After discarding the initial moisture contents above 12% (unusually high), six moisture content data sets from sensor A, twenty six sets from sensor B, and eighteen sets from sensor C were obtained.

Figure 12-15, Figure 12-16 and Figure 12-17 show plots of moisture content change per hour against three independent variables for sensor A, B and C. As can be seen from Figures 12-15, 12-16, 12-17 initial moisture content had the largest R-square value.

As shown in the regression equations below, Δmoisture content per hour in the CIR-foam layer can be predicted as a function of the initial moisture content, the average CIR pavement temperature, the average humidity and the average wind speed.

A: $\Delta MC/hr = 0.126316987 - 0.08254\ IMC + 0.003296\ Temp + 0.006625\ Hum + 0.101253\ Wind$ (R-square = 97.9%)

B: $\Delta MC/hr = -0.266312742 + 0.02592\ IMC + 0.000689\ Temp + 0.00093\ Hum - 0.00869\ Wind$ (R-square = 67.8%)

C: $\Delta MC/hr = -1.189184513 + 0.047769\ IMC + 0.006412\ Temp + 0.002592\ Hum - 0.00934\ Wind$ (R-square = 56.7%)

A, B and C: $\Delta MC/hr = -0.387972371 + 0.026593\ IMC + 0.002567\ Temp + 0.000221\ Hum - 0.00192\ Wind$ (R-square = 31.4%)

Overall, the R-square value for this project was reasonable, which suggests this equation can be used for predicting moisture level in a typical CIR-foam project. The individual sensors offered higher R-square values than the overall equation because of a significant variation among moisture contents measured by three different sensors.

12.7 CIR-foam Project Site in Black Hawk County

Moisture contents and climatic data were collected from the CIR-foam layer in Black Hawk County. A new set of moisture content data was created when the rainfall had occurred. After discarding the initial moisture contents above 12% (unusually high), thirty one moisture content data sets from sensor A, twenty five sets from sensor B, and thirty six sets from sensor C were obtained.

Figure 12-18, Figure 12-19 and Figure 12-20 show plots of moisture content change per hour against three independent variables for sensor A, B and C. As can be seen from Figures 12-18, 12-19, 12-20 initial moisture content had the largest R-square value.

As shown in the regression equations below, Δmoisture content per hour in the CIR-foam layer can be predicted as a function of the initial moisture content, the average CIR pavement temperature, the average humidity and the average wind speed.

A: $\Delta MC/hr = 1.562661004 + 0.057303\ IMC - 0.0135\ Temp - 0.00727\ Hum + 0.026461\ Wind$ (R-square = 40.6%)

B: $\Delta MC/hr = 3.075955244 + 0.045616\ IMC - 0.02578\ Temp - 0.01025\ Hum + 0.048878\ Wind$ (R-square = 41.0%)

C: $\Delta MC/hr = -0.040888315 + 0.028919\ IMC - 0.00146\ Temp + 0.001108\ Hum + 0.01161\ Wind$ (R-square = 24.5%)

A, B and C: $\Delta MC/hr = 1.316004832 + 0.049002\ IMC - 0.01172\ Temp - 0.00525\ Hum + 0.016429\ Wind$ (R-square = 35.9%)

Overall, the R-square value for this project was reasonable, which suggests this equation can be used for predicting moisture level in a typical CIR-foam project. The individual sensors offered higher R-square values than the overall equation because of a significant variation among moisture contents measured by three different sensors.

12.8 Compilation of Moisture Data from all CIR-foam Sites

The moisture contents and climatic data from each CIR-foam project site were compiled in order to develop a typical regression equation for all CIR-foam projects. By using the larger amount of data points from multiple sites may increase a reliability of the developed equation. The CIR-foam projects ranged from being performed in early June to October, which would provide one typical equation for the entire construction season. In the regression equation below, Δmoisture content per hour in CIR-foam layer can be predicted as a function of the initial moisture content, the average CIR pavement temperature, the average humidity and the average wind speed. The moisture loss indices and R-square values for each project site is shown in Table 12-1.

CIR-foam: $\Delta MC/hr = -0.04749354 + 0.02621\ IMC - 0.00048\ Temp + 0.000383\ Hum + 0.014683\ Wind$ (R-square = 45.0%)

Overall, the R-square value for CIR-foam projects is reasonable, which suggests this equation would be reliable for predicting moisture level in a typical CIR-foam project.

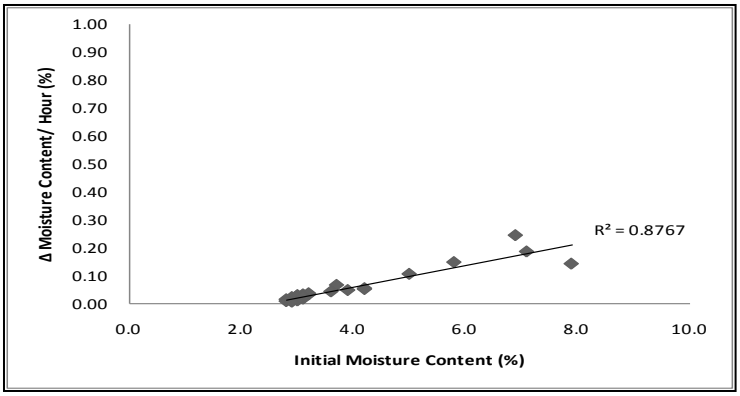

(a) ΔMC/h vs. IMC

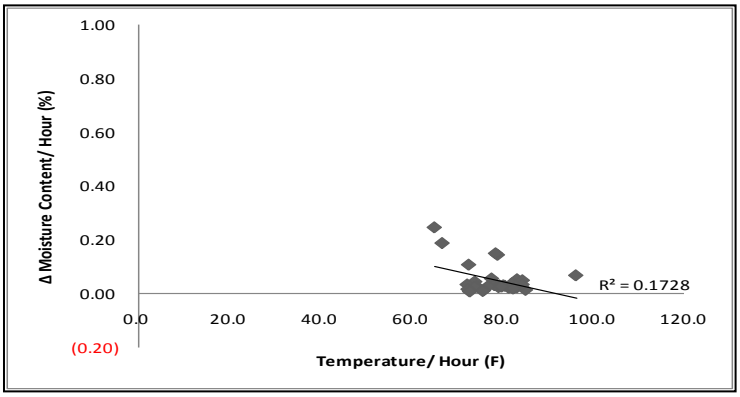

(b) ΔMC/hour vs. Temperature

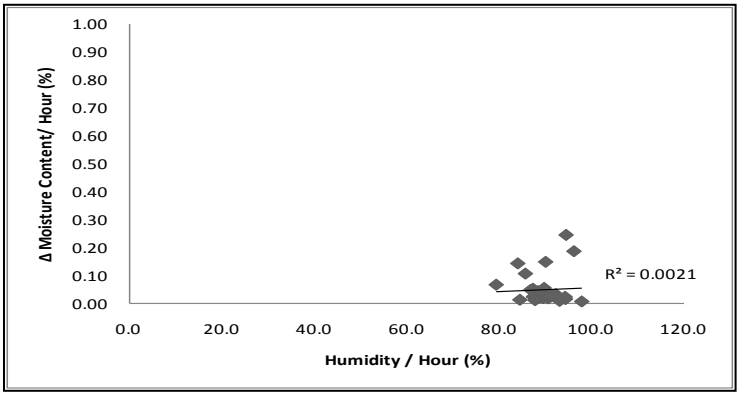

(c) ΔMC/h vs. Humidity

Figure 12-1. Plots of moisture change per hour against each of three independent variables at sensor A

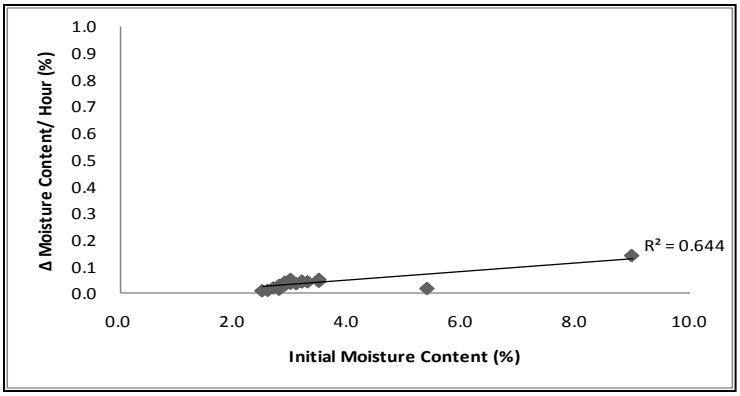

(a) ΔMC/h vs. IMC

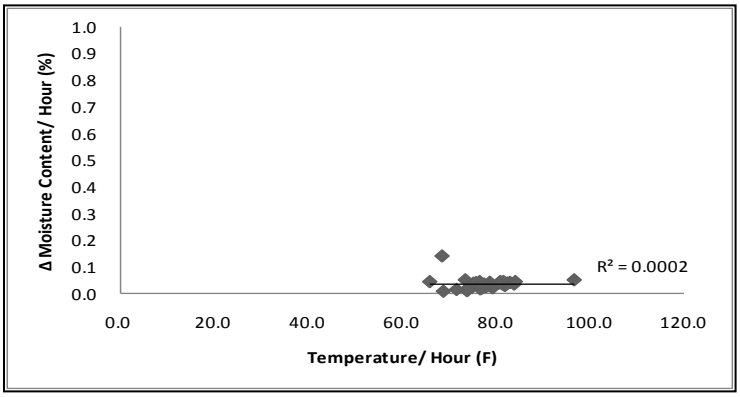

(b) ΔMC/hour vs. Temperature

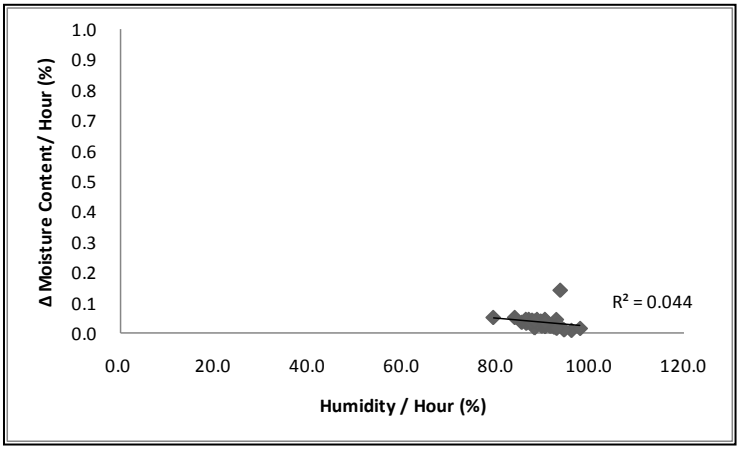

(c) ΔMC/h vs. Humidity

Figure 12-2. Plots of moisture change per hour against each of three independent variables at sensor B

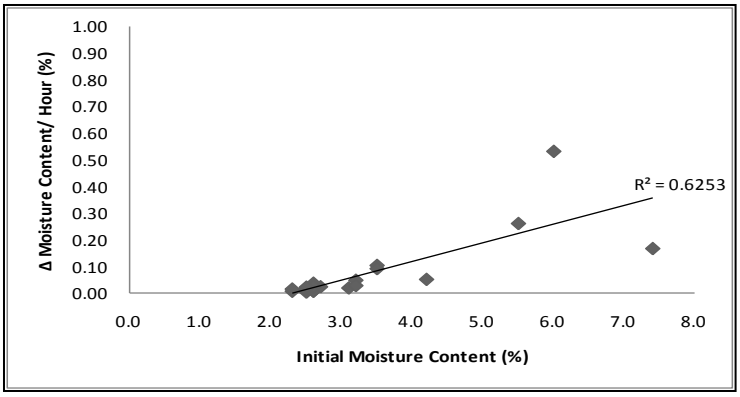

(a) ΔMC/h vs. IMC

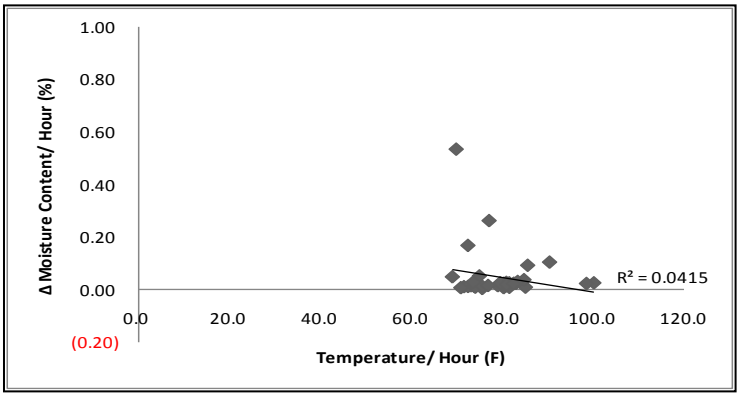

(b) ΔMC/hour vs. Temperature

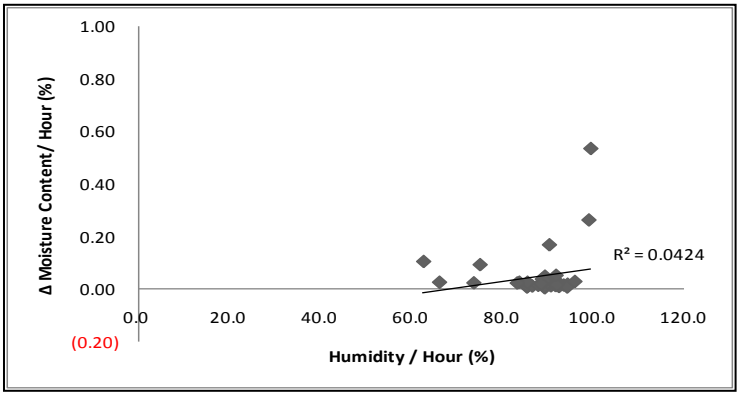

(c) ΔMC/h vs. Humidity

Figure 12-3. Plots of moisture change per hour against each of three independent variables at sensor C

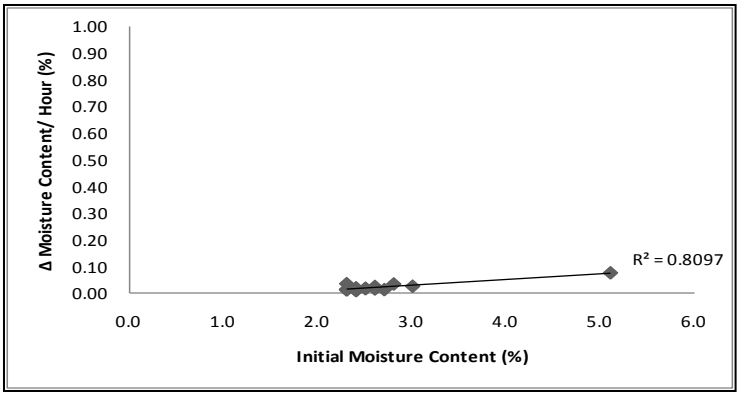

(a) ΔMC/h vs. IMC

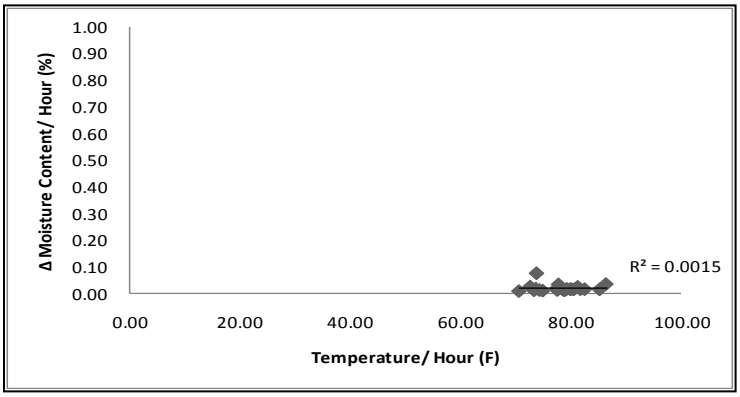

(b) ΔMC/hour vs. Temperature

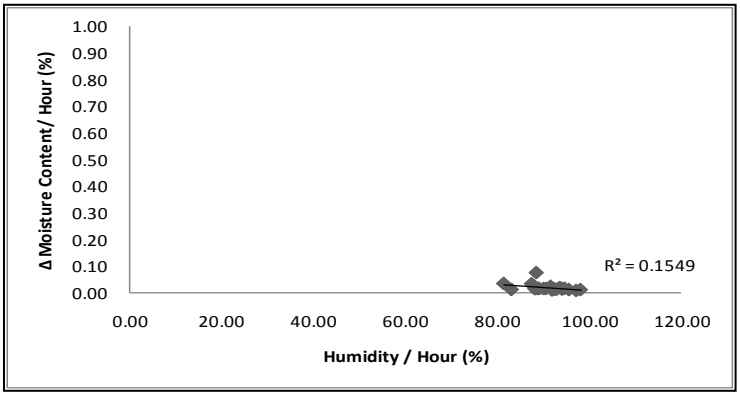

(c) ΔMC/h vs. Humidity

Figure 12-4. Plots of moisture change per hour against each of three independent variables at sensor A

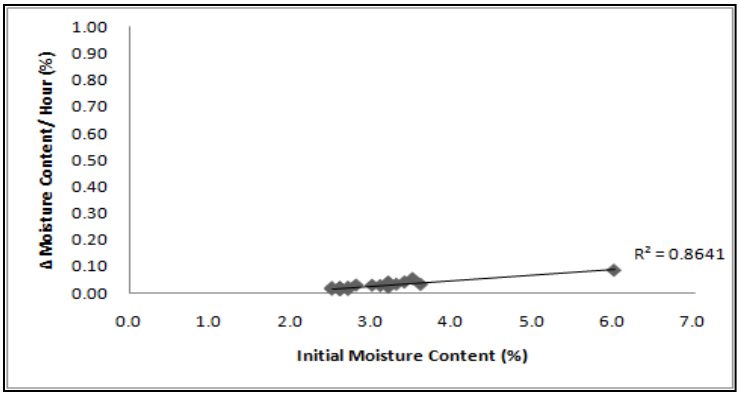

(a) ΔMC/h vs. IMC

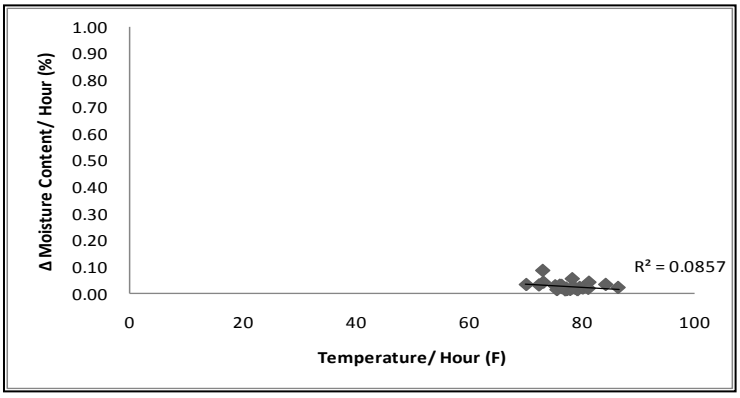

(b) ΔMC/hour vs. Temperature

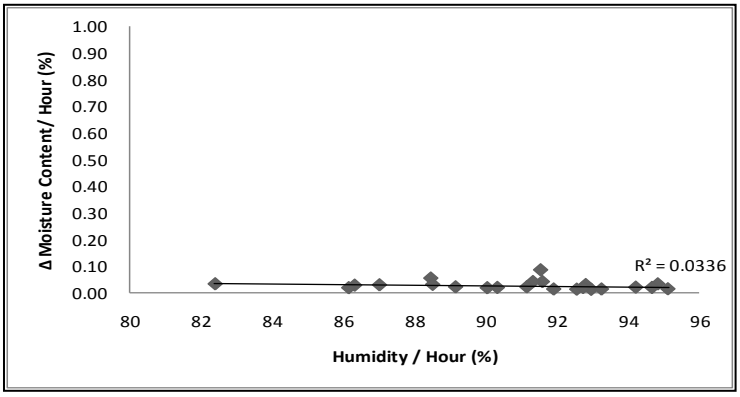

(c) ΔMC/h vs. Humidity

Figure 12-5. Plots of moisture change per hour against each of three independent variables at sensor B

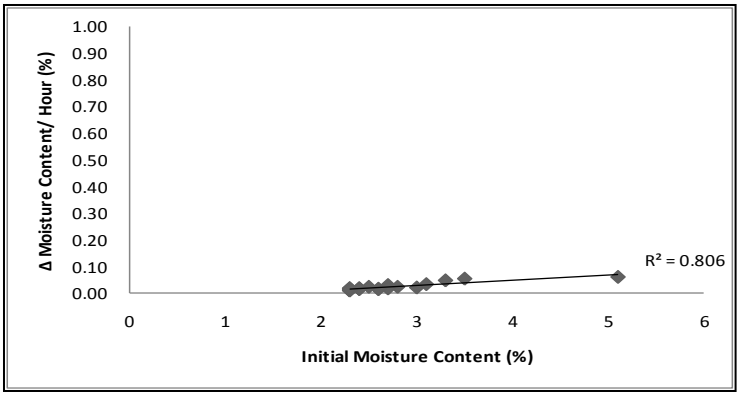

(a) ΔMC/h vs. IMC

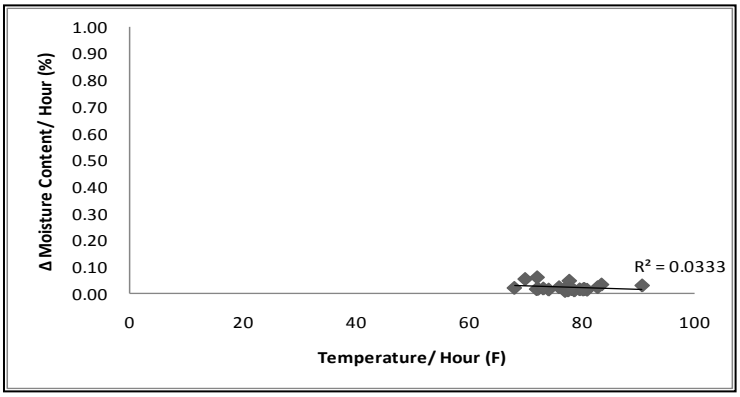

(b) ΔMC/hour vs. Temperature

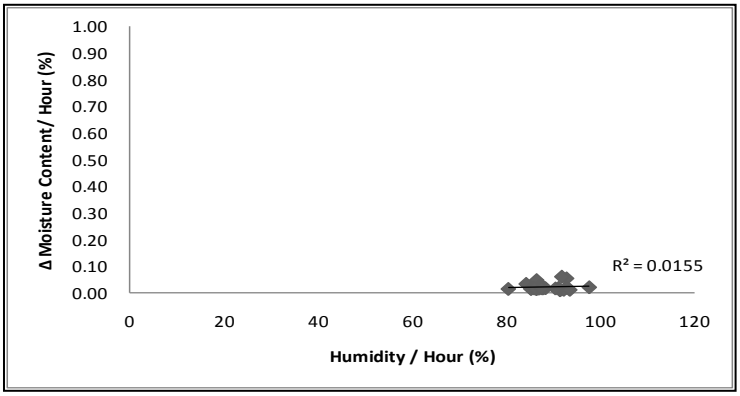

(c) ΔMC/h vs. Humidity

Figure 12-6. Plots of moisture change per hour against each of three independent variables at sensor C

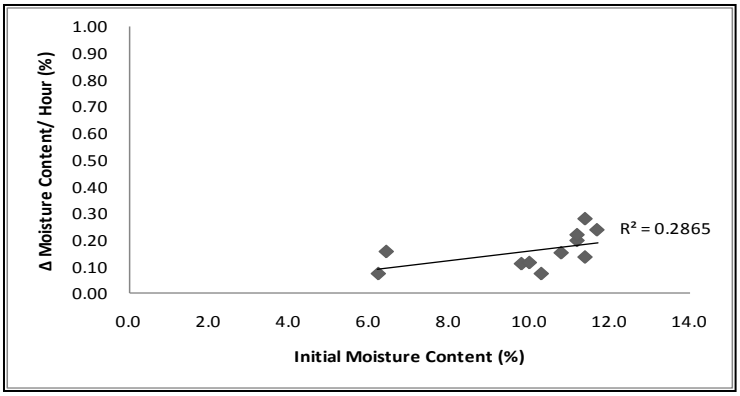

(a) ΔMC/h vs. IMC

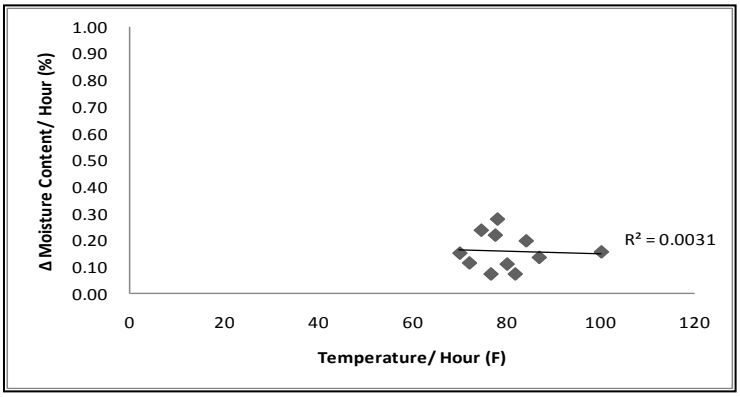

(b) ΔMC/hour vs. Temperature

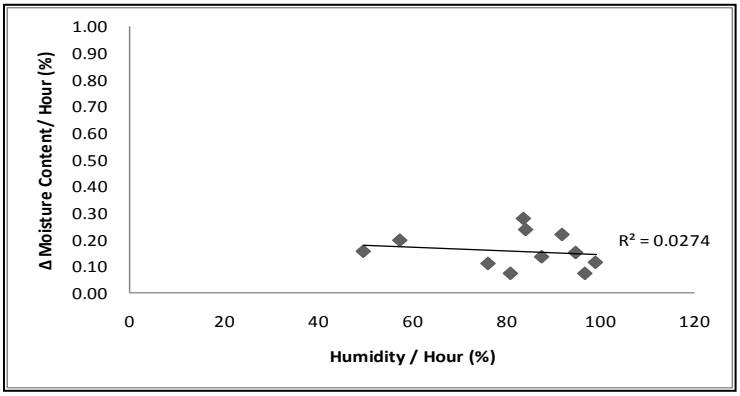

(c) ΔMC/h vs. Humidity

Figure 12-7. Plots of moisture change per hour against each of three independent variables at sensor A

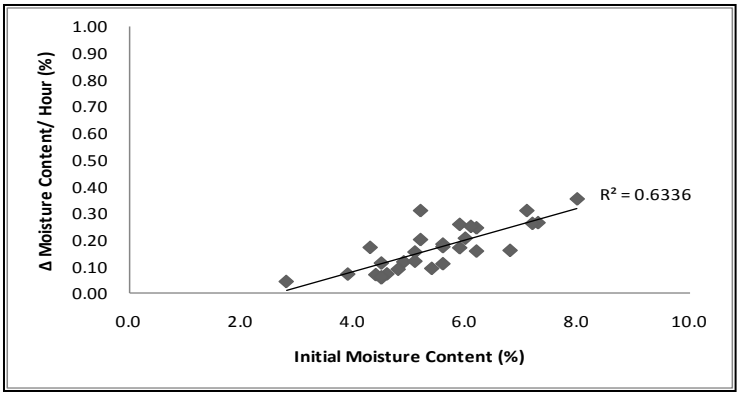

(a) ΔMC/h vs. IMC

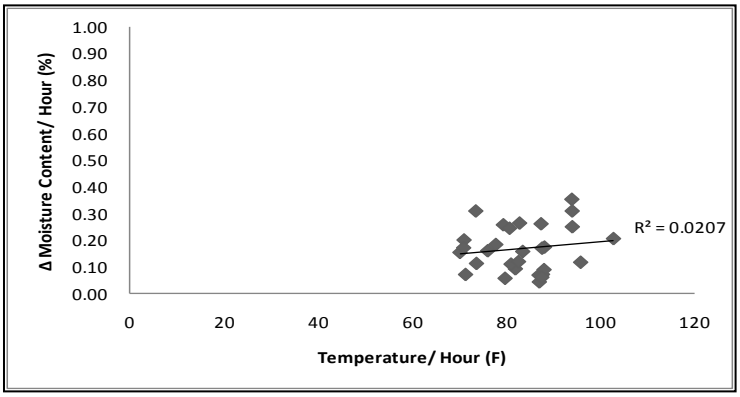

(b) ΔMC/hour vs. Temperature

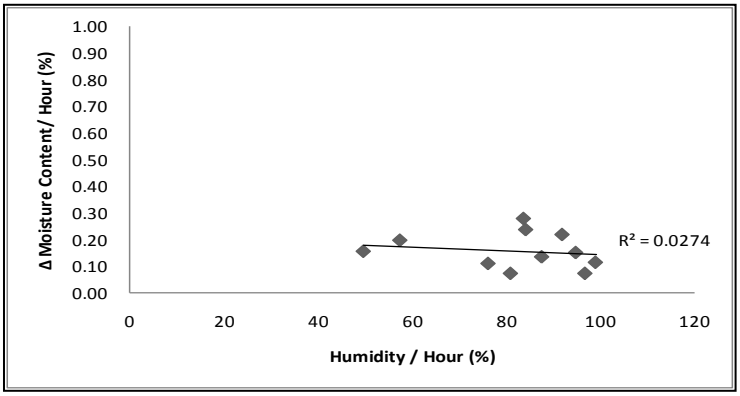

(c) ΔMC/h vs. Humidity

Figure 12-8. Plots of moisture change per hour against each of three independent variables at sensor B

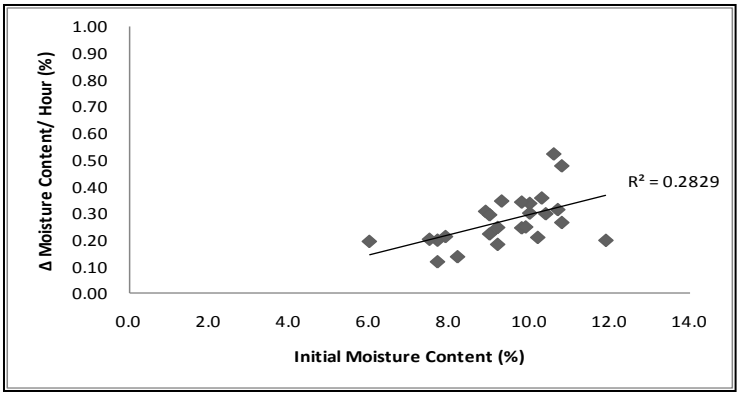

(a) ΔMC/h vs. IMC

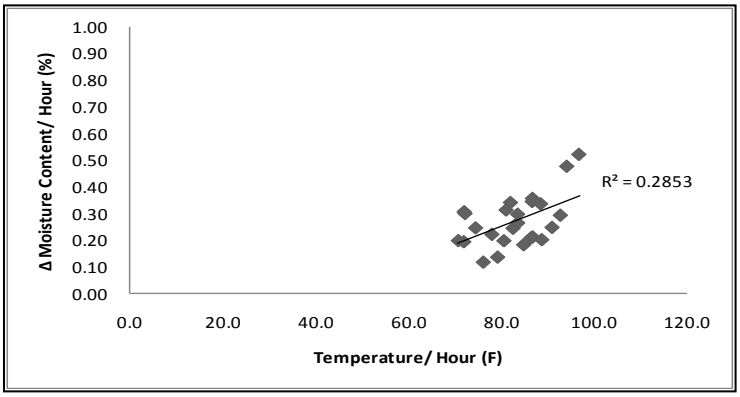

(b) ΔMC/hour vs. Temperature

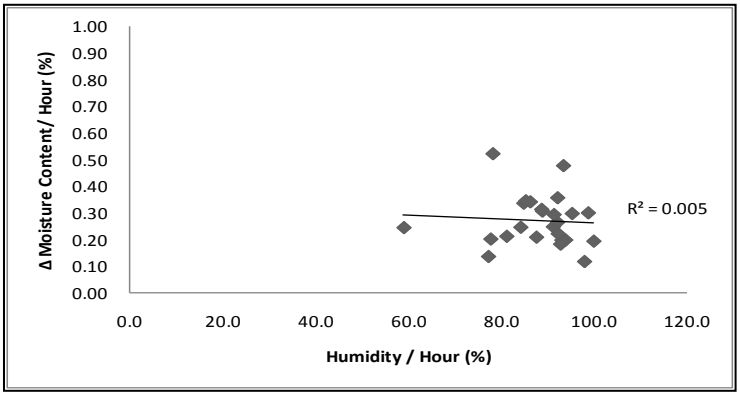

(c) ΔMC/h vs. Humidity

Figure 12-9. Plots of moisture change per hour against each of three independent variables at sensor C

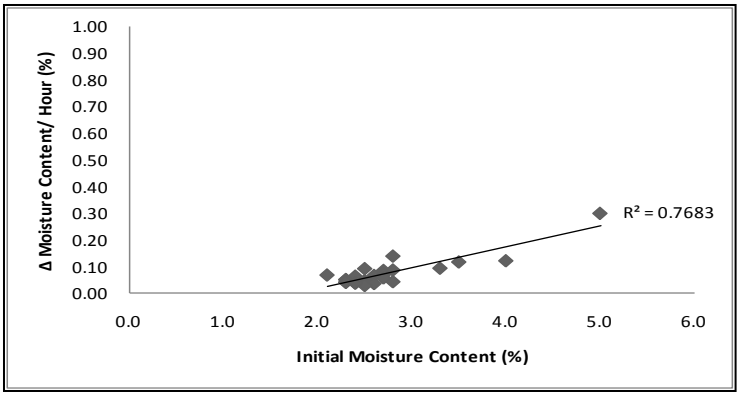

(a) ΔMC/h vs. IMC

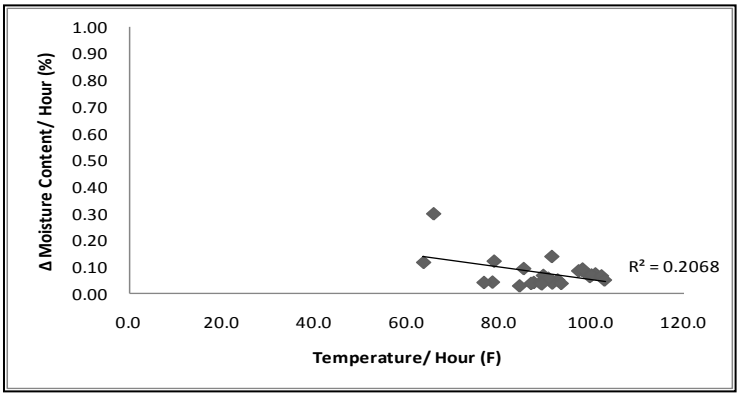

(b) ΔMC/hour vs. Temperature

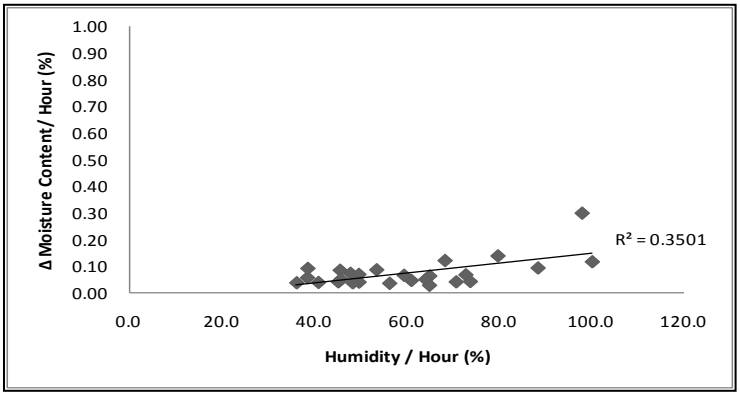

(c) ΔMC/h vs. Humidity

Figure 12-10. Plots of moisture change per hour against each of three independent variables at sensor A

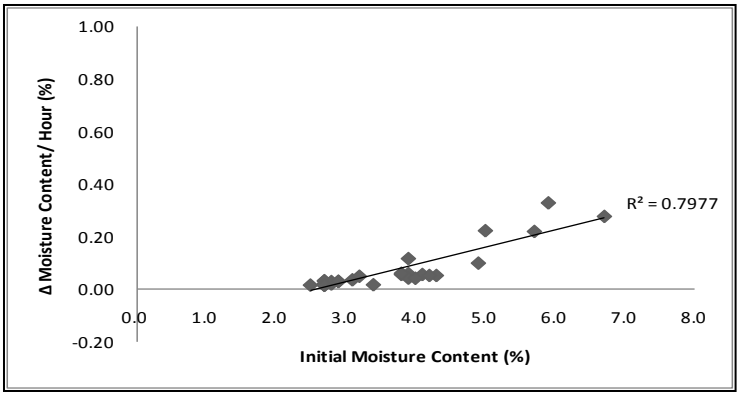

(a) ΔMC/h vs. IMC

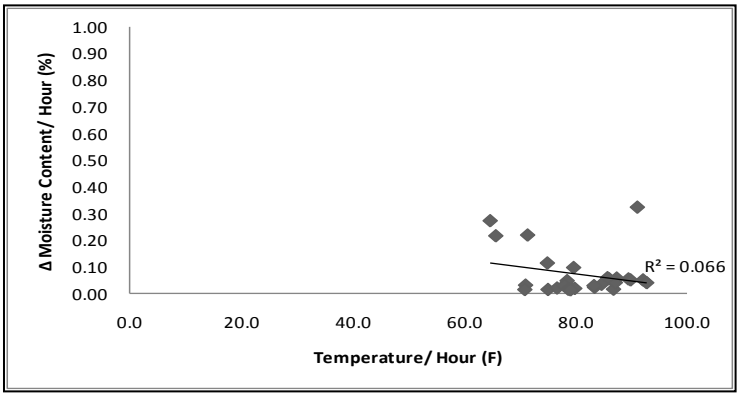

(b) ΔMC/hour vs. Temperature

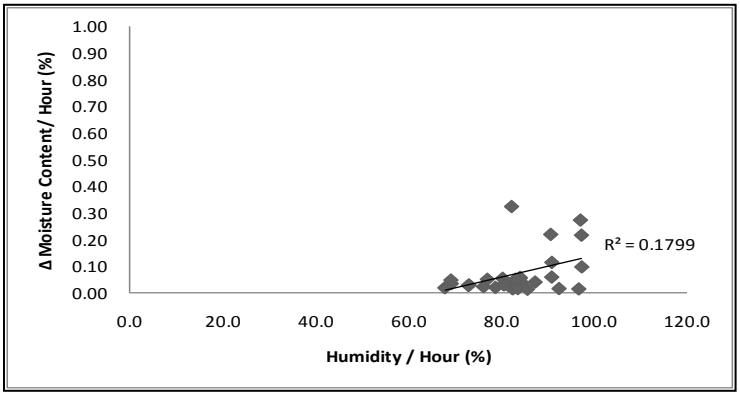

(c) ΔMC/h vs. Humidity

Figure 12-11. Plots of moisture change per hour against each of three independent variables at sensor C

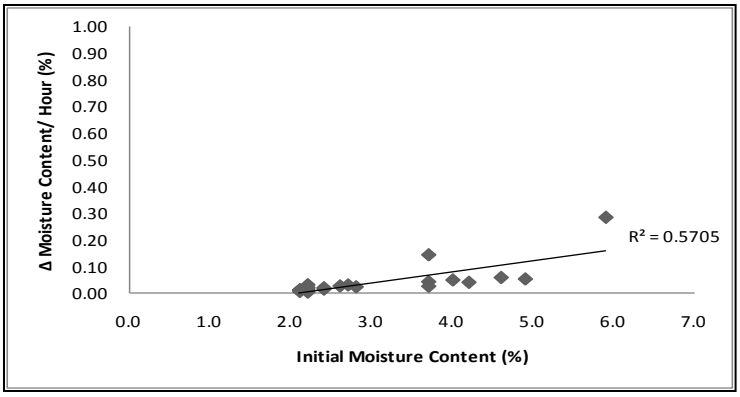

(a) ΔMC/h vs. IMC

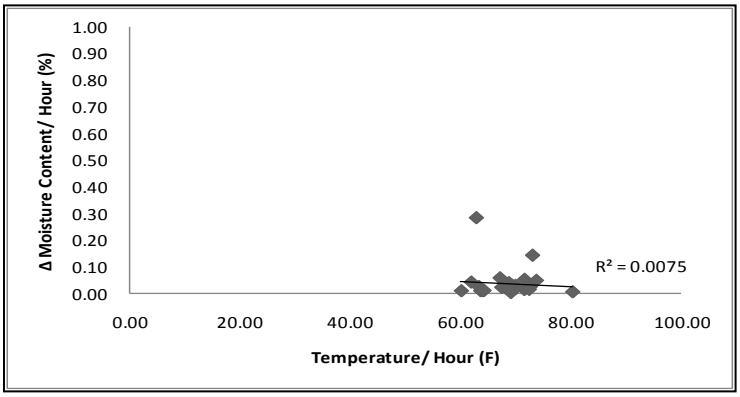

(b) ΔMC/hour vs. Temperature

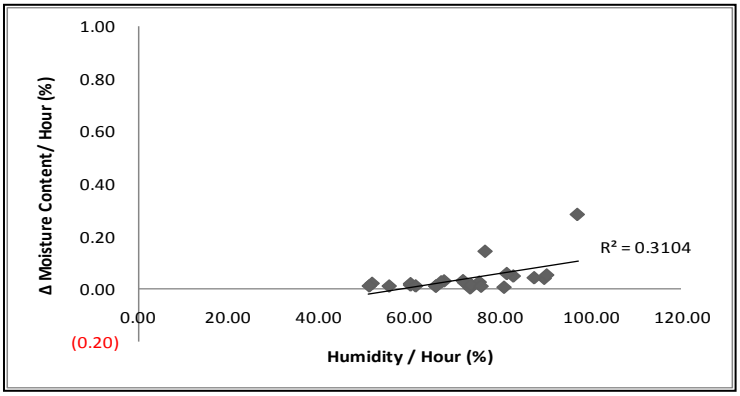

(c) ΔMC/h vs. Humidity

Figure 12-12. Plots of moisture change per hour against each of three independent variables at sensor A

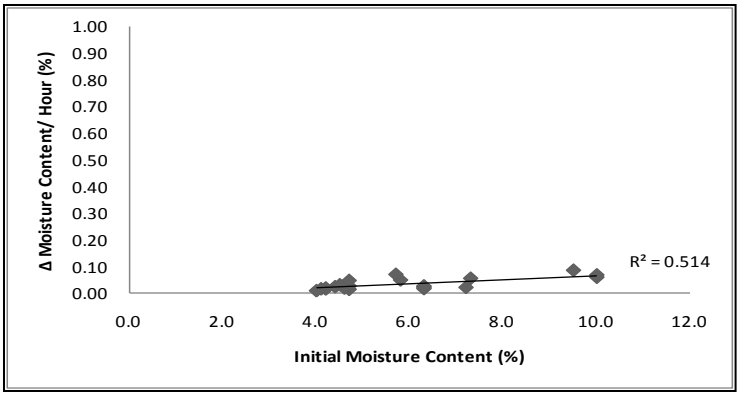

(a) ΔMC/h vs. IMC

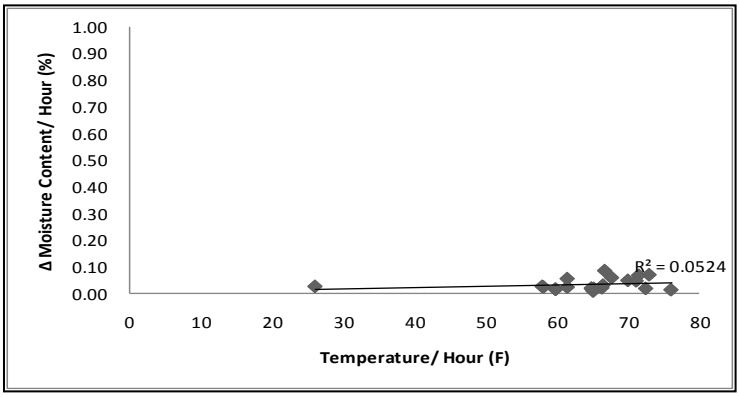

(b) ΔMC/hour vs. Temperature

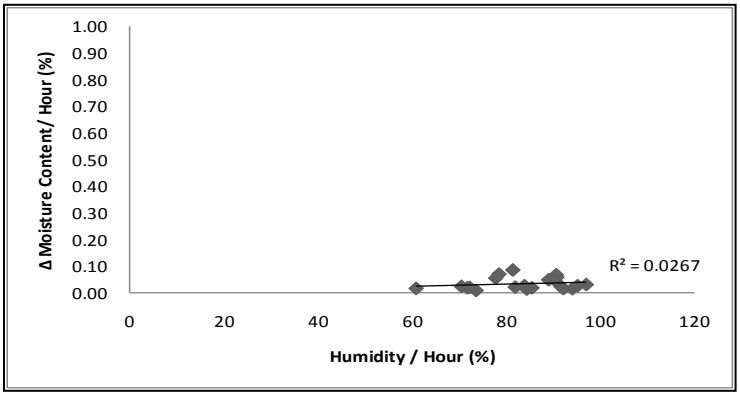

(c) ΔMC/h vs. Humidity

Figure 12-13. Plots of moisture change per hour against each of three independent variables at sensor B

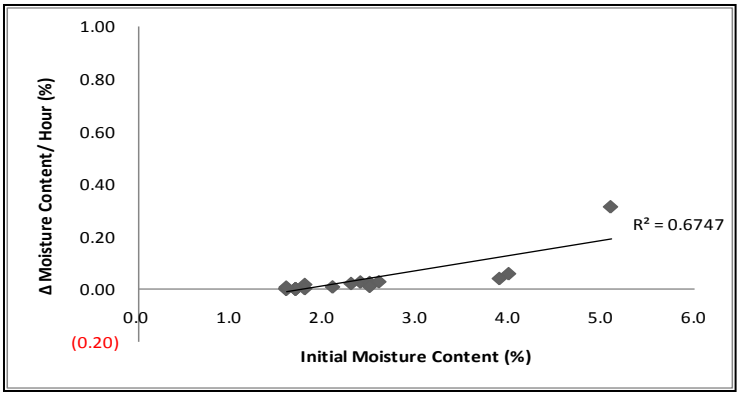

(a) ΔMC/h vs. IMC

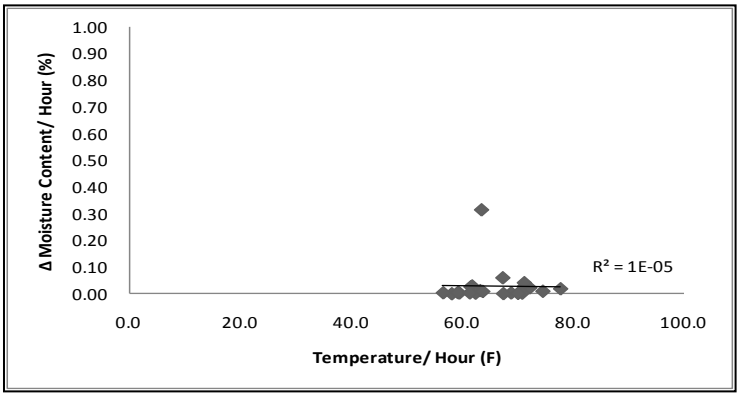

(b) ΔMC/hour vs. Temperature

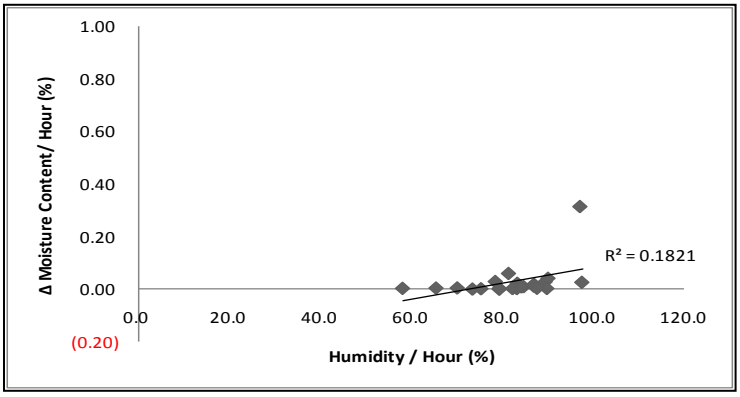

(c) ΔMC/h vs. Humidity

Figure 12-14. Plots of moisture change per hour against each of three independent variables at sensor C

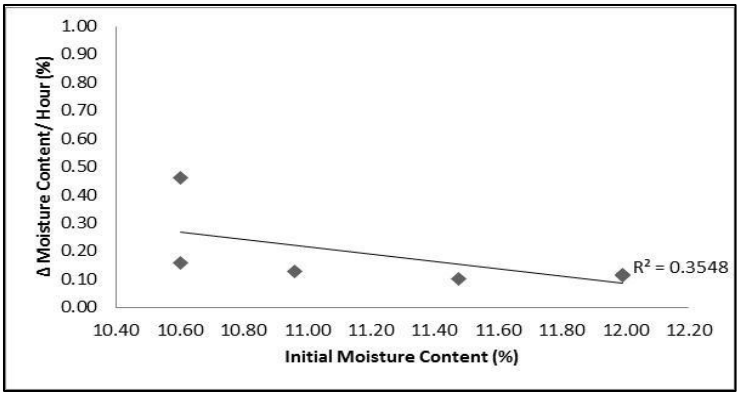

(a) ΔMC/h vs. IMC

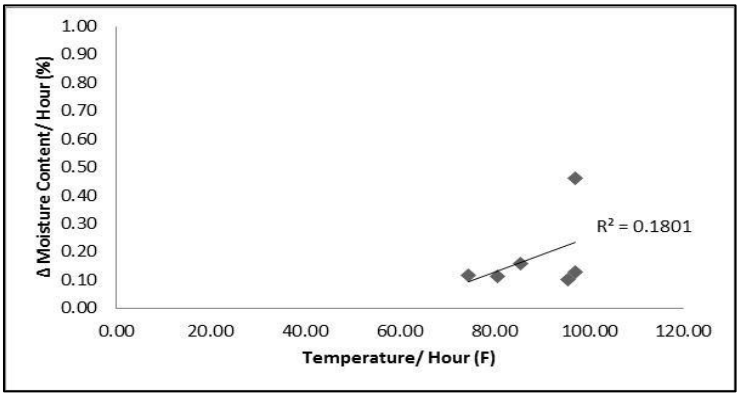

(b) ΔMC/hour vs. Temperature

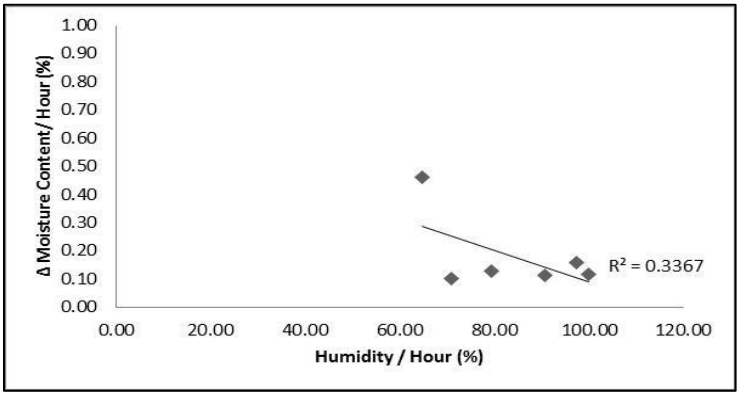

(c) ΔMC/h vs. Humidity

Figure 12-15. Plots of moisture change per hour against each of three independent variables at sensor A

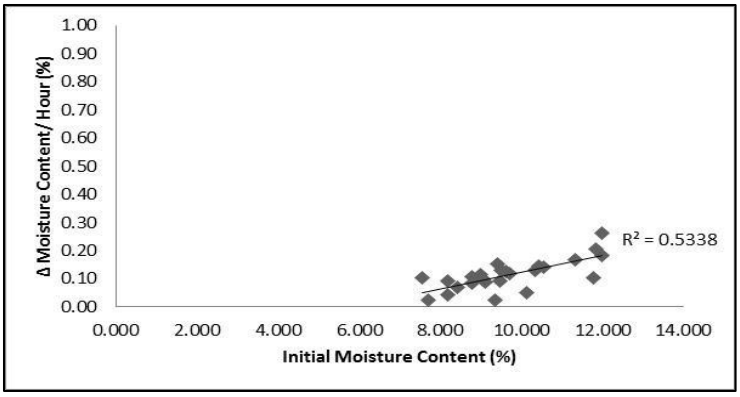

(a) ΔMC/h vs. IMC

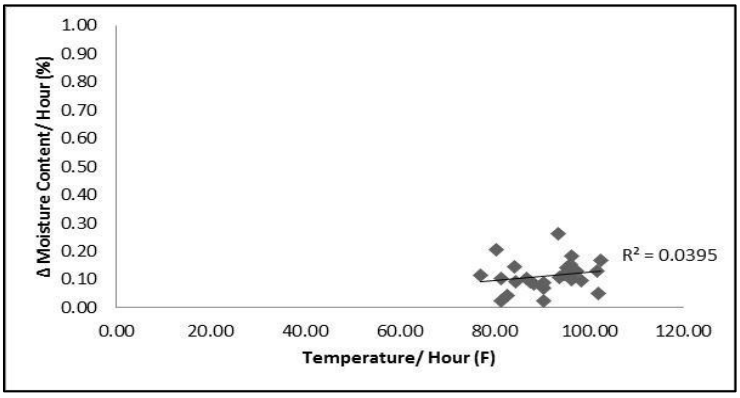

(b) ΔMC/hour vs. Temperature

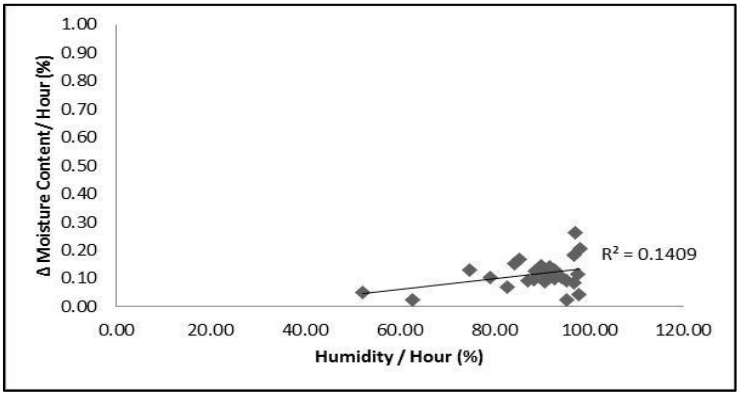

(c) ΔMC/h vs. Humidity

Figure 12-16. Plots of moisture change per hour against each of three independent variables at sensor B

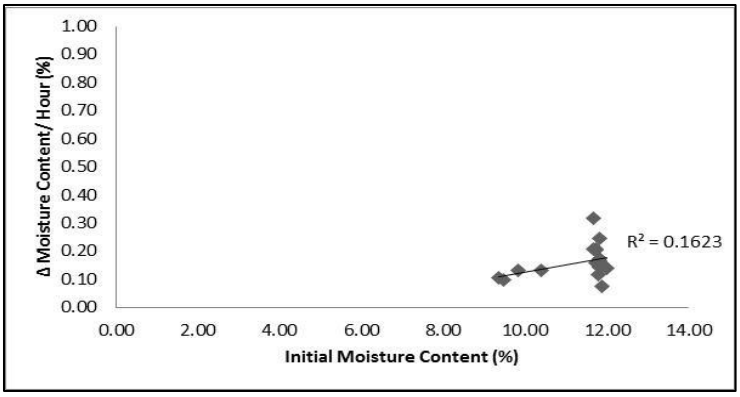

(a) ΔMC/h vs. IMC

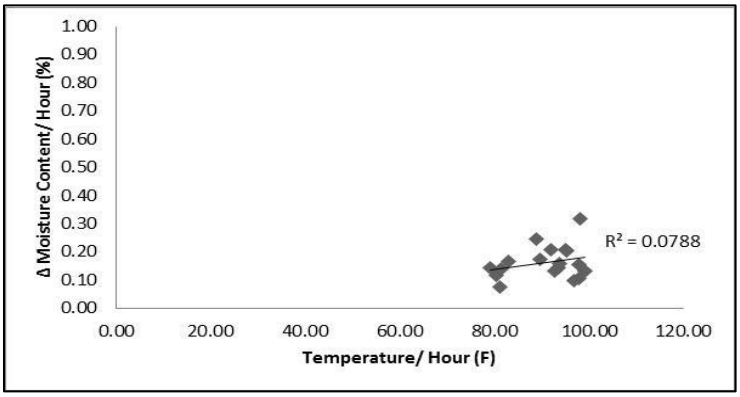

(b) ΔMC/hour vs. Temperature

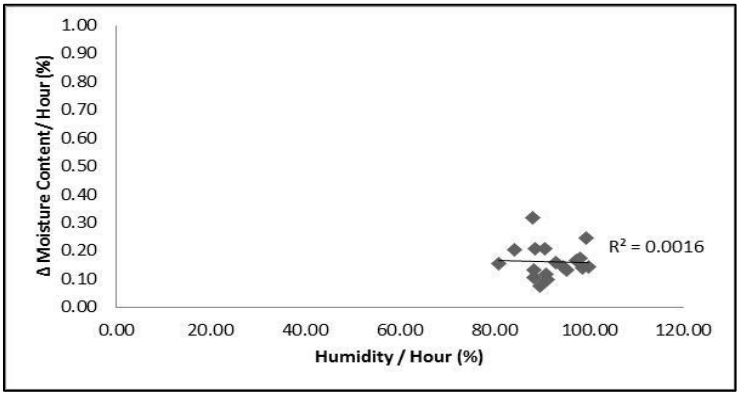

(c) ΔMC/h vs. Humidity

Figure 12-17. Plots of moisture change per hour against each of three independent variables at sensor C

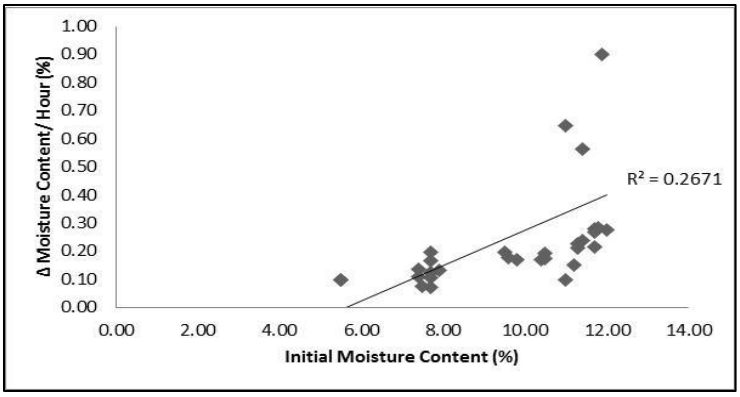

(a) ΔMC/h vs. IMC

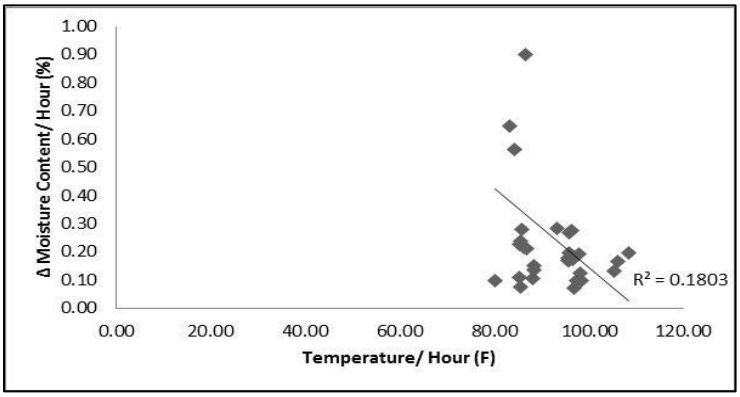

(b) ΔMC/hour vs. Temperature

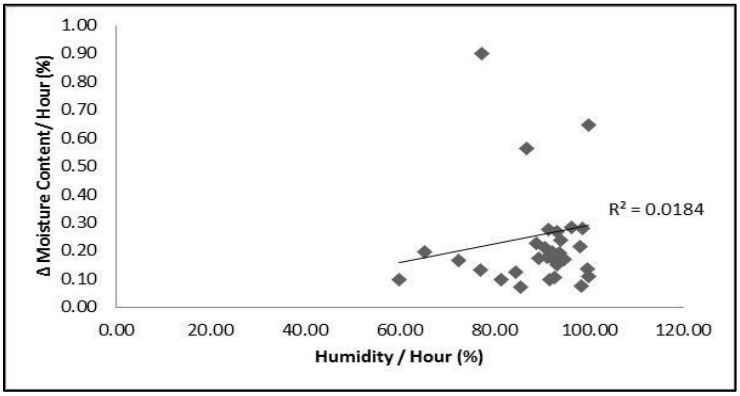

(c) ΔMC/h vs. Humidity

Figure 12-18. Plots of moisture change per hour against each of three independent variables at sensor A

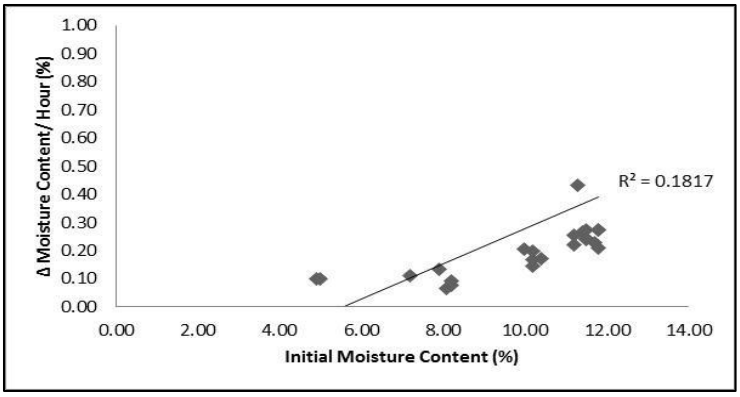

(a) ΔMC/h vs. IMC

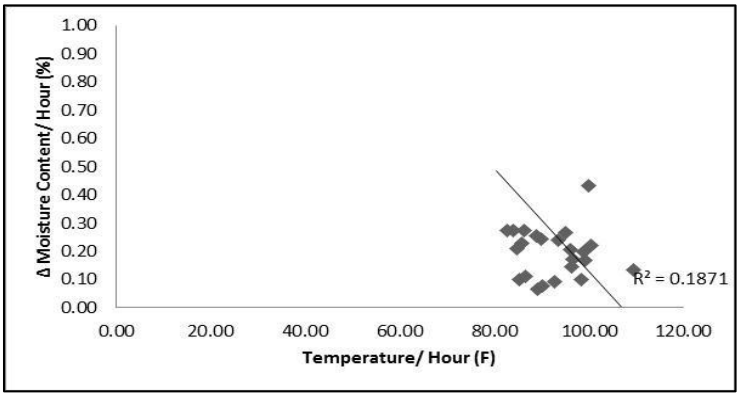

(b) ΔMC/hour vs. Temperature

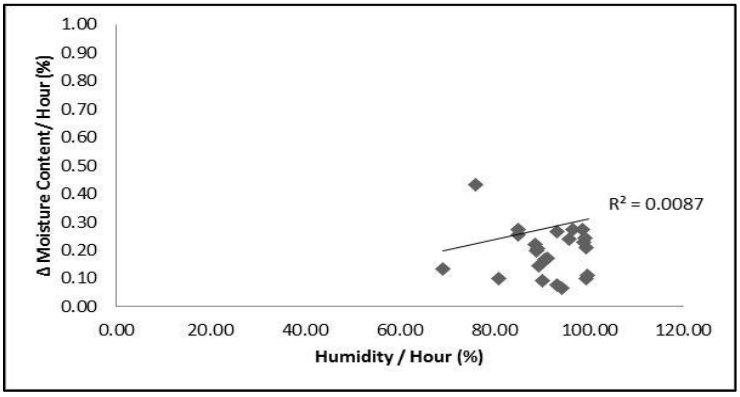

(c) ΔMC/h vs. Humidity

Figure 12-19. Plots of moisture change per hour against each of three independent variables at sensor B

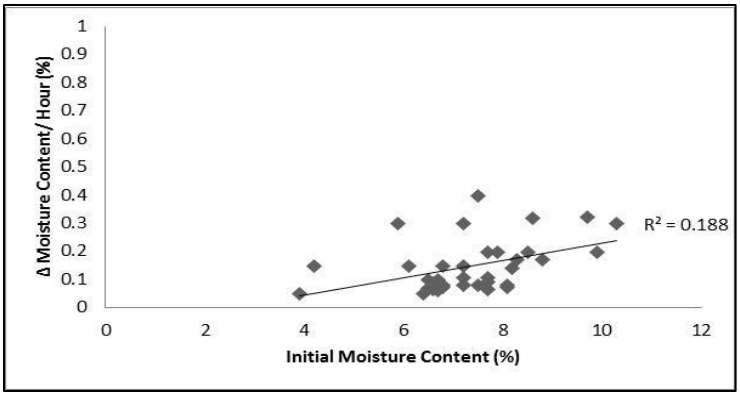

(a) ΔMC/h vs. IMC

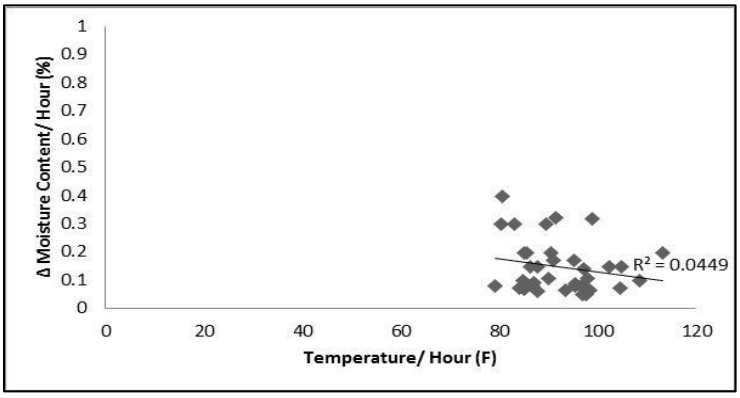

(b) ΔMC/hour vs. Temperature

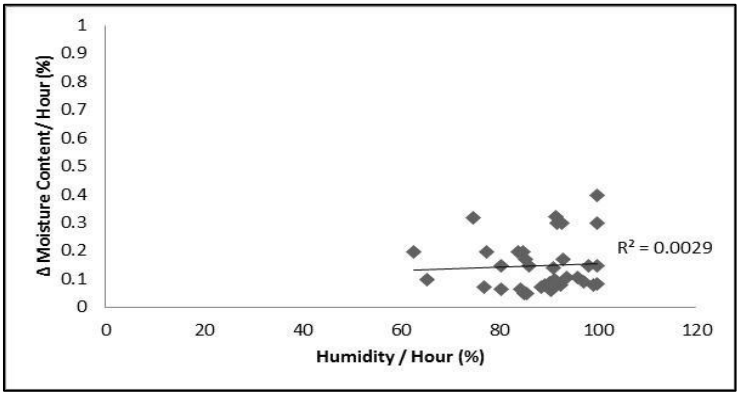

(c) ΔMC/h vs. Humidity

Figure 12-20. Plots of moisture change per hour against each of three independent variables at sensor C

Table 12-1. Comparisons between moisture loss indices for each project site

Site	y-intercept	Initial Moisture Content (1/1000 %)	Average CIR Layer Temperature (1/1000 °F)	Average Humidity (1/1000%)	Average Wind Speed (1/1000 mph)	R-square Value
Clinton County	-0.3767	43.1662	1.204	2.11	3.421	41.9%
Iowa County	-0.00996	6.015	0.145	-0.4	-6.18	83.2%
Benton County	-0.57728	25.464	4.615	2.316	13.437	41.9%
Marshall County	0.012526	73.734	--0.82	-1.41	3.206	62.3%
Delaware County	-0.14769	6.015	-0.13	1.933	18.711	27.4%
Delaware 2011	-0.38797	26.593	2.567	0.221	-1.92	31.3%
Black Hawk	1.316	94.002	-11.72	-5.25	16.429	35.9%
Combined Sites (7)	-0.04749	26.21	-0.48	0.383	14.683	45.0%

CHAPTER 13: DEVELOPMENT OF STIFFNESS CRITERIA

In order to supplement the moisture loss indices developed stiffness was measured and monitored at each project site during the curing period. Stiffness can be used to measure the resilient modulus of a pavement layer. States across the county are beginning to examine stiffness and its use in quality control of pavement layers. Previous studies of subgrade and base stiffness were examined in order to provide a comparison to this study's stiffness data and further create a criteria for curing.

13.1 Background and Other Studies

In a 2005 study by White et. al, subgrade/ subbase engineering properties at 12 Portland Concrete Cement project sites in Iowa were examined in order to evaluate the effect on pavement performance. One of the engineering properties examined was stiffness using the geogauge. Below, table 13-1 shows the stiffness values for each site as well as the subgrade/ subbase material used. Most values for the subgrade/ subbase were between the range of 2-8 MN/m. Projects 1, 11 and 12 had higher values around 15 MN/m. These projects with higher stiffness had fly ash and project 12 had a special granular subbase.

In 2003, Mohammad et. al performed a study on the use of foam recycled asphalt pavement base materials. A test section was established on US Highway 190 in Louisiana to test the potential use of foamed asphalt treated RAP as a base course material in lieu of a crushed lime stone base for continuously reinforced concrete pavement. 3 base type sections , A, B and C, were established. Base A was a crushed limestone base, Base B was a foam asphalt treated base with 100% of RAP materials and

Base C was a foam asphalt treated base with 75% of RAP and 25% of crushed concrete. The stiffness results from the test sections can be seen below in Table 13-2. Type B and C bases showed higher stiffness values than the crushed limestone. The difference in stiffness from 100% RAP to 75% RAP was very small indicating 100% RAP would perform as well as 75%.

Chen et. al performed an evaluation of In-Situ Resilient Modulus Testing Techniques. In this study approximately 100 field stiffness tests on different subgrade and base materials over 6 Texas Districts (Fort Worth, Pharr, Atlanta, Abilene, Austin and El Paso) were conducted. From this testing a ranking of base quality was established in regards to stiffness, as can be seen in Table 13-3. It was also concluded that density and stiffness showed a somewhat poor correlation with stiffness being 10 times more sensitive to the quality of a base than density. Based off of the rankings from this study the RAP bases from Mohammad et. al all are considered good bases.

13.2 Examination of Stiffness from Project Sites

The Geogauge was used to measure the stiffness of the CIR layer. Projects from 2009 and 2010, including sites in Clinton, Benton, Marshall, Iowa and Delaware 2010 counties, were tested roughly every 3-4 days for stiffness during the curing period. The results can be seen below in Figure 13-1. Stiffness reached a value of 20 MN/m at one point in every project. Stiffness trends were examined further previously in this report under each project section. The overall trend from the 2009 and 2010 sites suggests that stiffness increased over time, with the maximum stiffness recorded around 30 MN/m. According to the Chen et. al rating system each base was overlaid with a good or excellent rating except for Benton County. The low stiffness values in Benton County

could be a result of the frequent rainfalls that occurred during the curing period. The one question the data raised was the exact effect of rainfall on the stiffness. Benton and Marshall County both showed decreases in stiffness after significant rainfalls, however Iowa county showed steady increase despite a heavy rainfall on 8/28. In order to better understand the relationship between stiffness and rainfall it was decided that two more projects be examined and that stiffness measurements be taken every day, rather than 3-4 days, during the curing period.

In 2011 2 project sites were selected to examine. The projects occurred in Delaware and Black Hawk County. As previously stated, stiffness was measured every day in order to further examine the effect of rainfall on stiffness. The measurements can be seen in Figure 13-2 below. These plots show much more fluctuation than the previous year's mainly due to measurements being taken every day. For Delaware County it can be seen that there were decreases in stiffness around 7/15, 7/22 and 7/28. These dates all come after significant rainfalls. In each instance the stiffness began to recover after a day or two. Using the ranking previously mentioned from Chen et. al Delaware County always qualified as a good base and reached an excellent qualification at times. Black Hawk County also showed fluctuations in stiffness. There were drops on 7/22, 7/29 and 8/8. Again, these all coincided with significant rainfalls and the stiffness began to rebound after a day or two. For much of the curing period Black Hawk County would be considered an excellent base. From these two project sites it can be concluded that rainfall does indeed have an impact on stiffness. The stiffness begins to increase again after a day or two. This is very important if looking at stiffness as criteria for curing. It is recommended that overlay only occur once the pavement has reached a predetermined

value and that rainfall had not occurred within 24 hours of the measurement and that stiffness had shown increase for at least 2 days.

Table 13-1. Stiffness Results for 12 Portland Concrete Cement Projects in White et. al Study 2003

Project Number	Project Name	Subgrade/ Subbase Material	Number of Tests	Average Stiffness MN/m
1	Eddyville Bypass	Hydrated Fly Ash	33	14.82
2	Highway 330	Natural Soil	33	2.36
3	Knapp Street Subgrade	Natural Soil	51	1.60
4	Knapp Street Subbase	Granular Subbase	24	9.54
5	35th Street Subgrade	Granular Subbase	130	4.72
6	35th Street Subbase	Granular Subbase	24	5.88
7	Highway 34	Natural Soil	85	5.81
8	Highway 218	Natural Soil	85	7.22
9	Interstate 35	Natural Soil	85	4.68
10	Jack Trice Lot S1 Before Ash	Deteriorated Asphalt Pavement Subgrade	18	9.65
11	Jack Trice Lot S1 After Ash	Self-Cementing Fly Ash	18	16.30
12	University-Guthrie Avenue	Granular Subbase	30	15.72

Table 13-2. Stiffness Results for 3 Test Sections in Mohammad et. al 2003 Study

Test Section	Base Type	Stiffness (MPa)	Stiffness (MN/m)
A	Crushed Limestone	155.9	17.98
B	Foam Asphalt Treated Base with 100% of RAP Materials	197.8	22.81
C	Foam Asphalt Treated Base with 75% of RAP and 25% of Crushed Concrete	193.4	22.31

Table 13-3. Base Rankings in regards to Stiffness from Chen et. al Study

Base Quality	Stiffness (MPa)	Stiffness (MN/m)
Weak	< 87	<10
Good	156-208	18-24
Excellent	>260	>30

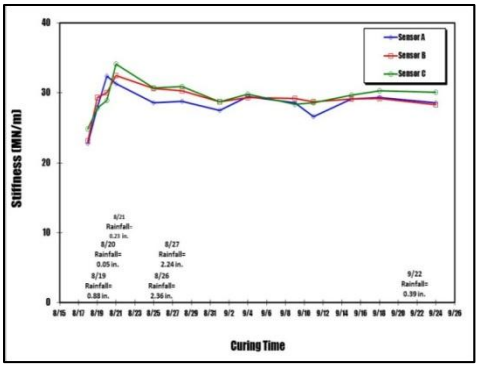

Clinton County

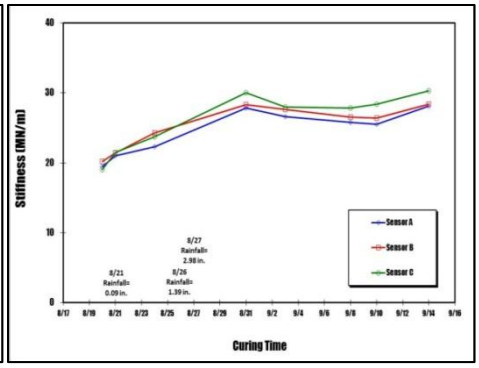

Iowa County

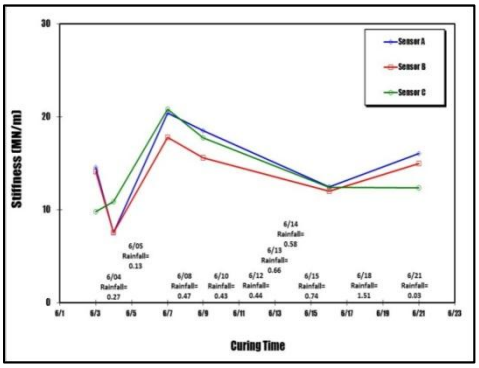

Benton County

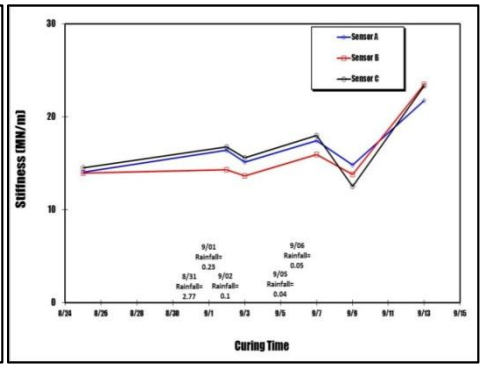

Marshall County

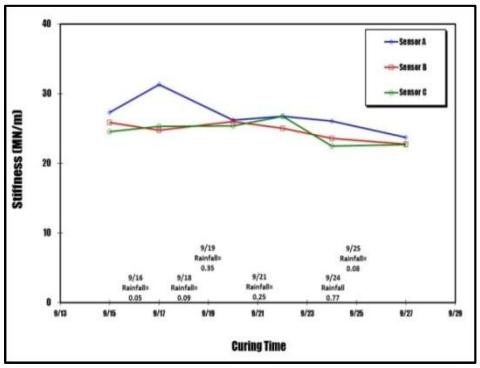

Delaware County

Figure 13-1. Plots of Stiffness Against the Curing Period for 2009 and 2010 Project Sites

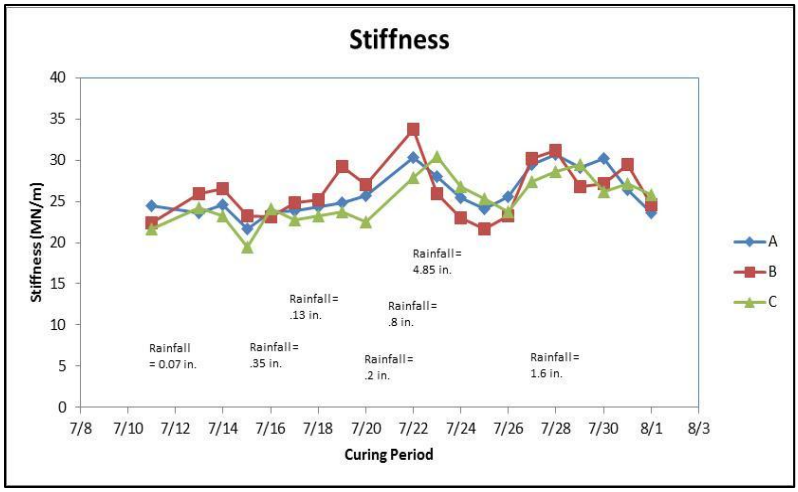

Delaware County 2011

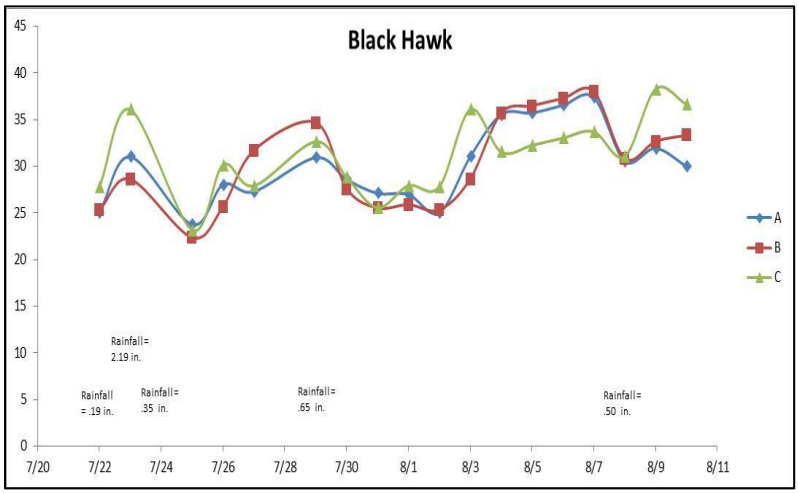

Black Hawk County

Figure 13-2. Plots of Stiffness Against the Curing Period for 2011 Project Sites

CHAPTER 14: SUMMARY AND CONCLUSIONS

The current practice in Iowa simply controls the maximum moisture content in the cold in-place recycling (CIR) of 1.5 percent, whereas all CIR projects evaluated in this study, struggling with unfavorable climate, have been overlaid successfully with higher amounts of moisture. To develop a better analysis tool to monitor the CIR layer in preparation for a timely placement of the wearing surface, a set of moisture loss indices were developed based on the field measurements of moisture contents from both CIR-foam and CIR-emulsion construction sites.

Moisture loss indices were developed for each sensor of each site. Next, a single moisture loss index based on the data from the multiple sensors was developed for each site. Lastly, a typical moisture loss index based on all sites was developed for each of CIR-foam and DIR-HFMS-2S emulsion projects.

The moisture sensor was very consistent with the time and amount of rainfall and it is an accurate tool to monitor moisture in CIR layer. The Geo-gauge provided reasonable stiffness values steadily increasing over time. It was found that significant rainfall decreased stiffness. This decrease was not always instant and often took 1-2 days to reach the minimum stiffness before it began to increase again. All project sites recorded stiffness values either in the good or excellent category of Chen et. als base rating system. The portable TDR device provided inconsistent result without a good correlation with an amount of rainfall.

14.1 Conclusions

Based on the field experiment the following conclusions were derived.

1. As expected, with no precipitation, stiffness of the CIR layers steadily increased over the curing time.

2. The stiffness measured by geo-gauge was effected by significant rainfall. The stiffness would decrease for around 1-2 days after a significant rainfall before rebounding and beginning to increase again.

3. The project sites all recorded stiffness values in either the good or excellent rating for Chen et. als base quality categorization.

4. The moisture indices developed for CIR-foam sites can be used for predicting moisture level in a typical CIR-foam project.

5. The moisture indices developed using data from one CIR-HFMS-2S emulsion project was not as reliable for the one developed for CIR-foam project. To increase the reliability of the moisture loss indices for a typical CIR-HFMS-2S emulsion project, more data should be collected.

6. The initial moisture content was the most significant in predicting the future moisture contents in a CIR layer.

7. The portable TDR device was not accurate in measuring the moisture contents in a CIR layer.

8. The nuclear gauge was not accurate in measuring the moisture contents in a CIR layer.

14.2 Recommendations/Future Studies

1. To further validate the moisture loss indices developed based on the data collected from one CIR-HFMS-2S emulsion project, one more CIR-HFMS-2S emulsion project site should be monitored.

2. To develop moisture loss indices for CIR-CSS-1 emulsion project, two CIR-CSS-1 emulsion project sites should be monitored.

3. Geo-gauge should be used to determine the optimum timing for an overlay. The suggested criteria for quality control be that the stiffness reach a value of at least 22 MN/m before overlay. This qualifies as a good quality base pavement. The minimum stiffness value must also be reached at a minimum two days after a significant rainfall when a beginning increase in stiffness is measured.

4. Nuclear gauge should not be used because its measurement is not consistent with the moisture contents in CIR layer.

REFERENCES

1. Asphalt Recycling and Reclaiming Association (ARRA). (2001). "Basic Asphalt Recycling Manual." Annapolis, MD, 2001, pp 225–226.

2. Asphalt Institute (AI). "A basic asphalt emulsion manual." Manual Series No. 19, Lexington, KY, 1988.

3. Kim, Y., S. Im., and H. Lee, "Impacts of Curing Time and Moisture Content on Engineering Properties of Cold In-place Recycling Mixtures Using Foamed or Emulsified Asphalt." Journal of Materials in Civil Engineering, Vol. 23, No. 5, ASCE, 2011, pp. 1-13.

4. AIPCR and PIARC. "Cold In-place Recycling of Pavements with Emulsion or Foamed Bitumen." Technical committee 7/8 Road Pavements, 2002.

5. Davidson, J. K., C. Blais, and J. Croteau, "A Review of In-place Cold Recycling/Reclamation in Canada." The Transportation Association of Canada Fall 2004 Meeting, 2004.

6. Kim, Y. and H. Lee, "Measurements of Moisture Conditions of Cold-in Place recycling Layer." CD ROM of the 90th Annual Meeting of the Transportation Research Board, Washington, D.C., 2011.

7. Tarantino, A., A. M. Ridley, and D. G. Toll, "Moisture Sensor Field Measurement of Suction, Water Content, and Water Permeability." Journal of Geotechnical and Geological Engineering, Vol. 26, No. 6, 2008, pp. 751-782.